SAHC

Non-destructive identification of the mechanical response of FRP strengthened brickwork walls with modal analysis

Hamidreza Taravat

Spain | 2013

ADVANCED MASTERS IN STRUCTURAL ANALYSIS
OF MONUMENTS AND HISTORICAL CONSTRUCTIONS

Master's Thesis

Hamidreza Taravat

Non-destructive identification of the mechanical response of FRP strengthened brickwork walls with modal analysis

UNIVERSITAT POLITÈCNICA DE CATALUNYA

University of Minho

Education and Culture

Erasmus Mundus

ADVANCED MASTERS IN STRUCTURAL ANALYSIS
OF MONUMENTS AND HISTORICAL CONSTRUCTIONS

Master's Thesis

Hamidreza Taravat

Non-destructive identification of the mechanical response of FRP strengthened brickwork walls with modal analysis

This Masters Course has been funded with support from the European Commission. This publication reflects the views only of the author, and the Commission cannot be held responsible for any use which may be made of the information contained therein.

Spain | 2013

ADVANCED MASTERS IN STRUCTURAL ANALYSIS
OF MONUMENTS AND HISTORICAL CONSTRUCTIONS

Master's Thesis

Hamidreza Taravat

Non-destructive identification of the mechanical response of FRP strengthened brickwork walls with modal analysis

This Masters Course has been funded with support from the European Commission. This publication reflects the views only of the author, and the Commission cannot be held responsible for any use which may be made of the information contained therein.

Spain | 2013

DECLARATION

Name: Hamidreza Taravat Najafabadi

Email: hamid_reza82@yahoo.com

Title of the Msc Dissertation: Non-destructive identification of the mechanical response of FRP strengthened brickwork walls with modal analysis

Supervisor(s): Professor. Lluis Gil

Dr. Ernest Bernat

Year: 2013

I hereby declare that all information in this document has been obtained and presented in accordance with academic rules and ethical conduct. I also declare that, as required by these rules and conduct, I have fully cited and referenced all material and results that are not original to this work.

I hereby declare that the MSc Consortium responsible for the Advanced Masters in Structural Analysis of Monuments and Historical Constructions is allowed to store and make available electronically the present MSc Dissertation.

University: Technical University of Catalonia, Spain

Date: 19-07-2013

Signature:

_____

Dedication

I dedicate this thesis to my father and mother

تقدیم به پدر و مادر عزیزم

ACKNOWLEDGEMENTS

I am especially thankful to Prof. Paulo Lourenço for his attention and help about everything during SAHC.

I am heartily thankful to Mr. Seifollahi who taught me how civil engineering and historical constructions can be improved culture and life.

I like to thank Prof. Lluis Gil and his group to learn and work under his guidance in the field of modal analysis and masonry. Also, I would like to express my gratefully appreciation to the tremendous help from Dr. Ernest Bernat.

Italy, Spain and Portugal are great and I am grateful to Prof. Pere Roca Fabregat and Prof. Claudio Modena because I understood how much the culture of Spain and Italy are great from them.

I would like to acknowledge the SAHC consortium for giving me an opportunity for this advanced master.

I also would like to express my gratitude to Prof. Halabian and Pro. Hashemolhosseini from Isfahan University of Technology who are helped me behalf Ministry of Science Research and Technology of Iran especially for my research and dissertation.

I am also grateful to my parents for the supports and helps.

ABSTRACT

Techniques for the non-destructive identification of the materials and structures properties have been recently developed and are rapidly improving their performance now. One of the main advantages of these testing procedures is their possible application for studying historical buildings without damaging these heritage elements, which is one of the basic requirements of conservation interventions.

Among non-destructive testing techniques, the vibration analysis or modal analysis outstands because of its easy implementation, quick data acquisition and reliable result. Hundreds of buildings and civil engineering structures have been studied with this technique to assess their performance through the elastic dynamic response. This testing technique is able to provide essential information for the safety study of existing structures or to evaluate the structural effectiveness of a strengthening system once it is applied.

Focusing the research on the historical buildings, brickwork walls are one of the most common structural elements. However, it has been noticed that there is a growing strengthening tendency which might change the structural behavior of these elements. Applying FRP laminates bonded on the wall's surface has turned to be a common practice in retrofitting structures. Nevertheless, this actuation shows several drawbacks which have been deeply studied. The elastic properties of the FRP strengthened walls are expected to be different from the ones of unreinforced walls. This strengthening system has been experimentally analyzed with destructive tests but using a non-destructive technique is still a new investigation branch.

The proposed tasks are aimed to perform an experimental campaign in order to evaluate the changes in the dynamic response of brickwork walls when strengthened with different patterns of FRP by using a modal analysis.

RESUMEN

Recientemente se han desarrollado técnicas no destructivas para la identificación de las propiedades de materiales y estructuras. Actualmente se está mejorando su rendimiento y capacidades. Una de las principales ventajas de estos procedimientos de ensayo es que se pueden aplicar en el estudio de construcciones históricas sin dañar estos elementos de la herencia cultural, cosa que es uno de los requisitos básicos de las intervenciones de conservación.

Entre las técnicas no destructivas de identificación de propiedades de materiales y estructuras, destaca el análisis de vibraciones o análisis modal por su fácil implementación, la rapidez en la adquisición de datos y la confianza de los resultados que ofrece. Cientos de edificios y estructuras civiles han sido estudiados con esta técnica para evaluar su capacidad de respuesta dinámica en el rango elástico. Esta técnica de ensayo es capaz de proporcionar información esencial para el estudio de la seguridad de estructuras existentes o para evaluar la efectividad estructural de un sistema de refuerzo una vez aplicado.

Centrando la investigación en edificios históricos, los muros de obra de fábrica son uno de los elementos estructurales más comunes. No obstante, se ha observado que hay una tendencia creciente orientada a su refuerzo, cosa que puede cambiar la respuesta estructural de estos elementos. Una práctica común en la rehabilitación de estructuras es la aplicación de laminados de FRP que se adhieren a la superficie del muro. Sin embargo, este tipo de actuación presenta varios problemas que han sido estudiados en profundidad. Las propiedades elásticas de los muros reforzados con FRP se espera que sean diferentes de las de los muros sin reforzar. Este sistema de refuerzo ha sido analizado experimentalmente a través de ensayos destructivos, pero el uso de técnicas no destructivas en este ámbito todavía resulta un línea de investigación novedosa.

Las tareas propuestas están orientadas a desarrollar una campaña experimental para evaluar los cambios en la respuesta dinámica de muros de obra de fábrica cuando se refuerzan con diferentes patrones de FRP mediante el uso del análisis modal.

خلاصه پژوهش

در حال حاضر تکنیک های شناسایی (تست های) غیر مخرب برای خصوصیت‌های سازه‌ای و مصالح ساختمانی با اصلاح کارایی به شدت در حال رشد می‌باشند. از مزایای اصلی این گونه از تست ها، امکان پذیری تست برای بناها و سازه های تاریخی به علت عدم تخریب بر روی المان های اینگونه از سازه های جهانی است که یکی از نیازهای اساسی از مداخلات در حفاظت می باشد.

از میان این گونه تست های غیر مخرب می‌توان به آنالیز لرزه یا آنالیز مودال به علت اجرای آسان، دریافت سریع داده ها و نتایج قابل اعتماد اشاره کرد. صدها گونه از ساختمان ها و سازه های عمرانی با این روش برای ارزیابی عملکرد خود از طریق پاسخ دینامیکی الاستیک مورد مطالعه قرار گرفته اند. این گونه تست قادر به فراهم کردن ارائه اطلاعات ضروری برای مطالعه ایمنی ساختمان های موجود و یا برای ارزیابی اثربخشی سیستم های مقاوم سازی شده، می باشد.

تمرکز این پژوهش بر روی ساختمان های تاریخی بوده که دیوارهای آجری یکی از مهمترین عناصر سازه‌ای آن می‌باشند. اما باید اشاره کرد گرایشی رو به رشد جهت تقویت برای این سازه ها وجود دارد که ممکن است رفتار سازه‌ای این عناصر را تغییر دهید. استفاده از صفحات FRP بر روی سطح دیوار ها تبدیل به یک عمل مشترک در مقاوم سازی سازه ها شده است گرچه این روش اشکالاتی دارد که به صورت عمیق مطالعه شده است. انتظار می‌رود که خواص الاستیکی دیواره های مقاوم شده با FRP متفاوت با دیوارهای تقویت نشده، باشند. این روش مقاوم سازی با تست های مخرب آزمایشگاهی آنالیز شده‌اند در حالی که تست های غیر مخرب هنوز یک شاخه جدید تحقیق هستند.

روش پیشنهادی جهت رسید به هدف: انجام یک کار تحقیقاتی با آنالیز مودال (تست مودال) برای شناسایی تغییرات در پاسخ دینامیکی دیوارهای آجری بوده زمانی که با الگوهای متفاوت FRP مقاوم سازی شده اند.

TABLE OF CONTENTS

1. INTRODUCTION 1

1.1 Objective 2
1.2 Thesis outline 2

2. DYNAMIC IDENTIFICATION 3

2.1 Single Degree of Freedom Systems 3
2.2 Multi Degree of Freedom Systems 6
2.3 Experimental modal analysis 8
2.3.1 Excitation mechanisms 9
2.3.2 Response transducers 10
2.3.2.1 Piezoelectric accelerometers 10
2.3.2.2 Piezoresistive and capacitive accelerometers 11
2.3.2.3 Force-balance accelerometers 11
2.3.3 Data acquisition systems 12
2.4 Identification Methods 12
2.4.1 Output-only identification techniques (Operational Modal Analysis) 13
2.4.2 Input-Output identification techniques 13
2.4.2.1 Measurement of the FRFs 14

3. PROPERTIES OF MATERIALS AND INSTRUMENTS 19

3.1 FRP 19
3.1.1 Preparation of substrate 20
3.1.2 Application 20
3.2 Primer 20
3.3 Adhesive 21
3.4 Bricks 22
3.5 Mortar 23
3.6 Masonry 23
3.7 Data Acquisition System (DAQ) 24
3.7.1 Hardware and software 24
3.7.2 Accelerometer and hammer 24

4. EXPERIMENTAL PROCEDURE 27

4.1 Constructing the walls 27
4.2 Transferring and setting up the specimens in the LITEM laboratory of UPC 29
4.3 Measuring and dimensions 30
4.3.1 Dimensions of grids for Modal Testing 31
4.4 Modal Testing before strengthening 34
4.4.1 Location of accelerometer 34
4.4.2 Setup the Data Acquisition System and software 35
4.4.3 Calibrating the errors 36
4.4.4 Obtaining the Frequency Response Spectrum and Function (FRF) before strengthening 37
4.5 Strengthening the walls 41
4.5.1 Preparing the specimens 41
4.5.2 Design of FRPs patterns 41
4.5.3 Measure, cut and location of the FRPs 43
4.5.4 Applying primer 45

4.5.5 Applying FRP and adhesive 47
4.6 Modal Testing after strengthening 51

5. POST PROCESS AND ANALYSIS OF DATA 55

5.1 Post processing the experiments 55
5.1.1 Mode indicator 55
5.1.2 Estimating real modes 57
5.1.2.1 Damping comparison 58
5.1.2.2 Repeated roots and closely coupled modes 58
5.1.3 Fit function and residues 59
5.2 Analysis and comparison of specimens 60
5.2.1 Location of accelerometer 60
5.2.2 Identification of the mechanical response of 15 specimens before and after strengthening for 5 FRP patterns 62
5.2.2.1 Obtaining the modal parameter and discarding the strange data 63
5.2.2.2 Damping ratio parameter 80
5.2.3 Comparison the results of specimens 81
5.2.3.1 Amount of FRP 82
5.2.3.2 Comparison the grid and vertical patterns 83
5.2.3.3 Influence of angle on FRP patterns. 84

6. CONCLUSIONS 87

6.1 Dynamic experimental testing 87
6.2 Analysis of data and results 88
6.3 Future works 89

7. REFERENCES 91

LIST OF FIGURES

Figure 1 - Single Degree of Freedom System 3
Figure 2 - Oscillating in a specific frequency in free vibration system 4
Figure 3 - Definition of multi degree of freedom system 7
Figure 4 - Impulse hammers (a); Response spectrum depending on the selected tip (b); Eccentric mass shaker (c) 10
Figure 5 - Piezoelectric accelerometer 11
Figure 6 - Piezoresistive accelerometer 11
Figure 7 - Force-balance accelerometers 12
Figure 8 - The Data AcQuisition system (DAQ) 12
Figure 9 - Classification of output-only identification techniques (Caetano, 2000) 13
Figure 10 - Classification of input-output identification techniques (Caetano, 2000) 14
Figure 11 - Beam 3 DOF Model 15
Figure 12 - FRFs of beam 3 DOF Model 15
Figure 13 - Drive Point FRF for Reference 3 and Cross FRFs for Reference 3 16
Figure 14 - Performance of used FRP 20
Figure 15 - Performance of used primer 21
Figure 16 - Performance of used adhesive 22
Figure 17 - Average dimensions of bricks 23
Figure 18 - Hardware of Data Acquisition System 24
Figure 19 - Characteristic of accelerometer 25
Figure 20 - Sensitivity and errors of accelerometer 25
Figure 21 - Hammer used in test 26
Figure 22 - Preparing the mortar for building the walls 27
Figure 23 - Controlling the uniform depth of the joints 28
Figure 24 - Process construction of the wall specimens 28
Figure 25 - The place and condition of completed walls 29
Figure 26 - Transporting and setting up the specimens in the laboratory 30
Figure 27 - The arrangement of walls in the laboratory 30
Figure 28 - Measuring the dimensions of the walls 31
Figure 29 - Supports in top of walls for next experiment 32
Figure 30 - Typical measuring of grids and walls 32
Figure 31 - Position of accelerometer on wall specimens 35
Figure 32 - The numbers of point and coordinate system of axis in each specimen 35
Figure 33 - Applying 2 horizontal impacts by hammer in each point 36
Figure 34 - The best coherence for 2 impacts in each point 36

Figure 35 - The worst coherence for 2 impacts in each point 37
Figure 36 - Rebound condition in hammer impact 37
Figure 37 - Results of Frequency versus Real for test 2V0H_1_nonstrengthened_a in points 1, 2, 55 and all points 38
Figure 38 - Results of Frequency versus Imaginary for test 2V0H_1_nonstrengthened_a in points 1, 2, 55 and all points 39
Figure 39 - Results of Frequency versus Magnitude for test 2V0H_1_nonstrengthened_a in points 1, 2, 55 and all points 40
Figure 40 - The processes of cleaning the surface 41
Figure 41 - Five groups of FRP patterns 42
Figure 42 - Positions of vertical and diagonal FRPs on walls 44
Figure 43 - Positions of horizontal FRPs on walls 44
Figure 44 - How to cut the FRP 45
Figure 45 - Removing the protection layer of FRPs for next steps 45
Figure 46 - Mixing the primer between 3 to 5 minutes 46
Figure 47 - Processes of applying primer 46
Figure 48 - Mixing and preparing the adhesive 48
Figure 49 - Process of applying the adhesive on walls and FRPs at the same time 48
Figure 50 - How to apply the FRPs on walls 49
Figure 51 - The operation of attaching the FRPs to each other 50
Figure 52 - Direction and turn of the second layer of FRP over the first layer of reinforcement 50
Figure 53 - Results of Frequency versus Real for test 2V0H_1_strengthened_a in points 1, 2, 55 and all points 52
Figure 54 - Results of Frequency versus Imaginary for test 2V0H_1_nonstrengthened_a in points 1, 2, 55 and all points 53
Figure 55 - Results of Frequency versus Magnitude for test 2V0H_1_nonstrengthened_a in points 1, 2, 55 and all points 54
Figure 56 - Estimation peak and modes from FRF 56
Figure 57 - Number of peaks for each FRF (4 modes for 1st FRF; 3 modes for 29th FRF) 56
Figure 58 - Difference of computing modes for the Real, Imaginary and Magnitude part 57
Figure 59 - Estimation frequencies and damping ratio 58
Figure 60 - Estimation modes in closely coupled conditions 59
Figure 61 - Curve fitting of mode shapes 59
Figure 62 - Example of residue parameter 60
Figure 63 - Estimation the same modes and same frequencies with different position of accelerometer 62
Figure 64 - FRFs of 2V0H_1 specimen before and after strengthening 63
Figure 65 - FRFs of 2V0H_2 specimen shows shift of peaks after strengthening 64
Figure 66 - Vague mode shapes of 2V0H_3 specimen 64
Figure 67 - Comparison of the difference of frequencies after and before strengthening for 2V0H specimens in Hz and percentage 66

Figure 68 - Mode shapes of 2V0H_3 specimen 67
Figure 69 - Mode shapes of 2V0H_1 specimen 68
Figure 70 - Mode shapes of 2V0H_2 specimen 69
Figure 71 - Graph of MAC value for 2V0H specimens 70
Figure 72 - Comparison of the frequency results for three specimens of 2V2H model 72
Figure 73 - Comparison of the difference of frequencies for 2V2H specimens in Hz and percentage . 73
Figure 74 - Vague mode shapes of 3V0H specimens 75
Figure 75 - Comparison between the non-strengthened and strengthened 3V5H_1 specimen (influence of homogenizing after strengthening) 77
Figure 76 - FRFs of 3V3I_1 and 3I3I_3 specimens 79
Figure 77 - Difference of damping ratio for the 2V0H_1, 2V0H_2 and 2V0H_3 specimens 80
Figure 78 - Comparison the difference average of frequencies for each mode shape 81
Figure 79 - Comparison the difference average of frequencies and amount of FRP 82
Figure 80 - Comparison the difference average of frequencies for grid and vertical patterns (2V0H-2V2H) 84
Figure 81 - Comparison the difference average of frequencies for grid and vertical patterns (3V0H-3V5H) 84
Figure 82 - Comparison the difference average of frequencies for angle (30-60 and 90) 85

LIST OF TABLES

Table 1 - Properties of FRP 19
Table 2 - Properties of primer 21
Table 3 - Properties of MBrace® LAMINATE ADHESIVE HT for structural reinforcement with FRP ... 22
Table 4 - Properties of the bricks 23
Table 5 - Properties of the mortar used in the joints 23
Table 6 - Properties of constructed brickwork walls 24
Table 7 - Characteristic of accelerometer 25
Table 8 - Dimensions and number of walls 31
Table 9 - Dimensions of vertical grids 33
Table 10 - Dimensions of Horizontal grids 34
Table 11 - The settings of DAQ system 36
Table 12 - How to number the specimens 42
Table 13 - Measurements and locations of FRPs 43
Table 14 - Dates of applying primer and FRPs 47
Table 15 - Dates of operating modal testing 51
Table 16 - Details of frequency and damping estimation for the 2V2H_1 specimen with different position of accelerometer 61
Table 17 - Summary of frequency and damping estimation for the 2V0H specimens 65
Table 18 - Summary of frequency and damping estimation for the 2V2H specimens 72
Table 19 - Summary of frequency and damping estimation for the 3V0H specimens 75
Table 20 - Summary of frequency and damping estimation for the 3V5H specimens 76
Table 21 - Summary of frequency and damping estimation for the 3I3I specimens 78
Table 22 - Comparison the difference average of frequencies for each mode shape 81
Table 23 - Comparison the difference average of frequencies and amount of FRP 82
Table 24 - Comparison the difference average of frequencies for grid and vertical patterns 83
Table 25 - Comparison the difference average of frequencies for angle (30-60 and 90) 85

1. INTRODUCTION

Among different non-destructive (ND) techniques that can be useful for the achievement of an advanced knowledge of historic masonry buildings, dynamic testing (successive modal analysis) can be considered a very effective tool. In the other hand, one of the main advantages of these testing procedures is their possible application for studying historical buildings without damaging these heritage elements, which is one of the basic requirements of conservation interventions. Also, dynamic testing is actually the only way to experimentally measure parameters related to the global structural behavior. Parallel to this subject, the estimation of the structural and material properties is usually not easy due to the complexity of historical structures. It should be mentioned that a lot of buildings and structures have been studied with the technique of input/output modal analysis to assess their performance through the dynamic response. However, this procedure has not been applied in historical construction yet.

In addition, modal analysis corresponds to the study of the dynamic properties of structures under vibration excitation. Dynamic properties resulting from experimental modal analysis are the frequencies, damping and mode shapes which are related to the physical and mechanical characteristics of the analyzed structure (mass, stiffness and energy dissipation). Due to mechanical characteristics of the structure, essential information for the safety study of existing structures could be reached with this method. One of the applications is to evaluate the structural effectiveness of a strengthening system.

In the masonry structures, brick walls will usually have the ability to support other parts of the building without any particular modification and under compression. These are load-bearing walls. This masonry element is among the most ancient architectural technologies, yet continues to provide boundless opportunities for both traditional and modern design. Any compression member usually fails due to the buckling when the wall is slender or vertical load is combined with horizontal load. When buckling reaction is expected, unreinforced masonry can be strengthened to increase its load-bearing capacity.

It has been noticed that there is a growing strengthening tendency which might change the structural behavior of wall element. Focusing the research on the historical buildings, brickwork walls are one of the most common structural elements. Applying Carbon Fiber Reinforced Polymer (FRP) laminates bonded on the wall's surface has turned to be a common practice in retrofitting structures. Nevertheless, this actuation shows several drawbacks which have been deeply studied. The elastic properties of the FRP strengthened walls are expected to be different from the ones of unreinforced walls. This strengthening system has been experimentally analyzed with destructive tests but using a modal analysis (Modal Testing) technique is still a new investigation branch.

1.1 Objective

The aim of this dissertation is to carry out a modal identification analysis of FRP strengthened brickwork walls. In addition, it is intended to evaluate the changes in the dynamic response of brickwork walls when strengthened with different patterns of FRP by using a modal analysis.

To achieve this goal several secondary objectives are going to be reached: a) a review about studying the scientific basis of the modal analysis, the data acquisition procedures and the post-processing theoretical formulation; b) defining the vibration tests and FRP patterns; c) applying FRP, performing the tests and obtaining relevant data for the mechanical characterization of the brickwork wall before and after the strengthening; Next, the main conclusions from the experiment are presented with proposing feasible improvements.

1.2 Thesis outline

This thesis study consists of six chapters as follows.

Chapter 1 gives general information about the motivation, concepts of dynamic experiments, the background of the necessity for strengthening unreinforced masonry wall and the outline of the study.

Chapter 2 presents a state of the art about the scientific basis of the modal analysis, dynamic based experimental dynamic tests and identification of the mechanical response.

Chapter 3 introduces the characteristics of the FRP, primer, brick, mortars and Data Acquisition System (DAQ).

Chapter 4 describes the process of making the masonry specimens and the procedure of the experimental test set-up (Modal Testing) before and after strengthening like estimation of dynamic properties and calibration the errors.

Chapter 5 discusses about post processing the experiments, analysis the estimated data and comparison of specimens.

Chapter 6 contains the conclusions. Brief summary of the study, difficulties faced during the work, recommendations, discussion of results and further works are explained.

2. DYNAMIC IDENTIFICATION

Structural dynamic analysis methods introduce the stress and response of the structure under arbitrary dynamic loadings. The dynamic properties of the structure can be defined as time dependent when the direction, position and magnitude of loads are varying with time.

The deterministic and stochastic are two approaches dynamic response. The system has been called deterministic when the time variation of dynamic forces acting on the system is known. Also, if the excitation is random, the problem can be analyzed with probabilistic concepts and it is possible to analyze the statistical description of the response (Chopra, 2001). In addition, the number of displacement components that must be taken into account to represent the effects of all significant inertial forces of a system is known as the number of (dynamic) degrees of freedom of the system (DOF). General overview on basic structural dynamics will be briefly discussed in this chapter.

2.1 Single Degree of Freedom Systems

Generally, the structural systems give response to the loads (external source of excitations or dynamic loadings) with their resistance of initial properties which are exposed to external source of excitations or dynamic loadings. This kind of properties are mass, stiffness and energy dissipation capability, damping.

The system is defined by a mass on top connected to ground by a column that has specified stiffness that contracts with the movements of the mass. Any force act on the mass **m** cause displacement proportional to the stiffness of the system **k**. When the forces replaced, the system starts to oscillate in a specific frequency. In damped structures, by the time passes the velocity of the cycles decreases until the initial position of the mass is satisfied. In damped systems, energy is dissipated in different mechanisms such transformation of kinetic energy to thermal energy, formation of cracks or friction between structural or non-structural elements as shown in Figure 1 (Chopra, 2001).

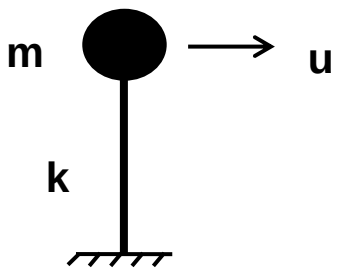

Figure 1 - Single Degree of Freedom System

The particular action itself can be defined by a mathematic expression with regard to Newton's second law of motion or dynamic equilibrium. If $\boldsymbol{u(t)}$ is defined as the time-dependent displacement of a system with one degree of freedom, the equation of motion is:

$$m\ddot{u}(t) + c\dot{u}(t) + ku(t) = p(t) \qquad \text{Eq.1}$$

where ***m*** is mass of the system, ***c*** is the damping constant, ***k*** is the system stiffness and ***p(t)*** is the acting force on the system depending on time. Here, the time derivatives $\boldsymbol{\dot{u}(t)}$and $\boldsymbol{\ddot{u}(t)}$ represents the velocity and the acceleration of the system, respectively.

Regarding the analytical solution, the equation of motion can be solved by derived from free vibration theory (Eq.2). It means vibration (caused by a disturbance) without any external dynamic excitation. The acting force equals to zero when the system is disturbed from its static equilibrium position by giving the mass some displacement and release. So, the system can oscillate in a specific frequency when it released that is shown by Chopra in Figure 2. Then the system will be solved by Eq.3.

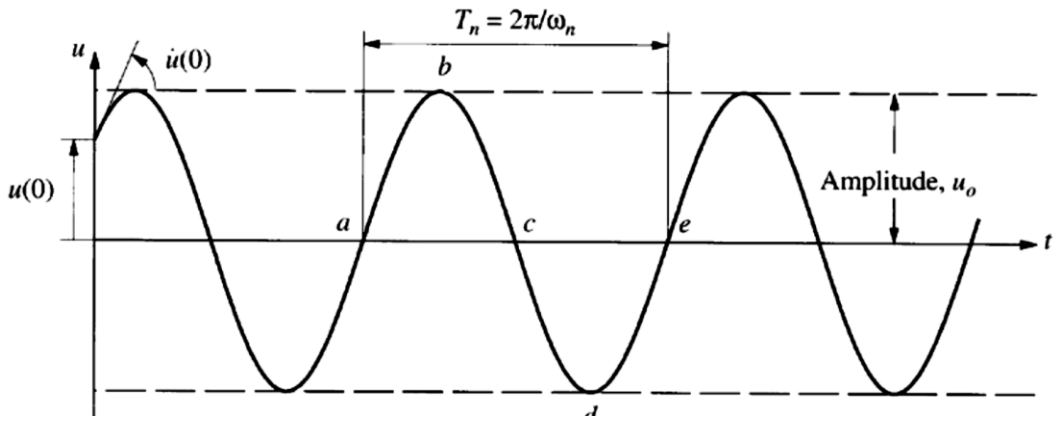

Figure 2 - Oscillating in a specific frequency in free vibration system

$$m\ddot{u}(t) + ku(t) = 0 \qquad \text{Eq.2}$$

$$u(t) = A\cos\omega_n t + B\sin\omega_n t \qquad \text{Eq.3}$$

When A and B are constants of integration and ω_n is natural circular frequency [rad/s].Also, the natural frequency (f_n) and period (T) can be derived easily from Figure 2-2.

$$\omega_n = \sqrt{\frac{k}{m}} \quad [rad/s\,] \qquad f_n = \frac{\omega_n}{2\pi} = \frac{1}{T} \ (Hz) \qquad \text{Eq.4}$$

Also, damping could be not zero in real life (Eq.5). So, it can be obtained by differentiating the equation of motion.

$$m\ddot{u}(t) + c\dot{u}(t) + ku(t) = 0 \qquad \text{Eq.5}$$

$$u = e^{-\xi\omega_n t}[u_0 cos\omega_D t + \frac{\dot{u}_0 + u_0\xi\omega_{Dn}}{\omega_D} sin\omega_D t] \qquad \text{Eq.6}$$

Where ξ is damping ratio and ω_D damped frequency given by;

$$\xi = \frac{c}{c_{cr}} \qquad \omega_D = \omega_n\sqrt{1-\xi^2} \qquad \text{Eq.7}$$

When an arbitrary force is acting in the system, the solution of this second order differential equation can be obtained by the Duhamel's integral (Chopra, 2001), valid for linear systems and given by the following expression:

$$u(t) = \frac{1}{m\omega_D}\int_0^t p(t)\, e^{-\xi\omega_n(t-\tau)} sin[\omega_D(t-\tau)]d\tau \qquad \text{Eq.8}$$

where τ is the reference instant.

System response can be calculated by Fourier Transformation in frequency domain; as an alternative; Definition of Fourier Transformation X for function $x(t)$ is;

$$u(t) = \int_{-\infty}^{+\infty} x(t)\, e^{-j\omega t} \qquad \text{Eq.9}$$

where j is the imaginary number $(j^2 = -1)$. In the process, $P(\omega)$ and $Q(\omega)$ represents the Fourier transforms of the excitation $p(t)$ and the response $u(t)$, respectively.

The Fourier transformation can be applied to the both sides of the motion equation;

$$m\omega^2 Q(\omega) + cj\omega Q(\omega) + kQ(\omega) = P(\omega) \qquad \text{Eq.10}$$

Solving the previous equation with respect to $Q(\omega)$ as presented in Eq.11 it can be concluded that the response Fourier transform function directly depends on the excitation and on a complex function $H(\omega)$. This is the so-called Frequency Response Function (FRF), defined as the ratio of the Fourier transforms of the response and the excitation force:

$$Q(\omega) = \frac{P(\omega)}{-m\omega^2 + cj\omega + k} = H(\omega)P(\omega) \qquad \text{Eq.11}$$

The advantage of this approach is the fact that a deterministic relationship between excitation and response can be obtained, as given by:

$$H(\omega) = \frac{Q(\omega)}{P(\omega)} = \frac{1}{k} \frac{P(\omega)}{1 - \left(\frac{\omega}{\omega_n}\right)^2 + j[2\xi\left(\frac{\omega}{\omega_n}\right)]} \quad \text{Eq.12}$$

It is noted that $H(\omega)$ is a complex function and to calculate its amplitude it is necessary to square root the sum of the squares from the real and imaginary parts, which results in

$$|H(\omega)| = \frac{1/k}{\sqrt{[1-(\omega/\omega_n)^2]^2 + [2\xi(\omega/\omega_n)]^2}} \quad \text{Eq.13}$$

This constitutes the bases of seismic analysis and experimental dynamic identification theories (Gavin H., 2010).

2.2 Multi Degree of Freedom Systems

The equation of movement can be obtained like single degree of freedom with regard to the Newton's second law when the system has n degree of freedom (Eq.14). Also, the multi degree of freedom systems can be solved like single degree freedom systems by means of simplifications. In addition, there are three possible types of displacements; the longitudinal, traversal and rotational. Figure 3 shows multi-degree of freedom systems can be solved regards to considering traversal displacements (Chopra, 2001).

$$M\ddot{u}(t) + C_2\ddot{u}(t) + Kq(t) = p(t) \quad \text{Eq.14}$$

In this equation M, C_2 and K are the order $n \times n$ matrices of mass, viscous damping and stiffness, with their components m_{ik}, c_{ik} and k_{ik} representing the generalized forces for coordinate i. $p(t)$ is the generalized excitation vector and $q(t)$ the generalized response vector when an acceleration is applied in the coordinate k.

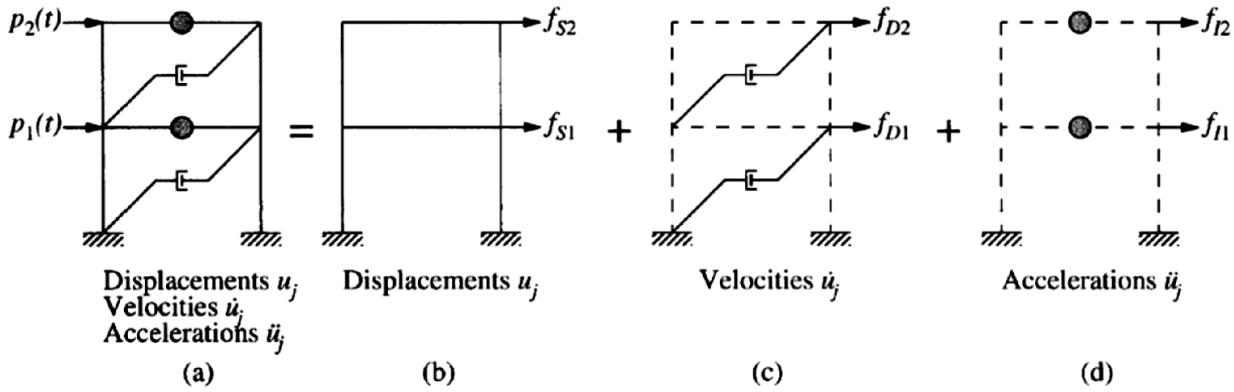

Figure 3 - Definition of multi degree of freedom system

The Fourier transform functions will be used for solving (Eq.14). Then, (Eq.15) will be established the direct relation between excitation and response like (Eq.12). This is Fourier Transform Function for multi degree of freedom systems. However, it is necessary to calculate the complex inverse of the matrix of $n \times n$ for each frequency ω (Caetano, 1992).

$$H(\omega) = [-\omega^2 M + j\omega\, C_2 + k]^2 \qquad \text{Eq.15}$$

Instead of solving (Eq.14), modal approach is preferred the solution which is based on assumptions of an undamped problem with eigenvalue solution that is shown in (Eq.16).

$$\mathrm{u(t)}=\varphi_i{}^{e^{\lambda_i t}} \qquad \text{Eq.16}$$

where φ_i are the real eigenvectors $(i = 1,\dots,m)$ and λ_i^2 are the eigenvalues. For free vibration systems, the equation reads by substituting $u(t)$,

$$[K - (-\lambda_i^2)M]\varphi_i = 0 \quad \vee\ \mathrm{K\Phi = M\Phi\Lambda} \qquad \text{Eq.17}$$

The modes are commonly grouped in the modal matrix Φ where each column represents the eigenvectors, and the eigen frequencies ω_i are grouped in a diagonal matrix Λ. Orthogonality properties of modal shape matrix allow normalizing matrices. Where I is the identity matrix of dimension $n \times n$.

$$\Phi_m^T M \Phi_m = I \qquad \Phi_m^T M \Phi_m = \Lambda^2 \qquad \text{Eq.18}$$

If (Eq.18) is pre-multiplied by $\Phi^T T$ and taking into account the (Eq.19), the natural undamped frequencies of each mode i can be obtained similarly to one degree of freedom system problem:

$$\omega_i^2 = \frac{K_{e,i}}{m_i} \qquad \text{Eq.19}$$

By adding damping properties and coordinate transformation, then equation of motion becomes;

$$I\,\ddot{u}_m(t) + \Gamma\dot{u}_m(t) + \Lambda^2 q_m(t) = \begin{bmatrix} \ddots & & \\ & \frac{1}{m_i} & \\ & & \ddots \end{bmatrix} \Phi^T\, p(t) \qquad \text{Eq.20}$$

where I is modal mass, Γ is modal damping and Λ^2 is modal stiffness.

Also, Fourier transform functions can be used to solve (Eq.21) because the equation is similar to the single degree of freedom system. The response now is related to the solicitation by a FRF in the modal space, in the following form:

$$Q(\omega) = H(\omega)P(\omega) \qquad \text{Eq.21}$$

where the diagonal terms of the FRF is a matrix $n \times n$ given by the expression:

$$H_{(i,K)}(\omega) = \sum_{j=1}^{n} \frac{\varphi_{i,j}\varphi_{k,j}}{(\omega_n^2 - \omega^2) + i(2\xi_n\omega_n\omega)} \quad , \quad i \wedge k = 1, \ldots, n \qquad \text{Eq.22}$$

The deterministic formulation for mass and stiffness can be calculated by extracting the mechanical material characteristics of the structural systems, but the information about damping cannot be calculated with those parameters. For further reading about deterministic formulation see Clough and Penzien (1993), Chopra (2001), Ewins (2000) and Maia and Silva (1997).

2.3 Experimental modal analysis

Regarding the modern conservation criteria and recommendation of International Scientific Committee for the Analysis and Restoration of Structures of Architectural Heritage (ISCARSA)-2005, the minimum intervention and preservation of construction techniques are requested for understanding any damage phenomena or evaluation of seismic vulnerability. Concerning this viewpoint, different non-destructive inspection techniques would be provided local information for the estimation of global properties. In addition, complete realistic behavioral model of masonry heritage structures is not possible when the experimentally verified data is not achieved.

Among different non-destructive (ND) techniques that can be useful for the achievement of an advanced knowledge of historic masonry buildings, dynamic testing (successive modal analysis) can be considered a very effective tool. Dynamic properties can be described a structure in terms of its natural characteristics which are the frequency, damping and mode shapes. In the case of masonry historical structures modal analysis may be considered for:

a) Evaluation of dynamic characteristics of structures like natural frequencies, modes, soil structure interaction, damping values, response to wind loads or traffic.

b) Validation of behavioral models in their elastic range, for successive structural (static, wind, seismic…) verifications.

c) Troubleshooting of structures experiencing problems in response like study of bells motion in bell towers, excessive vibration level in structural elements due to traffic and so on.

d) Control systems for structures (monitoring).

e) Checking repairs efficiency which is objective of this research

Considering in situ modal identification tests, there are three groups of experimental techniques: a) the input/output vibration (Operational Modal Analysis) tests that can measure the excitation forces and the vibration response are measured; b) the output/only tests, where only the response of the system is measured, and c) the free vibration tests, where the systems are induced with an initial deformation and then are quickly released.

The characteristics of measurement equipment should be described before discussion about the experimental techniques. This equipment can be generally divided in three groups: a) excitation mechanisms; b) response transducers; and c) data acquisition systems.

2.3.1 Excitation mechanisms

Excitation mechanisms are often preferred to use in dynamic test when the structure could not be under ambient vibrations. The shakers, drop weight systems and impact hammers are frequently used as excitation mechanisms as shown in Figure 4.

Shakers allow user to control both the frequency and force. They are used to study stationary dynamic responses and can induce large forces to the structure. Normally, the application of shakers is expensive and sometimes it is necessary to limit the use of the structure. Moreover, their use demands to stop the function of the structure during the experiment. While the shakers are used for big scale structures like bridges and dams, the impact hammer is frequently used in mechanical engineering structures because it gives sufficient results with for light/medium weight structures. Generally speaking, the exciter is a hammer with a selected tip for different spectral impact energy, coupled with a sensor to measure the impact force (Ramos 2007).Figure 4 shows kind of excitation mechanisms and the differences in spectral response by changing the tips of hammer. For control the

frequency contents of the impacts, the drop weight system could be used due to changing the damping properties and applying higher energy than impact hammers.

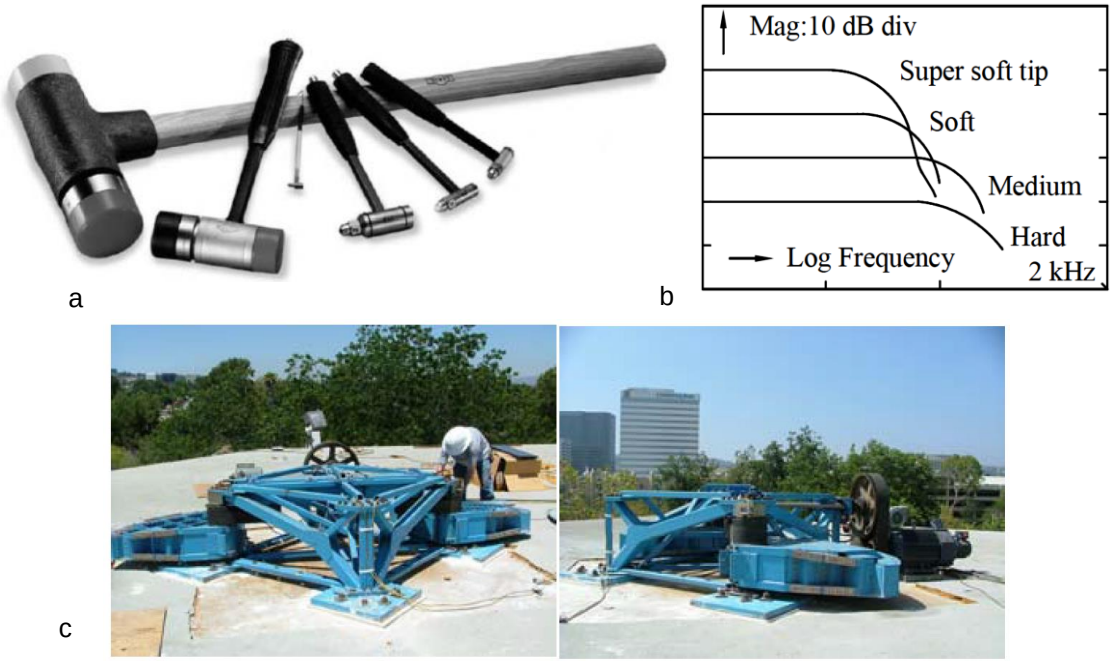

Figure 4 - Impulse hammers (a); Response spectrum depending on the selected tip (b); Eccentric mass shaker (c)

2.3.2 Response transducers

A transducer is kind of equipment able to transform a physic quantity into a proportional electrical signal, that usually defines the system response such as displacements, velocities, accelerations, strains, forces, etc..

In theory, the measure of the dynamic response can be achieved by any of the above physic quantities. However, displacements are better for low frequency response cases, e.g. civil engineering structures, and acceleration measurements are more adequate for higher frequency components, e.g. machinery (Caetano, 2000). In what concerns civil engineering structures, measuring displacements requests all sensors to be related to an external reference point and, often it is costly to do it. Therefore, test equipment based on accelerometers is usually preferred, providing accurate results with relatively low cost. Moreover, it is possible to calculate displacements by numerical integration of the acceleration records (Ramos 2007).

2.3.2.1 Piezoelectric accelerometers

Piezoelectric accelerometer can produce signals proportional to the acceleration of the mass in a frequency band below its resonant frequency and it is spring-mass-damper system. Those kinds of accelerometers require conditioning before starting to record.

The active part of the accelerometer is made of quartz crystals or ceramic materials, which produce an electrical output signal proportional to the acceleration. The principal disadvantage concerns the impossibility of measuring the DC components (0 Hz), like the permanent gravity acceleration g. Compared with others, the piezoelectric accelerometers have the advantages of not using external power source (active transducers), being stable, having a good signal-to noise ratio and being linear over a wide frequency and dynamic range as shown in Figure 5. This kind of accelerometer was used for this research.

Figure 5 - Piezoelectric accelerometer

2.3.2.2 Piezoresistive and capacitive accelerometers

The main advantage of the type is to capture uniform signals which cannot be captured by piezoelectric accelerometers. They are passive accelerometers, in the sense of requiring the supply of energy to measure accelerations and they are more expensive than the piezoelectrics. Also, they are in big size and limited band width with maximum 1000 Hz, Figure 6.

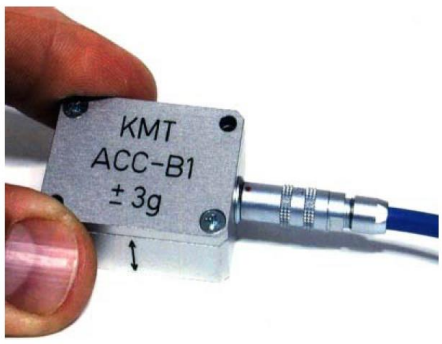

Figure 6 - Piezoresistive accelerometer

2.3.2.3 Force-balance accelerometers

Instead of directly measuring the inertia force exerted upon the mass by detecting its displacement, the force-balance system measures the compensated inertia force, generated by an electromagnetic force transducer, so that the mass of accelerometer moves as little as possible (Pospisil, 2011).

In addition, they are passive and particularly suitable for the measurements in low frequency range and used to test flexible structures and in ambient vibration tests. Also, they are used for the measurement of strong ground motions based on the force-balance principle, Figure 7.

Figure 7 - Force-balance accelerometers

2.3.3 Data acquisition systems

The Data AcQuisition system (DAQ) is used for recording the response signals and the excitation through a discrete-time series. In generally, DAQ converts the analogue data to digital data in discrete-time intervals as can be seen in Figure 8. They increase the resolution and reduce noise by amplifying the low level signals. They are transferred with high-voltage and voltage changes like ground potentials for isolating the transducer signals from computer.

Also, Noise filters are used to increase the measurement accuracy by excluding high frequencies signals that are out of the range of measured system frequencies. In addition, they can excite the transducers when they need external voltage or excitation. DAQ system is responsible of linearization of any nonlinear transducer response during the measurements.

Figure 8 - The Data AcQuisition system (DAQ)

2.4 Identification Methods

As discussed in section 2.3, modal testing has been comparing from viewpoint of the response observation of structure under excitation forces. They can be classified by excitation type in 2 groups; 1- output only (Operational Modal Analysis) identification techniques; 2- input-output identification techniques.

It should be mentioned, input-output identification technique was used in this experiment that will be discussed in chapter 4 and 5.

2.4.1 Output-only identification techniques (Operational Modal Analysis)

This type of modal analysis is done when the excitation forces are not measured. One or more reference (fixed) responses are used, and Cross Spectra or ODS FRFs are calculated instead of FRFs and the excitations are random nature in time and in the physical space of the structure. With devolution windowing, FRF-based curve fitting can be applied to these measurements to estimate operating modal parameters. This technique was used in large civil engineering constructions like bridge, tower and so on because artificial excitations and the determination of forces have been constituted problem. The modal parameters will be obtained very difficult where the modal parameters are estimated by simple peak picking. The frequency or time domains are two main group of this technique. The first group is also called “non-parametric methods” which is based on the signal analysis of each measured point (in frequency domain by the application of the FFTs) and on the correlation between the signals. The second group is “parametric methods” which is based on model fitting by the correlation functions or time history series of every measured point in the time domain. Figure 9 shows the classification of these techniques.

	Method	Characteristics
Frequency Domain	Peak Picking (PP)	Classical SDOF method
	Frequency Domain Decomposition (FDD)	MDOF method; application of SVD to reduce noise
	Enhanced Frequency Domain Decomposition (EFDD)	MDOF method; application of SVD to reduce noise
	Polimax	MDOF method
Time Domain	Random Decrement (RD)	Operates on time domain series, leading to a free decay curve analysis
	Recussive Techniques (ARMA)	Time series modelling using recursive algorithms
	Maximum Likelihood Methods	Stochastic methods based on the minimization of a covariance matrix
	Stochastic Subspace Identification Methods (SSI-DATA)	Stochastic methods based on the project of state vector on a vector of past realizations

Figure 9 - Classification of output-only identification techniques (Caetano, 2000)

2.4.2 Input-Output identification techniques

The response will be measured when the excitation force have been applied. In the other hand, the Frequency Response Function (FRF) will be making a related between excitation force and response with regard to section 2.1 and 2.2. These techniques are based on the control of the input excitation and the measurement of the structural time history response in a set of selected points. In the most of

experiment impact hammers are preferred. However, it can be used in small scale or lightweight structures. They can be applied while the structure is functioning and their implementation is cheap. The modal parameters like natural frequencies, mode shapes and damping coefficients will be calculated by estimating the FRFs or the Impulse Response Functions (IRF). Figure 10 shows the classification of output-input identification techniques.

The simpler tests are those with a single input and a single output measured the so called Single-Input-Single-Output (SISO) identification algorithm. Single input tests have difficulties in inducing all relevant modes and different input locations can be selected, together with different responses treated simultaneously or individually. The first case leads to Single-Input-Multi-Output (SIMO) algorithms, and the second case leads to Multi-Input-Multi-Output (MIMO) algorithms (Ramos 2007).

	Method	Type of formulation	Type of DOF	Type of estimates	Number of inputs/outputs
Frequency Domain	Peak Picking	Indirect (Modal)	SDOF	Local	SISO
	Circle-fit				
	Inverse				
	Dobson				SISO/SIMO
	Nonlinear LSFD		MDOF	Local Global	SIMO MIMO
	Orthogonal Polynomial				
Tuned-sinusoid	Mau		SDOF	Local	SISO
	Asher's		MDOF	Global	MIMO
Time Domain	Complex Exponential		SDOF	Local	SISO
	LSCE		MDOF	Global	SIMO/MIMO
	Ibrahim				MIMO
	ERA				
	ARMA	Direct			

Figure 10 - Classification of input-output identification techniques (Caetano, 2000)

2.4.2.1 Measurement of the FRFs

The frequency response function is very simply the ratio of the output response of a structure due to an applied force. The both applied force and the response of the structure will be misread due to the applied force simultaneously. The measured time data is transformed from the time domain to the frequency domain using a Fast Fourier Transform algorithm.

For instance, the evaluation system of a simple beam with only 3 measurement locations is shown in Figure 11. It can be seen the beam below with 3 measurement locations and 3 mode shapes. There are 3 possible places forces can be applied and 3 possible places where the response can be measured. This means that there are a total of 9 possible complex valued frequency response

functions that could be acquired; the frequency response functions are usually described with subscripts to denote the input and output locations as $h\,(out, in)$ or with respect to typical matrix notation this would be $h(row, column)$ (Peter Avitabile, University of Massachusetts Lowell).

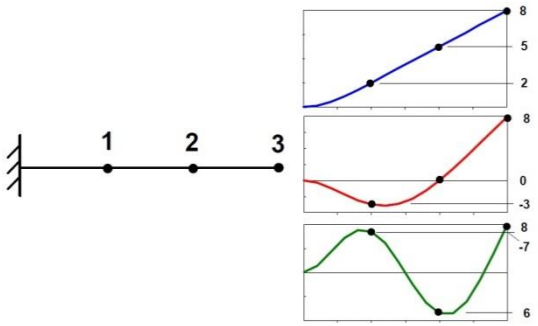

Figure 11 - Beam 3 DOF Model

Figure 12 shows the magnitude, phase, real and imaginary parts of the frequency response function matrix. A complex number is made up of a real and imaginary part which can be easily converted to magnitude and phase. Since the frequency response is a complex number.

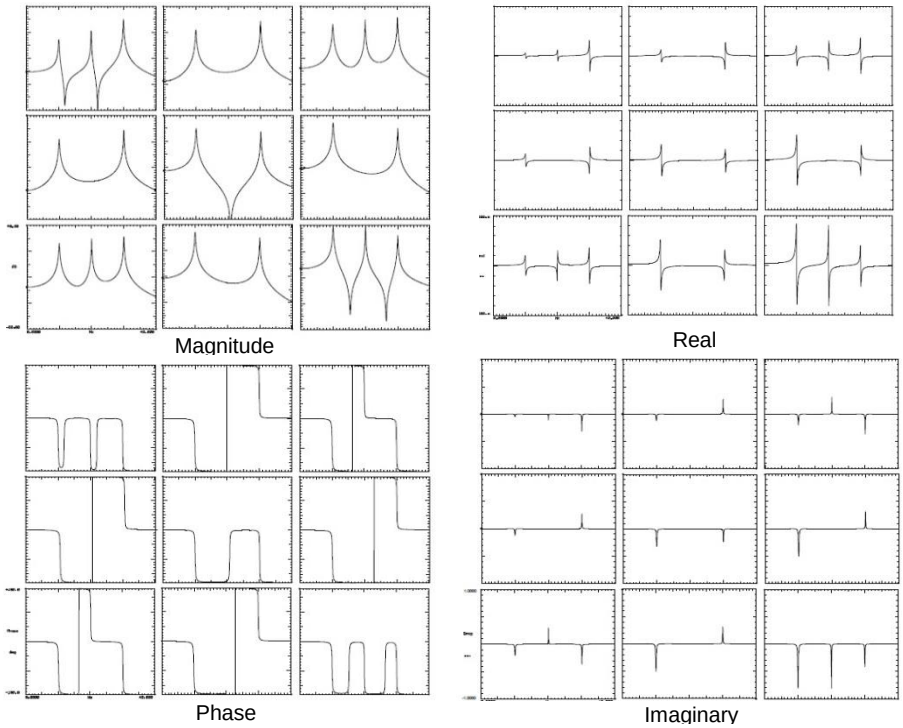

Figure 12 - FRFs of beam 3 DOF Model

It was derived the beam with a force from an impact at the tip of the beam at point 3 and measure the response of the beam at the same location, Figure 13. This measurement is referred to as $h33$. Also, this is a special measurement referred to as a drive point measurement. Some important characteristics of a drive point measurement are: a) All resonances (peaks) are separated by anti-resonances; b) The phase loses 180 degrees of phase as we pass over a resonance and gains 180

degrees of phase as The anti-resonance was passed; c) The peaks in the imaginary part of the frequency response function must all point in the same direction. (Peter Avitabile, University of Massachusetts Lowell)

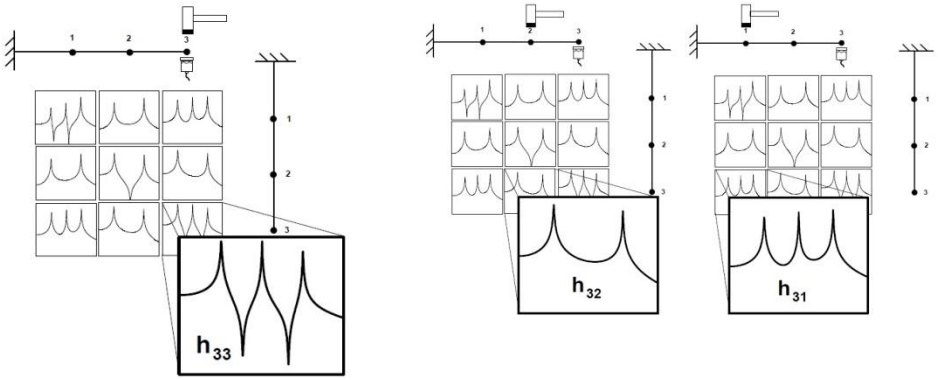

Figure 13 - Drive Point FRF for Reference 3 and Cross FRFs for Reference 3

Regarding (Eq.12) and (Eq.22), the first definition of the FRFs having the measured response time history $y(t)$ in the i degree of freedom and of the excitation time history $u(t)$ on the j degree of freedom, the FRF $H_{(i,j)}(\omega)$ can be calculated directly from the application of the FRFs to the time histories in theory by (Caetano, 2000):

$$H_{(i,j)}(\omega) = \frac{H_i(\omega)}{U_j(\omega)} \qquad \text{Eq.23}$$

where U and Y are the Fourier spectrums of the excitation and the response signals, respectively.

With regard to cross-spectra density functions between the excitation force and the response, another process to calculate $H(i,j)(\omega)$ is through the stochastic input-output relations, $S_{(i,j)}(\omega)$, and the Power Spectra Density (PSD) functions of the response or the excitation, $S_{(i,i)}(\omega)$ and $S(j,j)(\omega)$, respectively, where the following relations can be observed:

$$H_{(i,j)}(\omega) = \frac{S_{(i,j)}(\omega)}{S_{(j,J)}(\omega)} \qquad and \qquad \left|H_{(i,j)}(\omega)\right| = \frac{S_{(i,j)}(\omega)}{S_{(j,J)}(\omega)} \qquad \text{Eq.24}$$

Once the measurements are discrete in time with Δt spacing, the above equations can only be estimated at discrete frequency values ω on a frequency spacing $\Delta\omega$ defined by the sampling frequency fs given by (Eq.24) and the number of samples N in the time history by (Eq.25):

$$f_s = \frac{1}{\Delta t} \geq 2 \times f_{Nyq} \quad \leftrightarrow \quad f_s \geq 2 \times f_{max} \qquad \text{Eq.25}$$

$$\Delta\omega = \frac{2\pi}{N f_s} \qquad \text{Eq.26}$$

and the FRFs are then calculated as estimation of the real values by (the superscript ^ denotes estimate):

$$\widehat{H}_{(i,j)}(\omega) = \frac{\hat{S}_{(i,j)}(\omega)}{\hat{s}_{(j,J)}(\omega)} \qquad and \qquad \left|\widehat{H}_{(i,j)}(\omega)\right| = \frac{\hat{S}_{(i,j)}(\omega)}{\hat{S}_{(j,J)}(\omega)} \qquad \text{Eq.27}$$

$$\widehat{H}_{(i,j)}(\omega) = \frac{\hat{Y}_{(i,j)}(\omega)}{\widehat{U}_{(j,J)}(\omega)}$$

where every spectrum $S_{(X1,X2)}$ is given by the following expression:

$$\widehat{H}_{(i,j)}(\omega) = \frac{\hat{S}_{(i,j)}(\omega)}{\hat{S}_{(j,j)}(\omega)} \qquad \text{Eq.28}$$

(Ramos, 2007)

3. PROPERTIES OF MATERIALS AND INSTRUMENTS

For this experimental research, fifteen masonry walls were constructed as specimens. The instruments for modal testing, properties of the materials and the components of the structural strengthened that have been used in the constructions and experiment are described in this chapter. Also, the properties of bricks and mortar have evaluated from previous experiment in LITEM laboratory of the Polytechnic University of Catalonia.

3.1 FRP

The MBrace® Laminate System is a Carbon Fiber Reinforced Polymer (FRP) system for structural strengthening of masonry, concrete, steel and timber structures. MBrace® Laminate is a ready to use pultruded[1], carbon fiber laminate, normally externally bonded to structures, to provide additional load bearing capacity. It provides a lightweight, high tensile strength material (higher than steel reinforcement used in the concrete industry) and is largely utilized for additional flexural reinforcement of masonry, concrete, steel and timber members. Table 1 and Figure14 show the data of FRP.

Table 1 - Properties of FRP

MBrace® Laminate (Grade)	170/3100
Mean Tensile strength (MPa)	3100
Mean Tensile modulus E (GPa)	170
Laminate Width (mm)	80
Laminate Thickness (mm)	1.2
Ultimate Elongation (at break)	1.6%
Fiber content (%)	70
Density (g/cm^3)	1.6
Inter Laminar Shear Strength (MPa)	80
Thermal Expansion (m/m/°C)	0.6×10^{-6}

[1] **Pultrusion** is a continuous process for manufacture of composite materials with constant cross-section. Reinforced fibers are pulled through a resin, possibly followed by a separate preforming system, and into a heated die, where the resin undergoes polymerization.

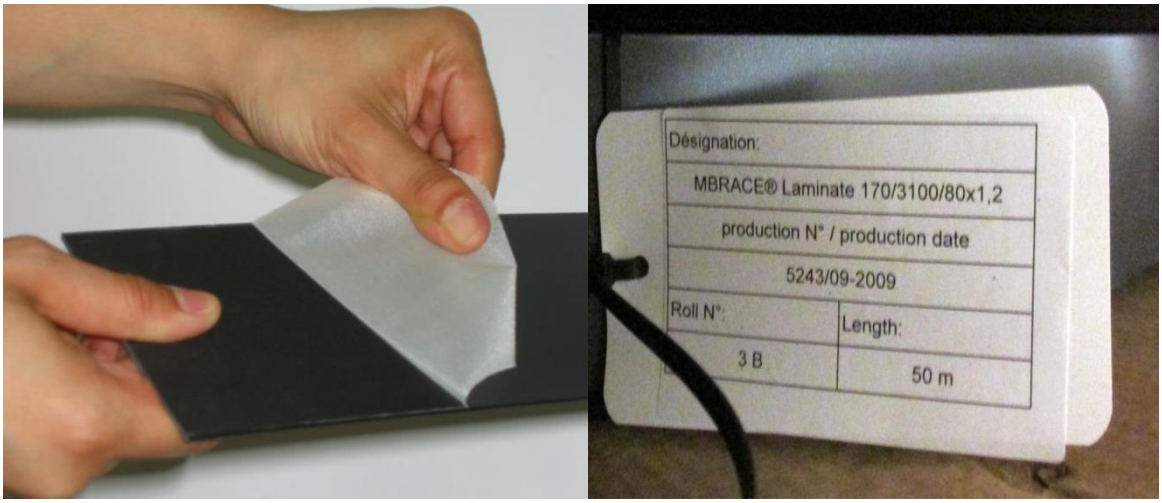

Figure 14 - Performance of used FRP

3.1.1 Preparation of substrate

The surfaces of elements should be sanded down and left clean and dry. With degraded structures, the whole damaged area should be removed by scarifying, hydro-demolition or similar, and then structural restoration would be carried out with mortar. Remove oils, grease, dust or any other loose material from the surface and leave dry.

3.1.2 Application

To ensure maximum adhesion, one coat of MBrace® Primer would be applied by roller or brush. If necessary, a coat of MBrace® Laminate Adhesive should be applied by using a putty knife, to fill any blow holes or imperfections to the masonry surfaces. Also, the protective peel-ply film from one surface of MBrace® Laminate would be removed to be adhered. If the type of Laminate is being used does not have a peel-ply surface, and then wipe clean the Laminate surface with a suitable solvent. The layer of MBrace® Laminate Adhesive should be applied 1–1.5 mm thick on both the surfaces (masonry and Laminate). After applying Adhesive on the Laminate, the minimum of 1 mm thick at each side, and 2 mm thick at the canter should be occurred by using a spatula. Finally, any excess MBrace® Laminate Adhesive (and air) from under the Laminate must be expelled and leaving a nominal 1-3 mm layer of adhesive.

3.2 Primer

MBrace® Primer is a low viscosity, 100% solids, polyamine cured epoxy. As the first applied component of the MBrace® System, it is used to penetrate the pore structure of cementitous substrates and to provide a high bond base coat for the MBrace® System. MBrace® Primer is based on a unique adduct curing technology that results in tolerance for surface moisture and for temperatures down to 35 °F (2 °C). MBrace® Primer is the first component of the MBrace® System

that is applied to concrete, steel and masonry substrates in vertical, horizontal, exterior and interior locations. MBrace® Primer is used to provide excellent adhesion of the MBrace® System to the substrate. The data and sample of prime are shown in Table 2 and Figure 15.

Packing		**Compressive Properties**	
Part A (liter)	2.85	Yield Strength (MPa)	26.2
Part B (liter)	0.95	Strain at Yield (%)	4
Handling Properties		Elastic Modulus (MPa)	670
Mixed Weight (g/L)	1103	Ultimate Strength (MPa)	28.3
Mixed Viscosity at 25 °C (cps)	400	Rupture Strain (%)	10
Physical Properties		**Flexural Properties**	
Installed Thickness (approx) (mm)	0.075	Yield Strength (MPa)	24.1
Density (kg/m3)	1102	Strain at Yield (%)	4
Tensile Properties		Elastic Modulus (MPa)	595
Yield Strength (MPa)	14.5	Ultimate Strength (MPa)	24.1
Strain at Yield (%)	2	Rupture Strain (%)	0
Elastic Modulus (MPa)	717	**Functional Properties**	
Ultimate Strength (MPa)	17.2	CTE (1/°C)	35.10^{-6}
Rupture Strain (%)	40	Thermal Conductivity (W/m·°K)	0.2
Poisson's Ratio	0.48	Glass Transition Temp (°C)	77

Table 2 - Properties of primer

Figure 15 - Performance of used primer

3.3 Adhesive

Product MBrace® ADHESIVE LAMINATE should be applied on both the surfaces of primed masonry and Laminate. The main adhesive will be combined from 2 parts and the layer thick of MBrace® Laminate Adhesive would be 1–1.5 mm. Also, applying the adhesive over the primer should not be

earlier than 90 minutes. For Mixing 2 parts of adhesive, the second part should be added to the part one. Then, the mixing should be occurred intensely with drill equipped and a stirrer at 400 rpm maximum rotation speed for 3 minutes until the mixed would be reached consistency. Not recommended in any case partial mixtures. The adhesive will be used approximately 1.7 Kg/m2/m. Table 3 and Figure 16 are presented the sample and properties of MBrace® LAMINATE ADHESIVE HT for structural reinforcement with FRP laminate.

Diagonal shear strength until 50 °C (MPa)	50
Bonding strength (MPa)	14
Shear strength (MPa)	12
Workability at 23 °C (min)	90
Workability at 30 °C (min)	35
Pot Life at 23 °C (min)	60
Pot Life at 30 °C (min)	60
Full Cure at 23 °C (day)	4
Elastic Modulus (GPa)	2

Table 3 - Properties of MBrace® LAMINATE ADHESIVE HT for structural reinforcement with FRP

Figure 16 - Performance of used adhesive

3.4 Bricks

The average dimensions of bricks in the masonry walls were 265 mm × 125 mm × 50 mm and the diagrammatical shape of them are shown in the Figure 17. Also, the average properties of brick are presented in Table 4.

- The compressive strength of the brick was determined according to the test procedure in BS EN 772-1:2000, with a few modifications. The specimen size used was half the brick.
- The water absorption capacity of the bricks in dry and wet conditions was determined according to the test procedure in BS EN 772-11:2000.
-

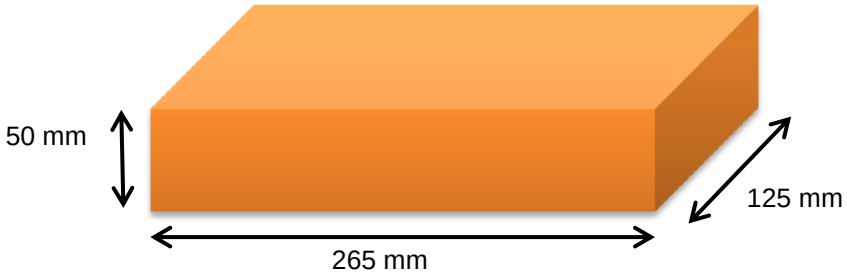

Figure 17 - Average dimensions of bricks

Property	Value
Tensile strength, f_{tb}	6.0 Mpa
Compressive strength, f_{cb}	27.93 Mpa
Water absorption(wet)	0.65 mg/mm^2.min

Table 4 - Properties of the bricks

3.5 Mortar

The compressive and flexural strength of the specimens was determined according to the test procedure in BS EN 1015-11:1999/A1:2006. The size of the mortar prisms used in the flexural tests was 160mm x 40mm x 40mm and for the compressive tests, the specimen size was half the size of these prisms. Mortar used was Durland of grade M7.5. The values of the compressive and flexural strength can be seen in Table 5.

Property	Value
Flexural strength	1.2 Mpa
Compressive strength, f_{cm}	3.3 Mpa

Table 5 - Properties of the mortar used in the joints

3.6 Masonry

The fifteen brickwork masonry walls were constructed and according to the tests the compressive, tensile strength and Young's modulus are presented in Table 6.

Property	Value
Tensile strength, f_{tm}	0.36 Mpa
Compressive strength, f_{cm}	10.8 Mpa
Young's modulus	780 Mpa

Table 6 - Properties of constructed brickwork walls

3.7 Data Acquisition System (DAQ)

From the general overview was discussed in the chapter two, the dynamic tests were on base of input-output experimental modal identification tests with one accelerometer and hammer.

3.7.1 Hardware and software

For data acquiring, an input-output hardware model 3050-B-060 with 6 channels and frequency range of 0 Hz to 51.2 kHz from Brüel&Kjær Company was used, Figure 18. Also, the impacts, coherence of impacts and Fast Fourier Transform (FFT) were controlled among tests by Brüel&Kjær-PULSE LabShop software.

Figure 18 - Hardware of Data Acquisition System

3.7.2 Accelerometer and hammer

In experimental modal analysis of brickwork walls, one accelerometer model 4370 V Brüel&Kjær was used. Table 7, Figure 19 and Figure 20 are shown its characteristics. Mounting was achieved by using the threaded steel studs and self-adhesive mounting discs, supplied as accessories.

Also, one hammer model 8206-003-55103 of Brüel&Kjær Company was used as input in modal analysis that is shown in Figure 21.

Model of accelerometer	4370 V - Brüel&Kjær
Refrence sensitivity at 159,2 Hz (ω=1000s^{-1}), 20 ms^{-2} and 23 ºC)	10,11 pC/ms^{-2} (99,2 pC/g)
Lower Frequency Limit	Determined by the amplifier used
Upper Frequency Limit (+10%)	4.8 kHz
Mounted Resonance Frequency	16 kHz
Calculated values for TEDS	
Resonance Frequency	17.9 kHz
Quality factor	18

Table 7 - Characteristic of accelerometer

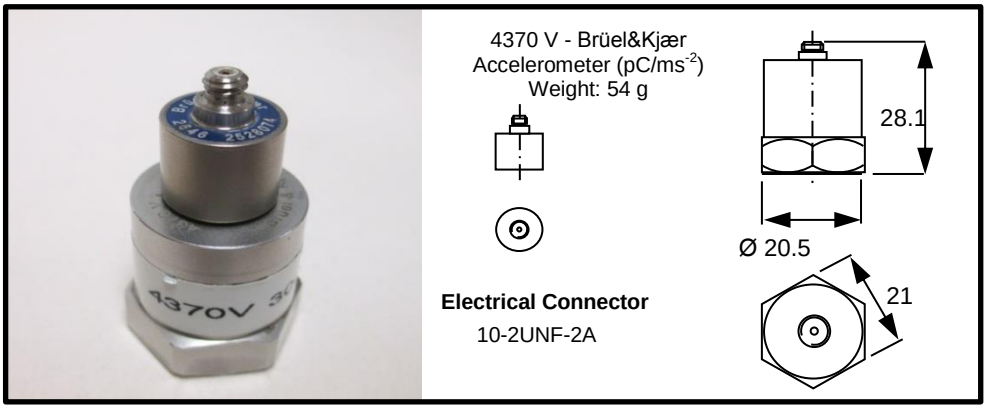

Figure 19 - Characteristic of accelerometer

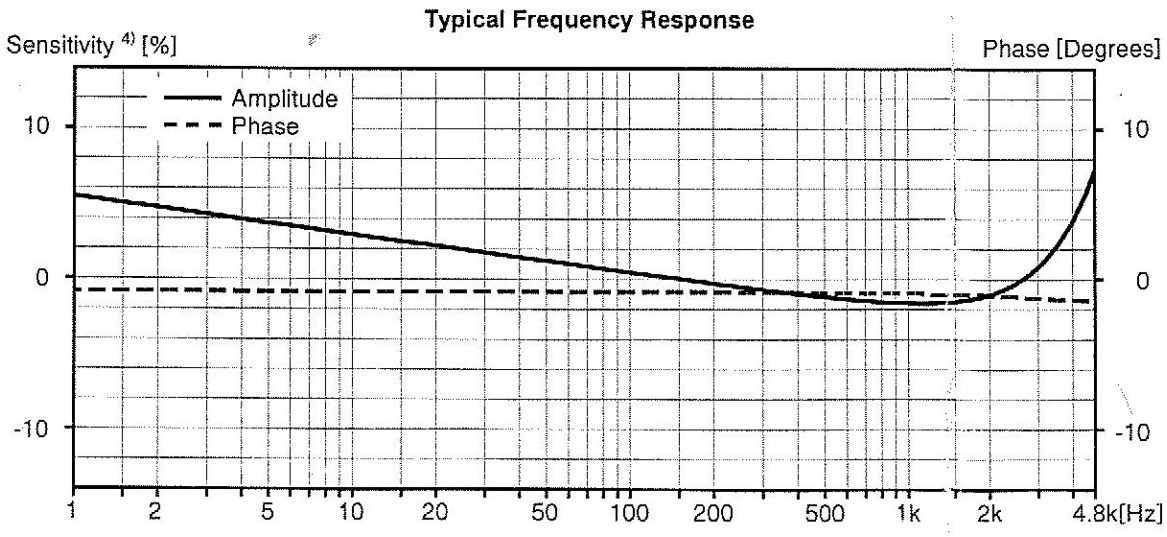

Figure 20 - Sensitivity and errors of accelerometer

Figure 21 - Hammer used in test

4. EXPERIMENTAL PROCEDURE

This chapter presents the processes in construction of the fifteen walls, modal testing before and after strengthening of specimens and the method of strengthening. For comparison specimens, five different patterns of FRP were used. Due to having one accelerometer, one specimen is tested again with different position of accelerometer. Then 32 tests were occurred totally.

4.1 Constructing the walls

For the comparison of five different patterns of FRP, the team of research decided to construct three brickwork walls for each patterns and fifteen walls totally. At first, the steel supports were provided in the same shape and dimension. Then, between two to three centimeters layer of mortar was used on side of wetted supports. The class and type of mortar used was M 7.5 but from the last experiment in LITEM laboratory that is mentioned in pervious chapter, the compressive strength of mortar was found 3.3 MPa. The required quantity of mortar was taken in a trough and mixed manually with water like other usual of fabrication in masonry field and the workers waited around 5 to 10 minutes to use the reached mortar, Figure 22.

Figure 22 - Preparing the mortar for building the walls

Also, the bricks were wetted with soaking them in dish of water and then they were put in open air to use for laying in rows.

The first brick row with full and half bricks was laid on the mortar which was on support and then another layer of mortar is applied on top of that. Two markers with one centimeter height are placed at diagonally opposite corners of the brick to control the uniform depth of the joints as shown on the Figure 23. Then, following one after another brick is put down in the layer of mortar and tapped down until the level and one centimeter thickness of joints are achieved. Also, the extra mortar was trimmed with the edge of the trowel which was come out from between the two bricks and then the spirit-level was used to control and ensure about the level and plumb of bricks.

Figure 23 - Controlling the uniform depth of the joints

This procedure is used to lay the successive 25 brick rows with checking of alignment to ensure that the walls are straight. However, three specimens were built with 24 brick rows that they were strengthened in 3V5H pattern. Figure 24 shows the process of construction of the wall specimens.

Figure 24 - Process construction of the wall specimens

Finally and after building the complete wall, the sides were cleaned with a brush to remove extra mortar and to ensure that surface which the FRP and primer will be applied is clean and regular. Though, the cleaning happened again before the applying the FRP because the FRP laminate and primer were too sensitive to stick to walls completely. Then, the fifteen brickwork walls were left for 146 days in open air condition but they were under big and high roof from ground. The brickwork walls were constructed between 18th and 20th of December, 2012 outside the LITEM laboratory at the UPC Campus of Terrassa. Also, it should mention these work were carried out in average 6 to 14 centigrade temperature and 64% to 81% humidity. The place and condition of completed walls are shown in Figure 25.

Figure 25 - The place and condition of completed walls

4.2 Transferring and setting up the specimens in the LITEM laboratory of UPC

The wall specimens were transferred from outside, place of preparation, to inside of LITEM laboratory by a stacking machine and two persons. Also, the specimens and their supports are fixed again completely with some pieces of steel to avoid kind of sliding as shown in Figure 26. In among of this experiment, we learned how to arrange the specimens for future experiments, the minimum space between walls are equal maximum height of walls. By the way, wall arrangement was not ideal because there could be domino effect if some wall had been fallen down accidentally. However, there was not enough space to setup another arrangement. This is shown in Figure 27. Also, the walls were not transported until the last part of process to have same boundary condition before and after strengthening.

Figure 26 - Transporting and setting up the specimens in the laboratory

Figure 27 - The arrangement of walls in the laboratory

4.3 Measuring and dimensions

The walls were measured with using measuring tape, scale and caliper. The average of three readings from top, bottom and middle of each parameter of walls were assumed as final dimension. Also, the dimension and the values are presented in Table 8 and the measuring the dimensions of the walls and instruments are shown in Figure 28.

It should be pointed it out the walls were numbered with patterns of FRP to avoid confusing situation about number of tests that will be explained in section 5.2.

Number	Height (cm)			Average	Width (cm)			Average	Thickness (cm)
2V0H-1	158.70	158.60	158.90	158.73	83.70	83.80	83.60	83.70	12.50
2V0H-2	161.00	160.90	160.90	160.93	84.10	83.70	83.40	83.73	12.50
2V0H-3	158.60	159.40	159.20	159.07	84.10	84.00	83.30	83.80	12.40
3V0H_1	160.00	160.30	160.20	160.17	82.50	82.60	82.50	82.53	12.60
3V0H_2	160.20	160.20	160.20	160.20	83.30	83.20	83.40	83.30	12.50
3V0H_3	161.20	161.20	161.30	161.23	83.30	83.40	83.20	83.30	12.40
2V2H_1	157.90	157.80	157.90	157.87	83.50	83.70	83.70	83.63	12.50
2V2H_2	158.70	159.10	158.90	158.90	83.40	83.60	83.50	83.50	12.50
2V2H_3	159.20	159.20	159.10	159.17	82.60	82.60	82.50	82.57	12.50
3V5H_1	157.70	157.30	157.50	157.50	82.90	83.50	83.00	83.13	12.40
3V5H_2	157.80	158.10	158.00	157.97	83.10	83.00	82.50	82.87	12.60
3V5H_3	155.10	155.20	155.20	155.17	83.00	82.90	82.80	82.90	12.50
3I3I_1	162.50	162.60	162.50	162.53	82.50	82.50	82.50	82.50	12.50
3I3I_2	162.00	162.20	162.40	162.20	83.60	83.40	82.30	83.10	12.50
3I3I_3	160.80	160.80	160.80	160.80	83.10	83.00	83.10	83.07	12.60

Table 8 - Dimensions and number of walls

Figure 28 - Measuring the dimensions of the walls

4.3.1 Dimensions of grids for Modal Testing

Before starting the process of modal testing, it was decided to have similar mesh on surface of walls because one purpose of this experiment was about the comparison the mode shapes in same patterns of FRP. So it was needed to prepare similar mesh in different walls with minimum difference of dimension to measure frequency and damping of walls.

In all walls except 3V5H pattern, two rows of bricks from bottom and two rows from top were left because first row was inside of supports (bottom in this experiment and top in next experiment) as seen in Figure 29. Also, location of mortar between two bricks in the even rows should be made problem about impact of hammer. It was needed to smooth surface for impacting hammer of modal testing and establish a formula to pass even rows.

Figure 29 - Supports in top of walls for next experiment

Vertical grids: finally, 21 rows were reminded which were estimated 11 vertical grids with these distances in Table 9 and Figure 30 from this formula.

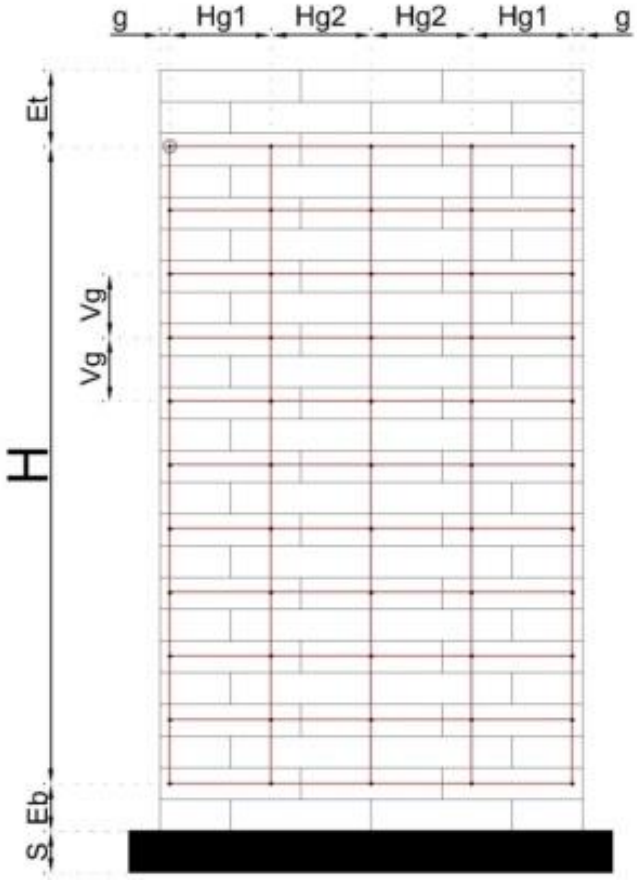

Figure 30 - Typical measuring of grids and walls

$$Vg = \frac{H}{\left(\frac{(Nb-1)}{2}\right)} \quad \text{Eq. 29}$$

H: Height of total mesh (center to center of rows of brick, 3rd from top and 3rd from down)

V_g: Distance of vertical points

N_b: Number of rows

	Number of brick rows	Height of total mesh	Distance of vertical grids
Number	Nb	H (cm)	Vg (cm)
2V0H-1	21	126.10	12.61
2V0H-2	21	128.17	12.82
2V0H-3	21	125.87	12.59
3V0H_1	21	127.33	12.73
3V0H_2	21	127.03	12.70
3V0H_3	21	127.70	12.77
2V2H_1	21	125.27	12.53
2V2H_2	21	127.03	12.70
2V2H_3	21	126.30	12.63
3V5H_1 *	21	130.17	13.02
3V5H_2 *	21	130.83	13.08
3V5H_3 *	21	128.13	12.81
3I3I_1	21	128.97	12.90
3I3I_2	21	129.13	12.91
3I3I_3	21	128.13	12.81
*: These walls have just 24 rows. Therefore, center to center of rows of brick are started from 2nd brick row from up to 3rd brick row from down			

Table 9 - Dimensions of vertical grids

Horizontal grids: 2 centimeters from right and left side in each wall are remained, symbolized g, because the mesh of modal testing need to be rectangular exactly for comparison of results in behavior of mode shapes. Then, 20 centimeters (H_{g1}) are separated from both sides of surface. The reminded distance was divided per two parts that are called H_{g2}. The measurements of the specimens can be seen in Table 10.

	Real width	Tolerance of edge	First-Fixed distance	Distance of horizontal points
Number	Width (cm)	g (cm)	Hg1 (cm)	Hg2=(b-44)/2 (cm)
2V0H-1	83.70	2.00	20.00	19.85
2V0H-2	83.73	2.00	20.00	19.87
2V0H-3	83.80	2.00	20.00	19.90
3V0H_1	82.53	2.00	20.00	19.27
3V0H_2	83.30	2.00	20.00	19.65

3V0H_3	83.30	2.00	20.00	19.65
2V2H_1	83.63	2.00	20.00	19.82
2V2H_2	83.50	2.00	20.00	19.75
2V2H_3	82.57	2.00	20.00	19.28
3V5H_1	83.13	2.00	20.00	19.57
3V5H_2	82.87	2.00	20.00	19.43
3V5H_3	82.90	2.00	20.00	19.45
3I3I_1	82.50	2.00	20.00	19.25
3I3I_2	83.10	2.00	20.00	19.55
3I3I_3	83.07	2.00	20.00	19.53

Table 10 - Dimensions of Horizontal grids

Finally, eleven rows and five columns are calculated and drawn in each walls with color thread. Also, for controlling the error of drawing, the meshes are measured and compared with calculated mesh. The maximum error was around 3 millimeters. In addition, it should be mentioned, it is better to do the meshing from center to edges in historical elements but here the walls are made exactly from first step and the maximum error is around 2 mm that is so exact for this kind of testing.

4.4 Modal Testing before strengthening

The dynamic tests performed are input-output experimental modal identification tests as it is stated in chapter 2. The tests consist of fixing the sensor (accelerometer), recording the response of the structure to successive impacts of hammer from first to last point and finally using the Data Acquisition (DAQ) equipment with its software. Also, the factors such as types of the data to be acquired, number and locations of impacts, dynamic range, power and processor/memory requirements, sampling intervals and etc. should be considered.

4.4.1 Location of accelerometer

As there was only one accelerometer, it was decided to place accelerometer at top in left side of all walls because of its high amplitude, maximum displacement and contribution in each mode. The position of accelerometer is important to avoid the locations of zero displacement for each mode of vibration of walls. Moreover, two tests were carried out with different position of accelerometer in one specimen (2V2H_1) to compere discrepancy of left and right side locations that would be explained in section5.2.1. Figure 31 shows the arranged position of the accelerometers on wall specimens. One setup and 55 points were decided to be measured for each specimen. In addition, the coordinate system of axis had been located in point number 11 as shown in Figure 32. Also, the impact was carried out in X direction to simulate the load-bearing walls (here is self-weight) plus horizontal forces.

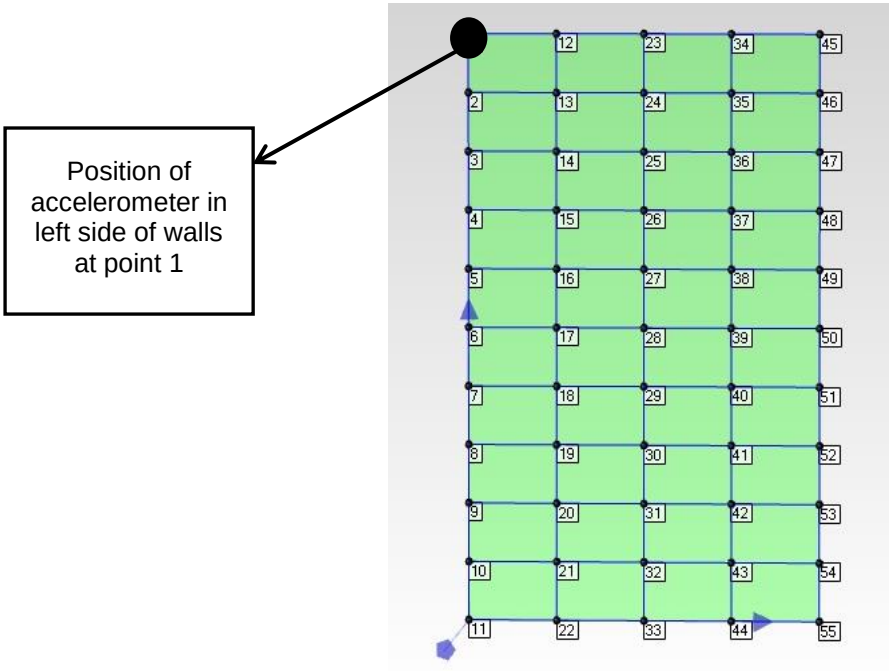

Figure 31 - Position of accelerometer on wall specimens

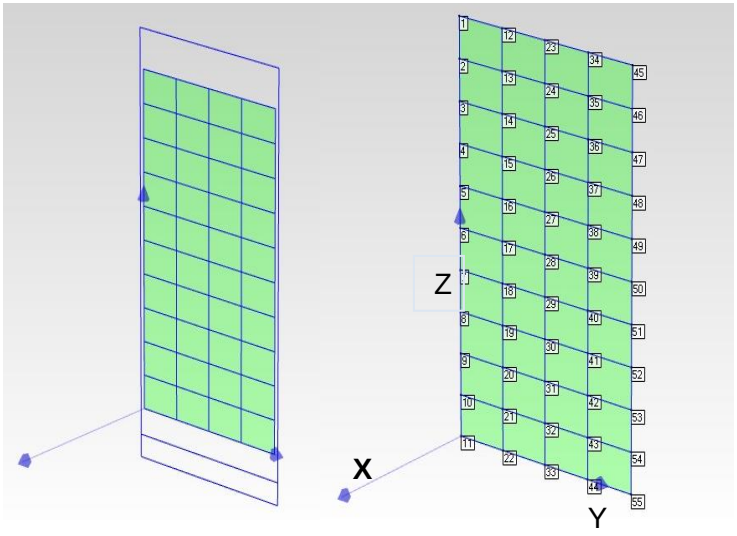

Figure 32 - The numbers of point and coordinate system of axis in each specimen

4.4.2 Setup the Data Acquisition System and software

As it is discussed in chapter 2 and 3 about the Data Acquisition System (DAQ), Table 11 tabulates the instrumentation and test settings used for the modal testing. For each point, two Fast Fourier Transform (FFTs) were measured. The wall was excited by applying a horizontal impact by hammer. In each point, the 2 impacts were applied every 3.2 seconds at same points on wall and frequency response function (FRF) is computed for each point, Figure33. A standard modal analysis was performed on the collected data. The set of transfer functions and modal parameters for the structure are extracted.

Data Acquisition System	Software	Domain of span (Hz)	Range of frequency (mHz)	Time (s)	Numbers of impacts
3050-B-060 Brüel&Kjær	PULSE LabShop Brüel&Kjær	500	312.5	3.2	2

Table 11 - The settings of DAQ system

Figure 33 - Applying 2 horizontal impacts by hammer in each point

4.4.3 Calibrating the errors

To avoid errors and calibrate the specimens, measurements were taken for 4 seconds between 2 hammer impacts in each point. In addition, coherence of 2 hammer impacts was checked among test with PULSE LabShop Brüel&Kjær software and sometimes the impacts were repeated 2 until 5 times to find best coherence that is presented in Figure 34 and Figure 35. Moreover, the coherence function is used as a data quality assessment tool which identifies how much output signal remains in comparistonto the measured input signal. Also, if rebound condition had been happened by hammer, the impacts were repeated to avoid errors in FRFs. Figure 36 shows the sample of rebound situations. Furthermore, the sensitivity of range of frequency (mHz) has been setup 0.3125 Hz meanwhile the minimum variation before and after strengthening was around 2 Hz as can be seen in chapter 5. Also, it was tried that the tests were carrying out in silent time of laboratory during the experiment to avoid influence of any noise.

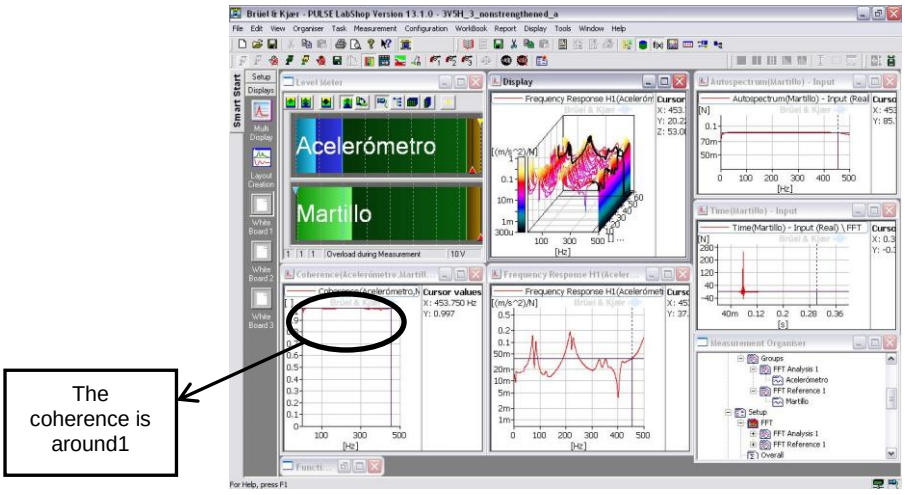

Figure 34 - The best coherence for 2 impacts in each point

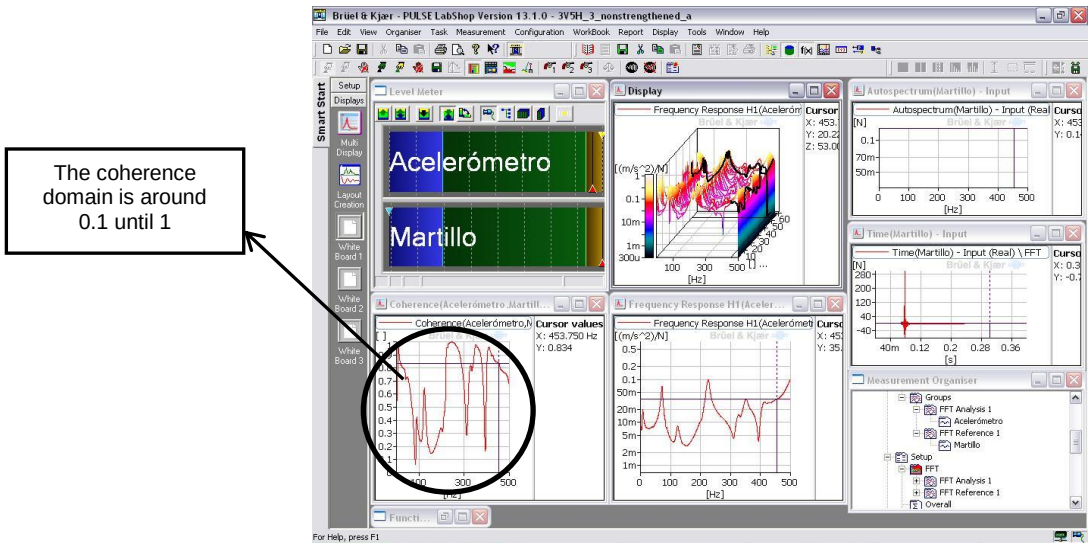

Figure 35 - The worst coherence for 2 impacts in each point

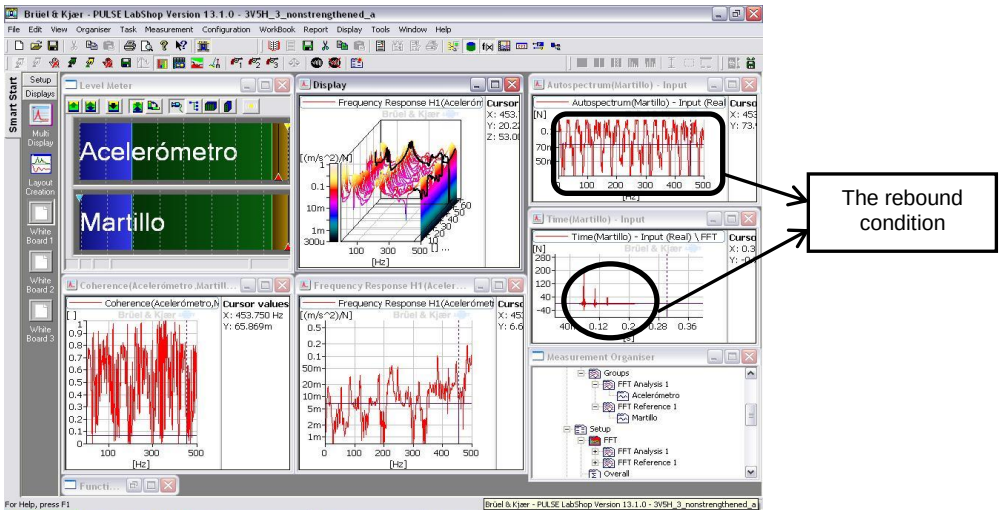

Figure 36 - Rebound condition in hammer impact

4.4.4 Obtaining the Frequency Response Spectrum and Function (FRF) before strengthening

Figure 37, Figure38 and Figure 39 are shown examples of the results of frequency versus Real, Imaginary and Magnitude for test 2V0H_1_nonstrengthened_a in points 1, 2, 55 and all points. By performing the Fast Fourier Transform (FFT) analysis, the results are transformed from the time domain to the frequency domain, which are called frequency response function (FRF). The frequency values can be obtained by picking up the peaks of the FRSs shape that would be discussed in next chapter.

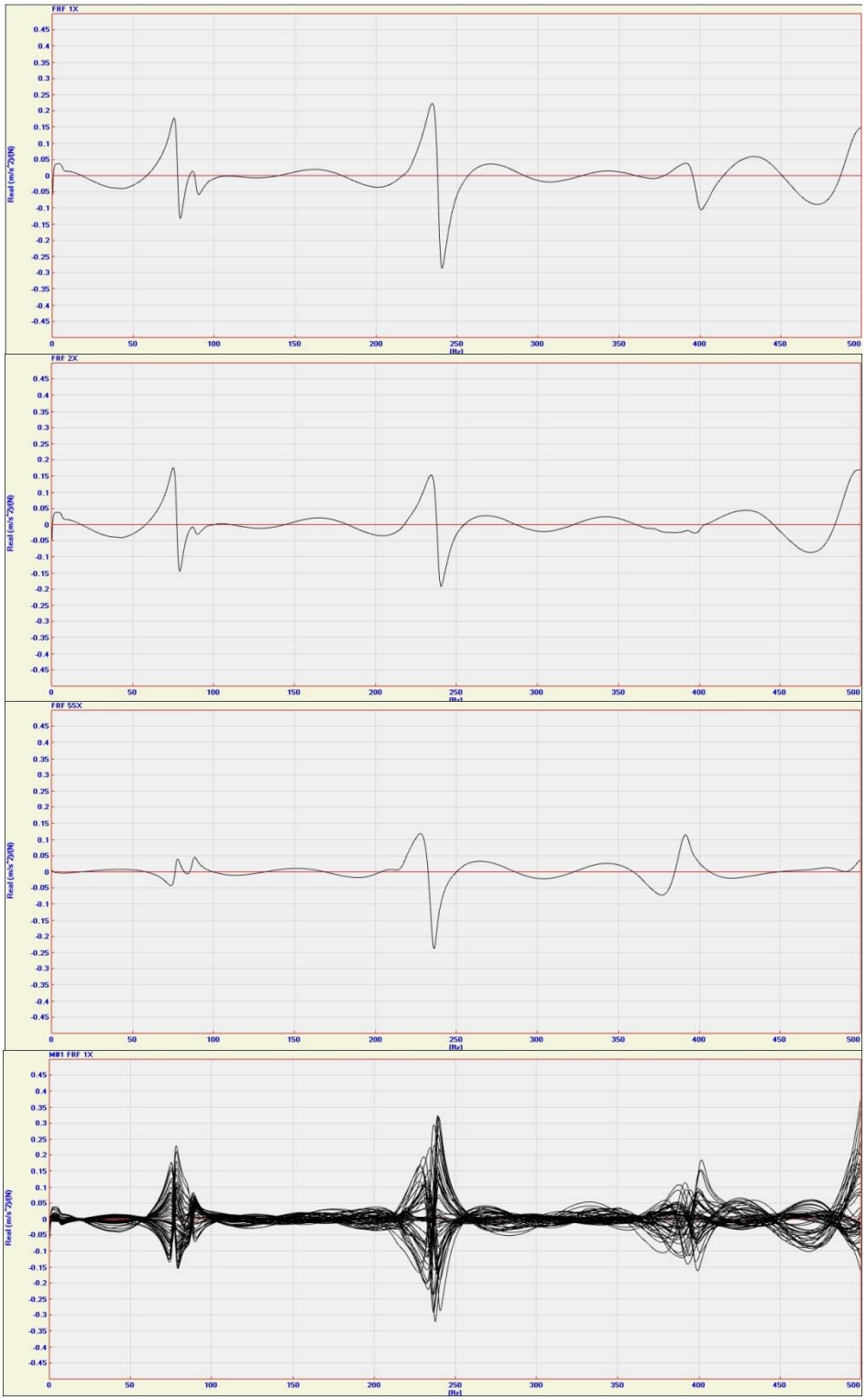

Figure 37 - Results of Frequency versus Real for test 2V0H_1_nonstrengthened_a in points 1, 2, 55 and all points

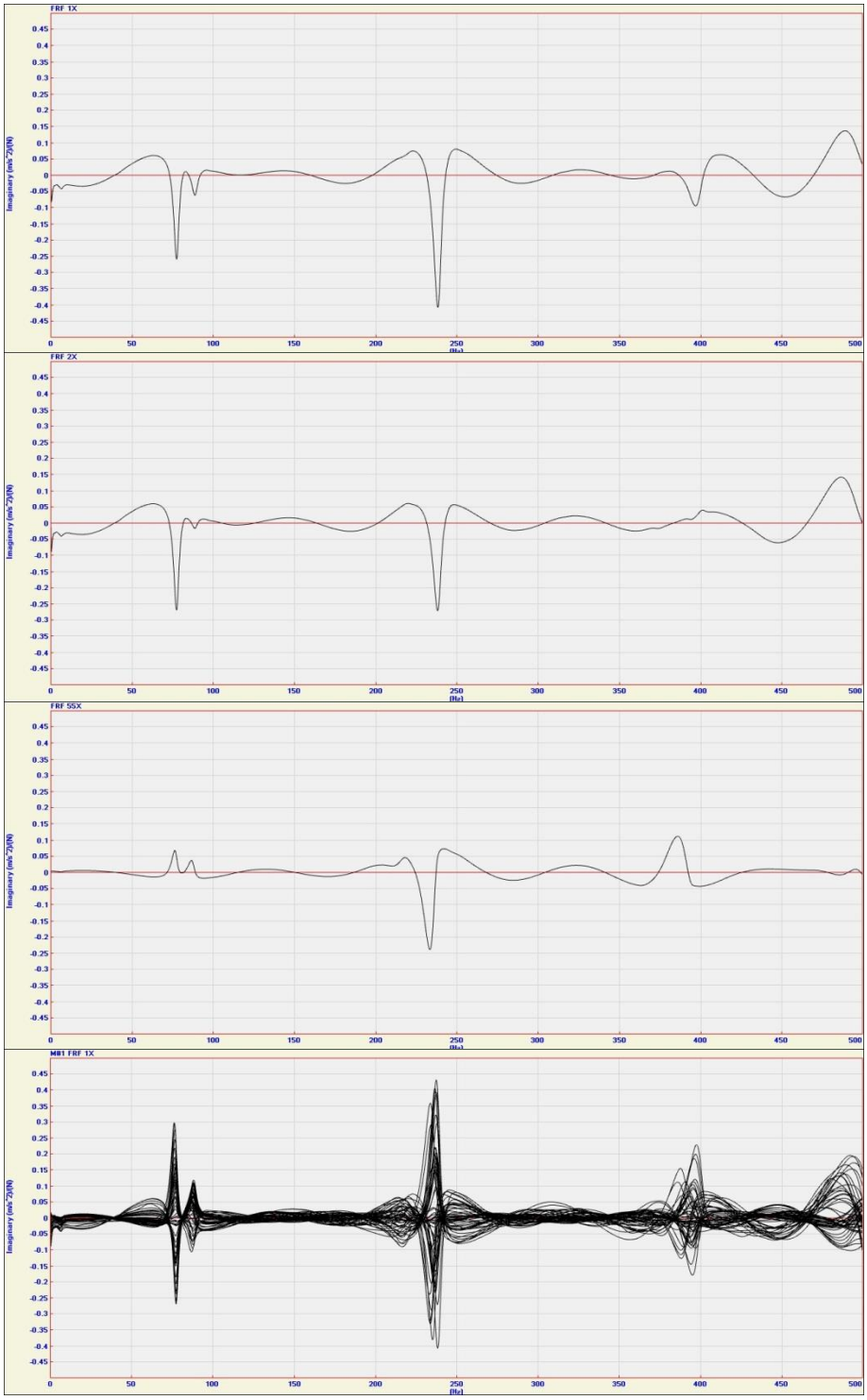

Figure 38 - Results of Frequency versus Imaginary for test 2V0H_1_nonstrengthened_a in points 1, 2, 55 and all points

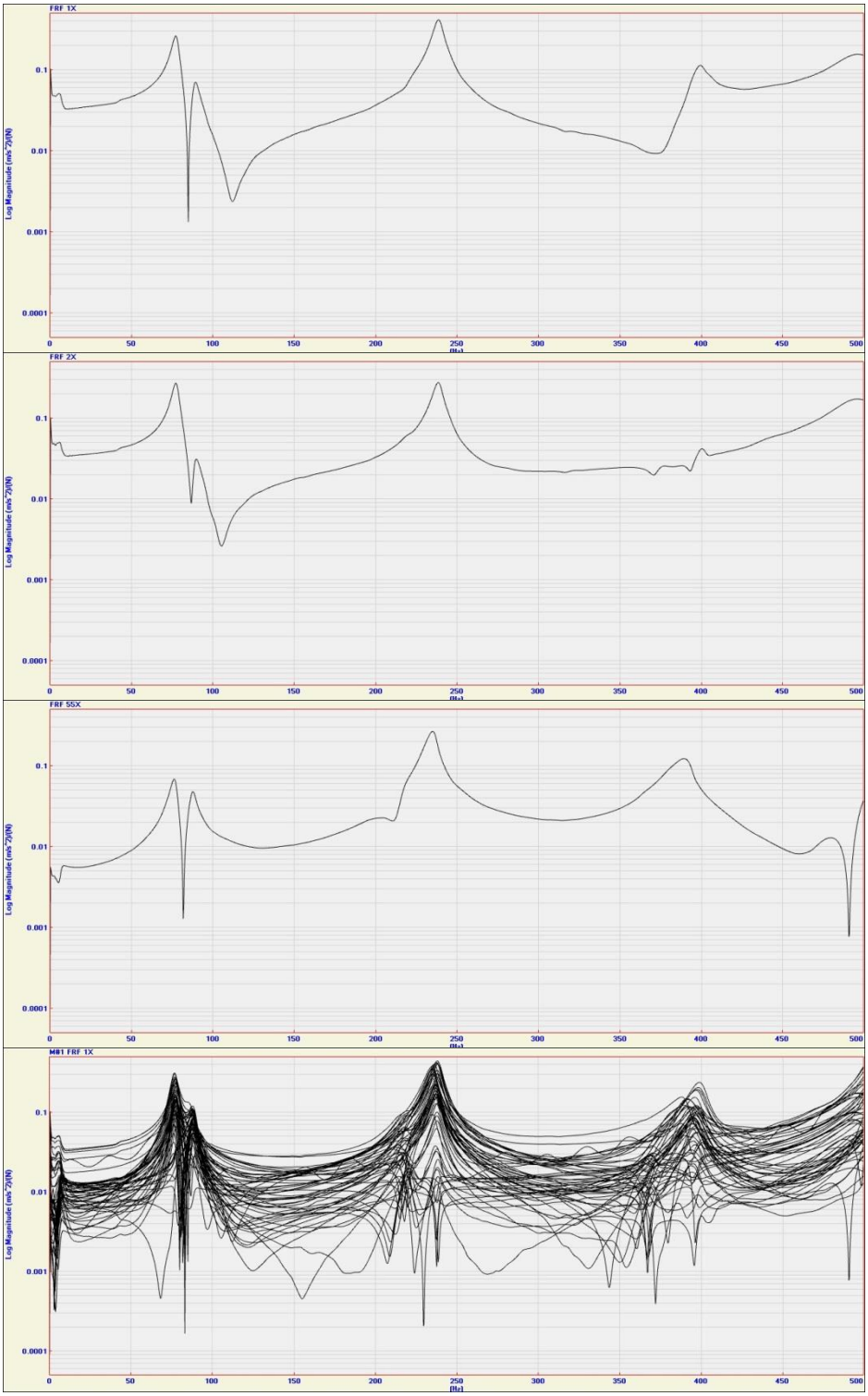

Figure 39 - Results of Frequency versus Magnitude for test 2V0H_1_nonstrengthened_a in points 1, 2, 55 and all points

4.5 Strengthening the walls

In this research one of the main objectives is to evaluate the changes in the dynamic response of brickwork walls when they are strengthened with different patterns of FRP that is intended to be reached. In order to determine whether which patterns of FRP will be more suitable for strengthening unreinforced masonry walls. The dynamic response of FRP patterns will be compared and discussed in next chapter but the patterns of FRP will be designed and applied in this section. The following sections explain the method and procedure of reinforcing the masonry specimens with 5 patterns of FRP.

4.5.1 Preparing the specimens

The requirements for applying FRP for strengthening the specimens are clean surface. The surface of walls must be smooth and clean without any extra mortar because the FRP would not be stuck with high efficiency. Hence, the substrates were cleaned again with brush, emery and water for removing extra mortar. The processes are presented in Figure 40.

Figure 40 - The processes of cleaning the surface

4.5.2 Design of FRPs patterns

It was decided to specify three main patterns to design in vertical, vertical-horizontal and diagonal. For each category except diagonal pattern, two different numbers of FRP were used, five groups and fifteen walls in total. Also, the walls were numbered with counts of FRPs. Also, it was decided to use FRPs of diagonal pattern in 60 and 30 degrees due to used Golden ratio ($\frac{a+b}{b}=\frac{a}{b}$) in elements dimension of historical constructions and monument. In addition, the below formulas are used for numbering of specimens. Table 12 and Figure 41 are shown the 5 groups of walls.

(#V#H_*_strengthened or nonstrengthened_a, b or c)

(#I#I_*_strengthened or nonstrengthened_a, b or c)

#	Counting the number of FRPs
V, H, I	Condition of FRPs
*****	Counting the walls number in each group
strengthened or nonstrengthened	Situation of walls that is explained the FRPs are applied or not
a, b, c	counting the number of modal analysis tests

Table 12 - How to number the specimens

For instance, 3I3I_2_nonstrengthened_b: The wall has 3 diagonal FRPs in both direction and it is second wall in groups of diagonal that is not strengthened and b is shown that the modal testing is carried out for second time.

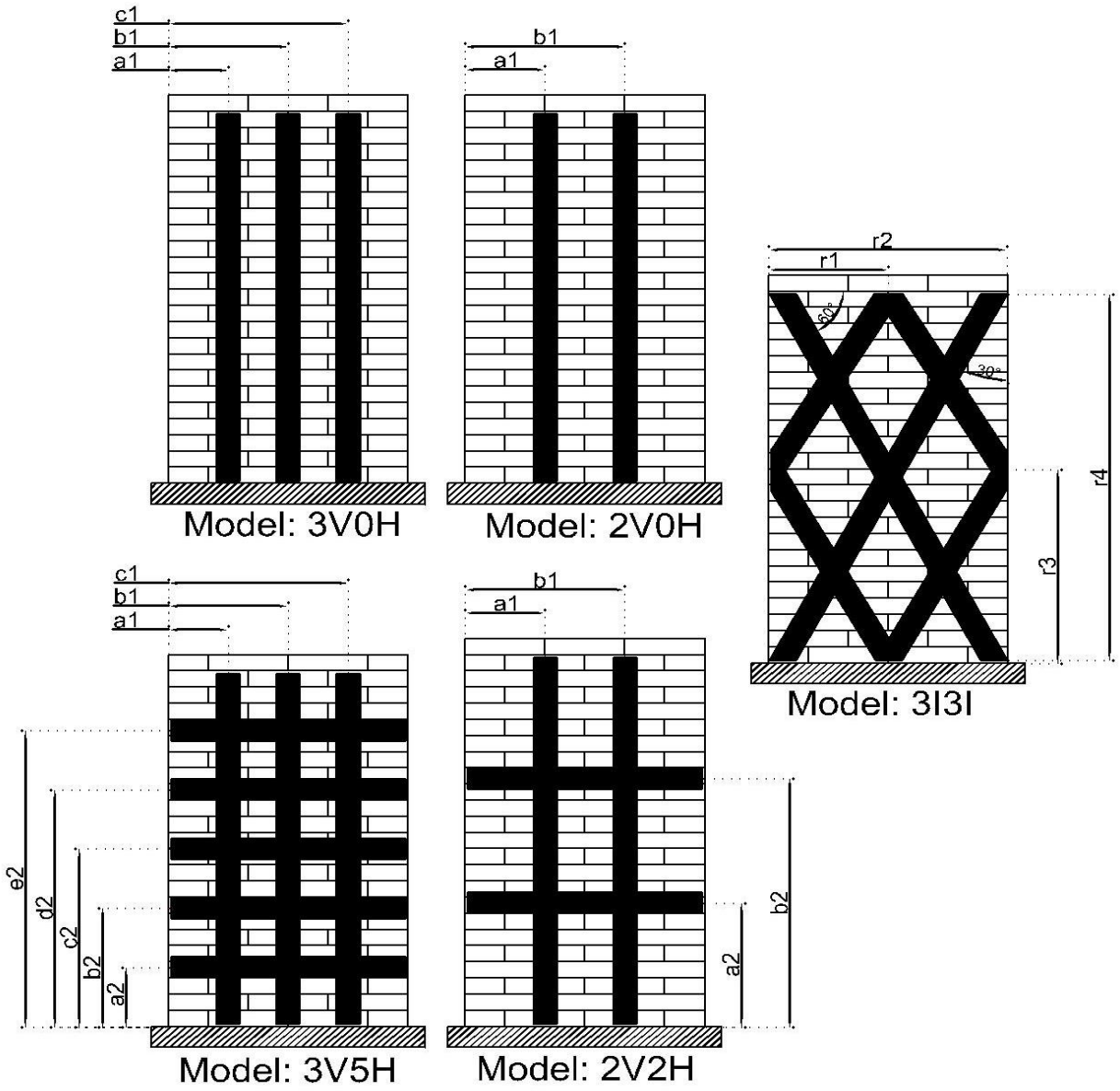

Figure 41 - Five groups of FRP patterns

4.5.3 Measure, cut and location of the FRPs

Because of the next experiment, the vertical and diagonal FRPs were measured and cut two centimeters lesser than height of walls without computing the supports in bottom and 6 cm for support in top were assumed for next experiment as seen in Figure 42 and Table 13. Furthermore, the horizontal FRPs were measured one centimeter lesser than the width of specimens because FRPs should not be glued on walls exactly with liquid adhesive. Figure 42, Figure 43 and Table 13 are shown the measurements. After measuring the length and angle of FRPs, they were cut for all walls. The cuttings of FRPs are carried out with simple handsaw and prop device that is presented in Figure 44. Finally, the center locations of FRPs on each wall were calculated with dividing the dimensions of walls per numbers of FRPs that would be used as vertically, horizontally and diagonally as shown in Table 13. Then, the width of FRPs was marked on walls for applying them in next steps. Figure 45 shows a piece of protection layer of FRPs in one side were removed with cutter and hand to prepare for next steps.

Table 13 - Measurements and locations of FRPs

	Dimension		Distance							
Number	length of vertical FRP	length of horizontal FRP	a1	b1	c1	a2	b2	c2	d2	e2
2V0H-1	142.53		28.07	55.63						
2V0H-2	144.63		28.08	55.66						
2V0H-3	142.77		28.10	55.70						
3V0H_1	143.57		20.88	41.27	61.65					
3V0H_2	144.00		21.08	41.65	62.23					
3V0H_3	145.03		21.08	41.65	62.23					
2V2H_1	141.37	82.63	28.04	55.59		48.12	95.24			
2V2H_2	142.60	82.50	28.00	55.50		48.53	96.07			
2V2H_3	142.87	81.57	27.69	54.88		48.62	96.24			
3V5H_1	141.30	82.13	21.03	41.57	62.10	24.55	48.10	71.65	95.20	118.75
3V5H_2	141.67	81.87	20.97	41.43	61.90	24.61	48.22	71.83	95.44	119.06
3V5H_3	139.07	81.90	20.98	41.45	61.93	24.18	47.36	70.53	93.71	116.89

	Dimension						Distance			
Number	2 sides of N.1 and N.4 with angles 60°-30°		2 sides of N.2 and N.5 with angles 60°-60°		2 sides of N.2 and N.5 with angles 30°-60°		r1	r2	r3	r4
3I3I_1	83.00	104.50	160.50	160.50	102.00	81.00	41.25	82.00	74.17	147.33
3I3I_2	83.00	104.00	162.00	162.00	103.00	82.50	41.55	82.60	74.05	147.10
3I3I_3	82.00	101.00	161.00	161.00	100.50	80.50	41.53	82.57	73.30	145.60

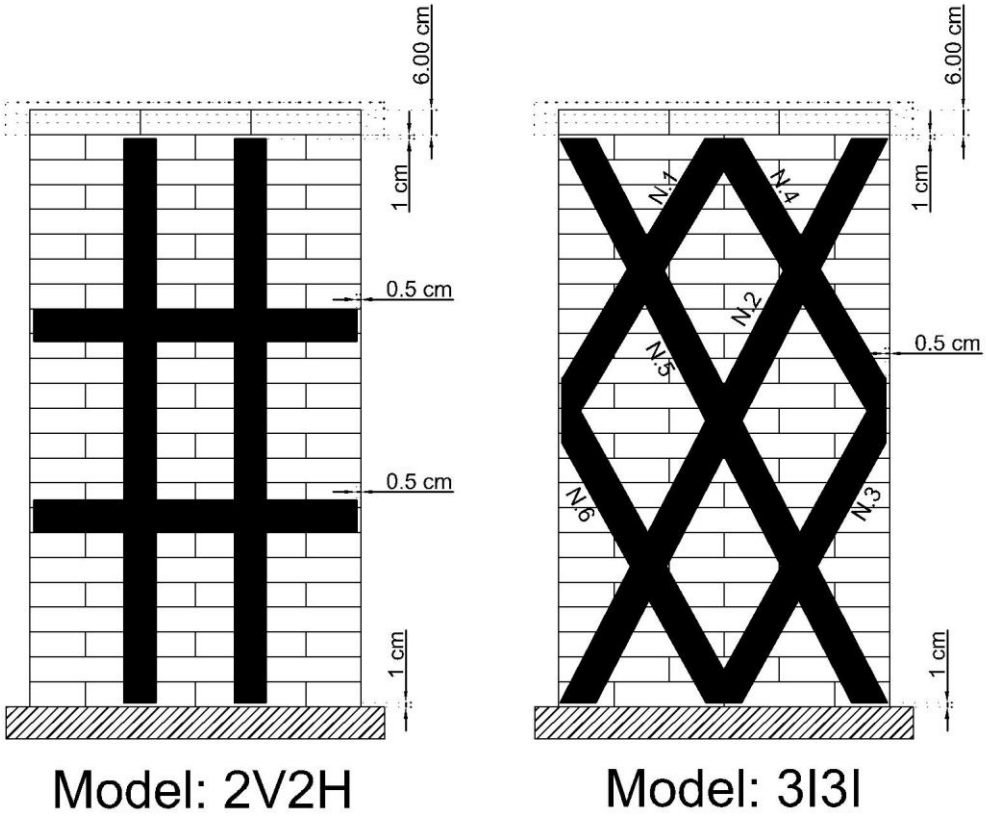

Figure 42 - Positions of vertical and diagonal FRPs on walls

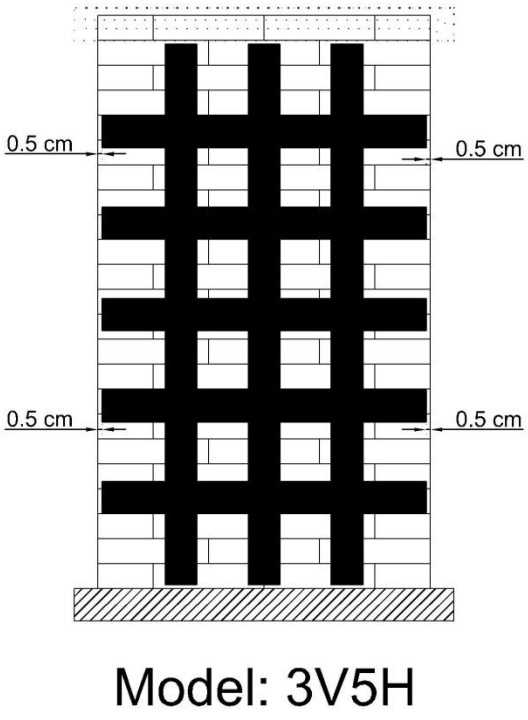

Figure 43 - Positions of horizontal FRPs on walls

Figure 44 - How to cut the FRP

Figure 45 - Removing the protection layer of FRPs for next steps

4.5.4 Applying primer

Before applying primer in specimens, it was decided to divide walls in three groups and applying primer was carried out in three times with one package of primer because the specimens were a lot and the process should be occurred maximum in 20 minutes at 25° C before hardening the primer. Figure 46 are presented the main primer was polymerized from two primary primers and they were mixed together between three to five minutes with low-speed drill (600 rpm). Then, the all primer was separated into 3 or 4 parts to carry out the process quickly and avoid hardening the primer due to hot

chemical activity less than 20 minutes. Finally, the positions of FRPs were brushed like painting with primer. For normal masonry walls, the average thickness of the primer layer should be between 1 and 2 mm. These processes and date are shown in Figure 47 and Table 14. It should be mentioned the primer of 3V5H_2 wall was painted defectively and then the hardened primer was removed completely and the process of applying primer was carried out again.

Figure 46 - Mixing the primer between 3 to 5 minutes

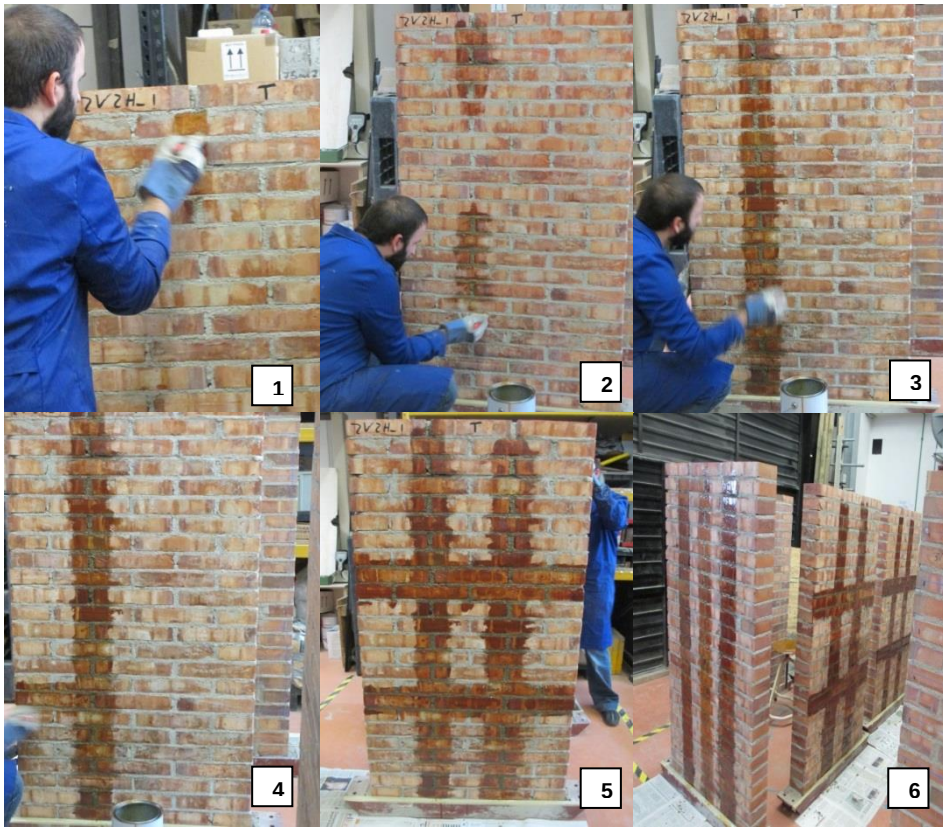

Figure 47 - Processes of applying primer

Number	Date of applying primer		Date of applying FRP	
	Vertical or right to left positions	Horizontal or left to right position	Vertical or right to left positions	Horizontal or left to right position
2V0H_1	21.05.2013		22.05.2013	
2V0H_2	21.05.2013		22.05.2013	
2V0H_3	28.05.2013		29.05.2013	
3V0H_1	21.05.2013		22.05.2013	
3V0H_2	28.05.2013		29.05.2013	
3V0H_3	21.05.2013		22.05.2013	
2V2H_1	21.05.2013	28.05.2013	22.05.2013	29.05.2013
2V2H_2	21.05.2013	28.05.2013	22.05.2013	29.05.2013
2V2H_3	21.05.2013	28.05.2013	22.05.2013	29.05.2013
3V5H_1	28.05.2013	04.06.2013	29.05.2013	05.06.2013
3V5H_2	28.05.2013*	04.06.2013	29.05.2013	05.06.2013
3V5H_3	28.05.2013	04.06.2013	29.05.2013	05.06.2013
3I3I_1	28.05.2013	04.06.2013	29.05.2013	05.06.2013
3I3I_2	28.05.2013	04.06.2013	29.05.2013	05.06.2013
3I3I_3	28.05.2013	04.06.2013	29.05.2013	05.06.2013

*: Prime had been applied in 21.05.2013 but it was removed in 27.05.2013 due to apply after 20 minutes and bad quality of primer

Table 14 - Dates of applying primer and FRPs

4.5.5 Applying FRP and adhesive

This process usually was occurred 24 hours after applying primer. However, the minimum time for applying adhesive and FRP after process of primer is around 90 minutes. Table 14 was shown the date of process.

The adhesive was prepared with mixing two materials around 3 minutes as seen in Figure 48. Also, the process of applying FRP and adhesive should be finished before 35 minutes at 30° centigrade for each mixed adhesive because after that the strengthening would be started. It was decided to apply adhesive on wall and FRP in the same time as presented this step in Figure 49. The average thickness of the adhesive layers on FRP and walls should be between 1 and 2 millimeters, but it should be more than 2 millimeters in some specimens that two FRPs were laid in each other.

The prepared FRPs were put on the surface of walls with rubbing FRPs on wall slowly and heavy pressing with hands subsequently. Then, the extra adhesive was removed from both sides of FRP by spatula as seen in Figure 50.

Figure 48 - Mixing and preparing the adhesive

Figure 49 - Process of applying the adhesive on walls and FRPs at the same time

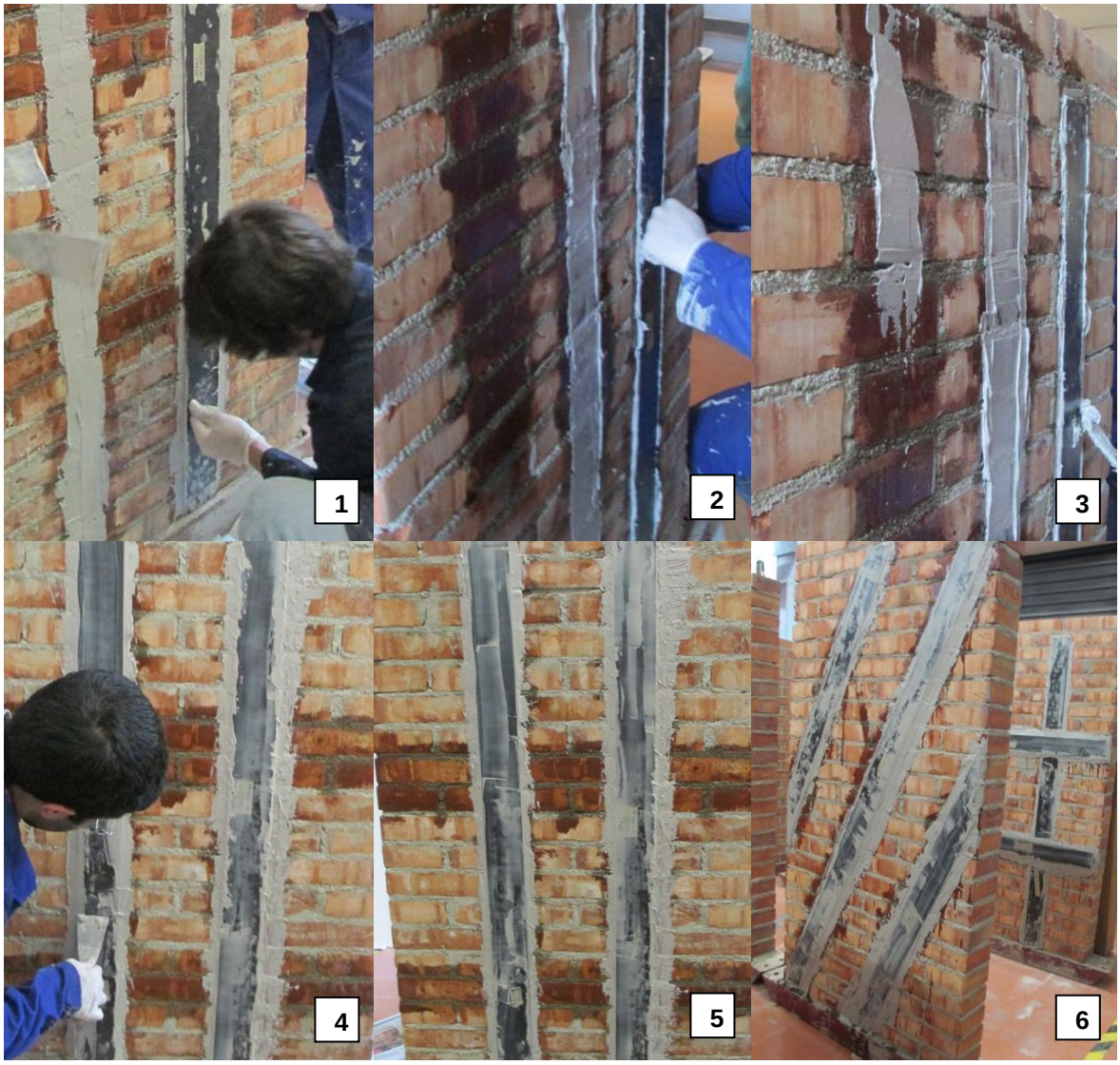

Figure 50 - How to apply the FRPs on walls

For specimen numbers 3V5H, 2V2H and 3I3I, two layers of FRP were needed to lay in each other. The second layer of FRPs was usually positioned when the first layer of FRPs and adhesive were applied and dried after minimum 4 days. However, in this experiment the second FRP was laid after seven days. Table 14 was shown the date of this process. Also, for attaching the FRP on another FRP should not need to use primer. However, the second protection covers just should be removed and applied adhesive that operation is seen in Figure 51. In addition, it was decided to apply vertical FRPs and diagonal FRPs from right to left side of walls (when you stand in front of the walls, their direction are from northwest to southeast). Figure 52 shows the direction an turn of the second layer of FRP over the first layer of reinforcement. In next chapter would have been seen the turn of gluing of transverse FRPs from left to right or right to left side would have not affected on identification of the mechanical response of strengthened brickwork walls.

Figure 51 - The operation of attaching the FRPs to each other

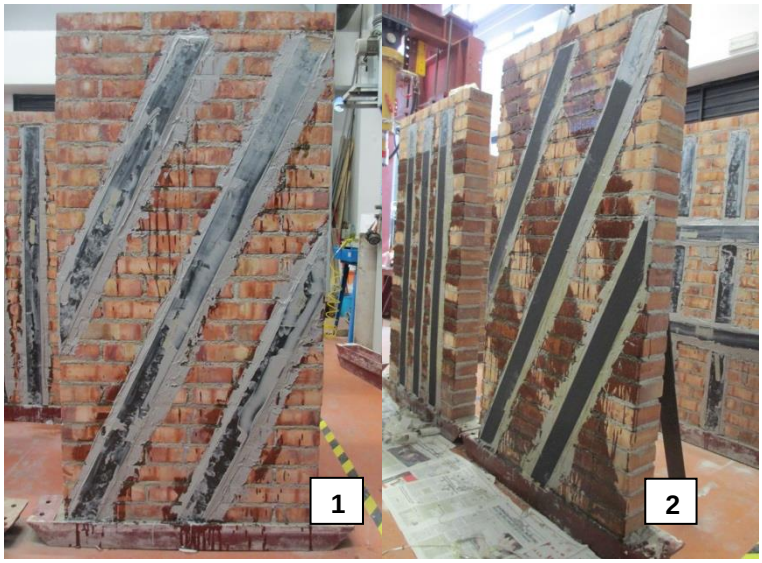

Figure 52 - Direction and turn of the second layer of FRP over the first layer of reinforcement

4.6 Modal Testing after strengthening

The dynamic tests were occurred after strengthening and in the same location of accelerometer like section 4.4, setup the Data Acquisition System and software, calibrating the errors and obtaining the Frequency Response Spectrum and Function (FRF) parts. However, it was considered more about the obtaining the FFTs and FRFs among test because the main purpose of experiment was about this. Also, it should be indicated the strengthening and modal testing was occurred in different side of walls because the surface of impacting must be the same before and after strengthening in modal testing.

For primary comparison, Figure 53, 54 and 55 are presented examples of the results of frequency versus Real, Imaginary and Magnitude for test 2V0H_1_strengthened_a in points 1, 2, 55 and all. However the all results of the frequency response spectrums (FRSs) and FRFs are shown and discussed in next chapter. The dates of operating modal testing after strengthening are shown in Table 15.

Number	**Date of applying FRP**		**Modal Testing after strengthening**	**Divergence of days**
	Vertical or right to left positions	Horizontal or left to right position		
2V0H-1_strengthened_a	22.05.2013		30.05.2013	8
2V0H-2_strengthened_a	22.05.2013		10.06.2013	19
2V0H-3_strengthened_a	29.05.2013		10.06.2013	12
3V0H_1_strengthened_a	22.05.2013		30.05.2013	8
3V0H_2_strengthened_a	29.05.2013		10.06.2013	12
3V0H_3_strengthened_a	22.05.2013		30.05.2013	8
2V2H_1_strengthened_a	22.05.2013	29.05.2013	11.06.2013	13
2V2H_1_strengthened_b _right side*	22.05.2013	29.05.2013	26.06.2013	28
2V2H_2_strengthened_a	22.05.2013	29.05.2013	11.06.2013	13
2V2H_3_strengthened_a	22.05.2013	29.05.2013	11.06.2013	13
3V5H_1_strengthened_a	29.05.2013	05.06.2013	18.06.2013	13
3V5H_2_strengthened_a	29.05.2013	05.06.2013	18.06.2013	13
3V5H_3_strengthened_a	29.05.2013	05.06.2013	18.06.2013	13
3I3I_1_strengthened_a	29.05.2013	05.06.2013	18.06.2013	13
3I3I_2_strengthened_a	29.05.2013	05.06.2013	18.06.2013	13
3I3I_3_strengthened_a	29.05.2013	05.06.2013	18.06.2013	13

*:The accelerometer had been located on right side of wall

Table 15 - Dates of operating modal testing

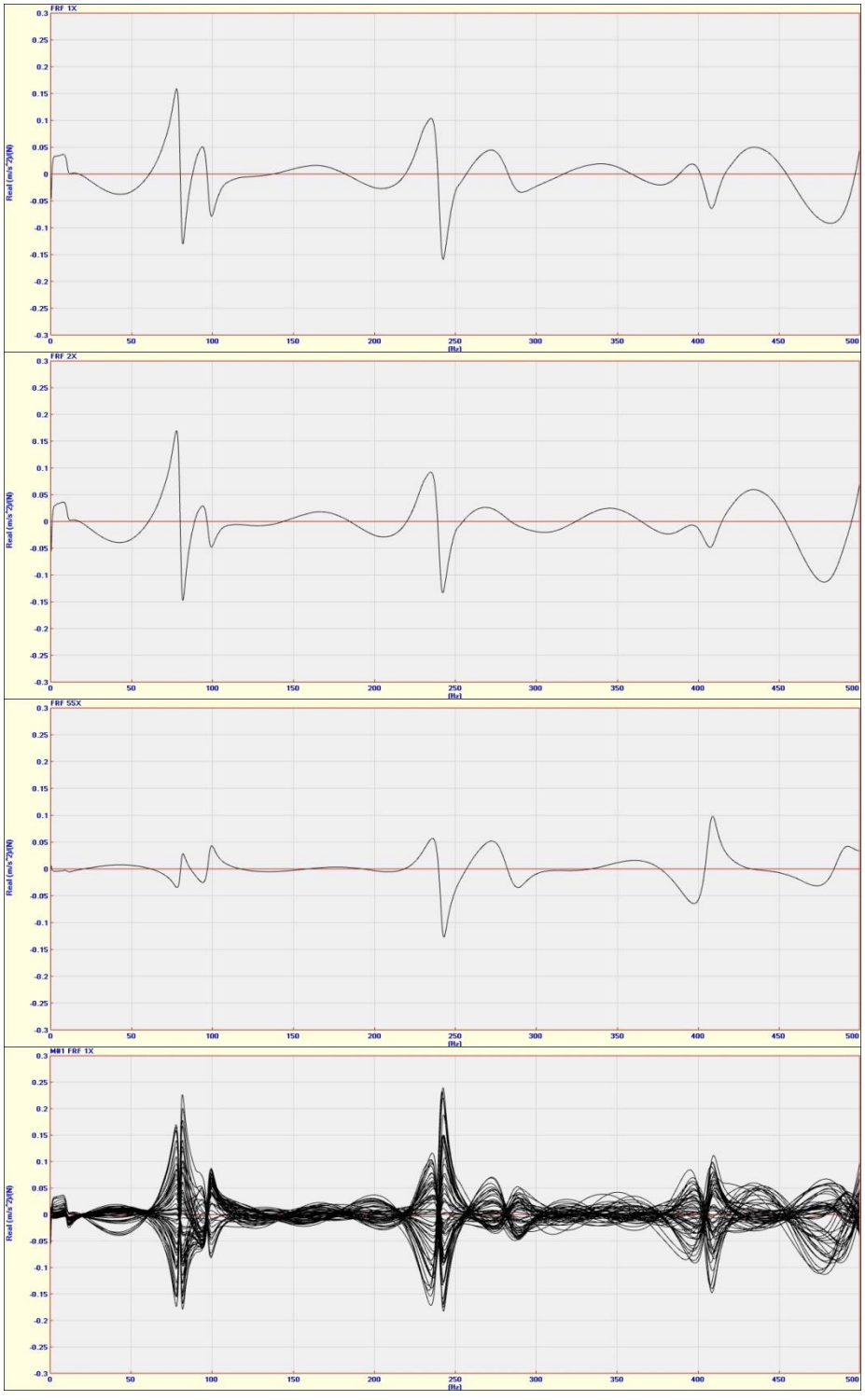

Figure 53 - Results of Frequency versus Real for test 2V0H_1_strengthened_a in points 1, 2, 55 and all points

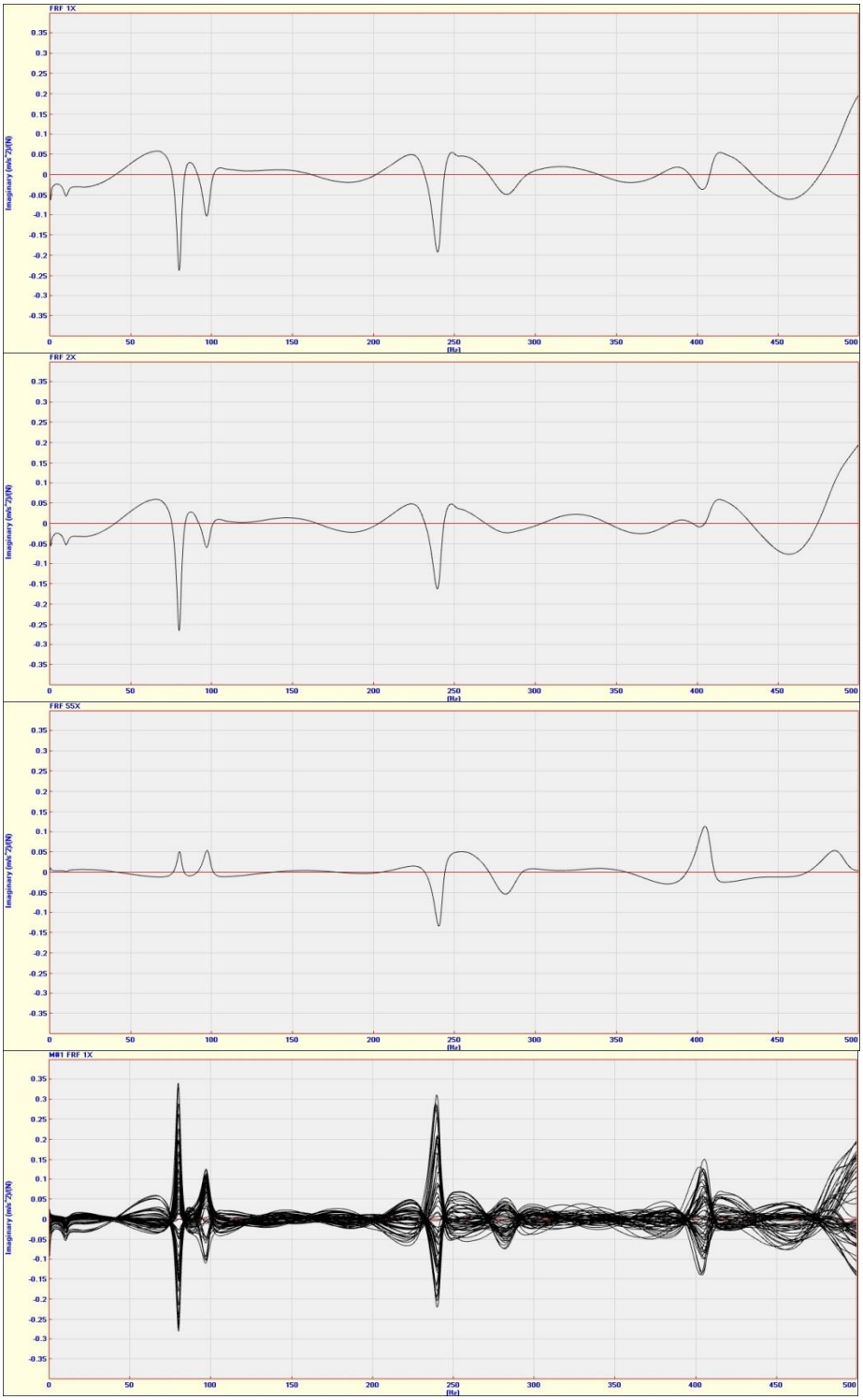

Figure 54 - Results of Frequency versus Imaginary for test 2V0H_1_nonstrengthened_a in points 1, 2, 55 and all points

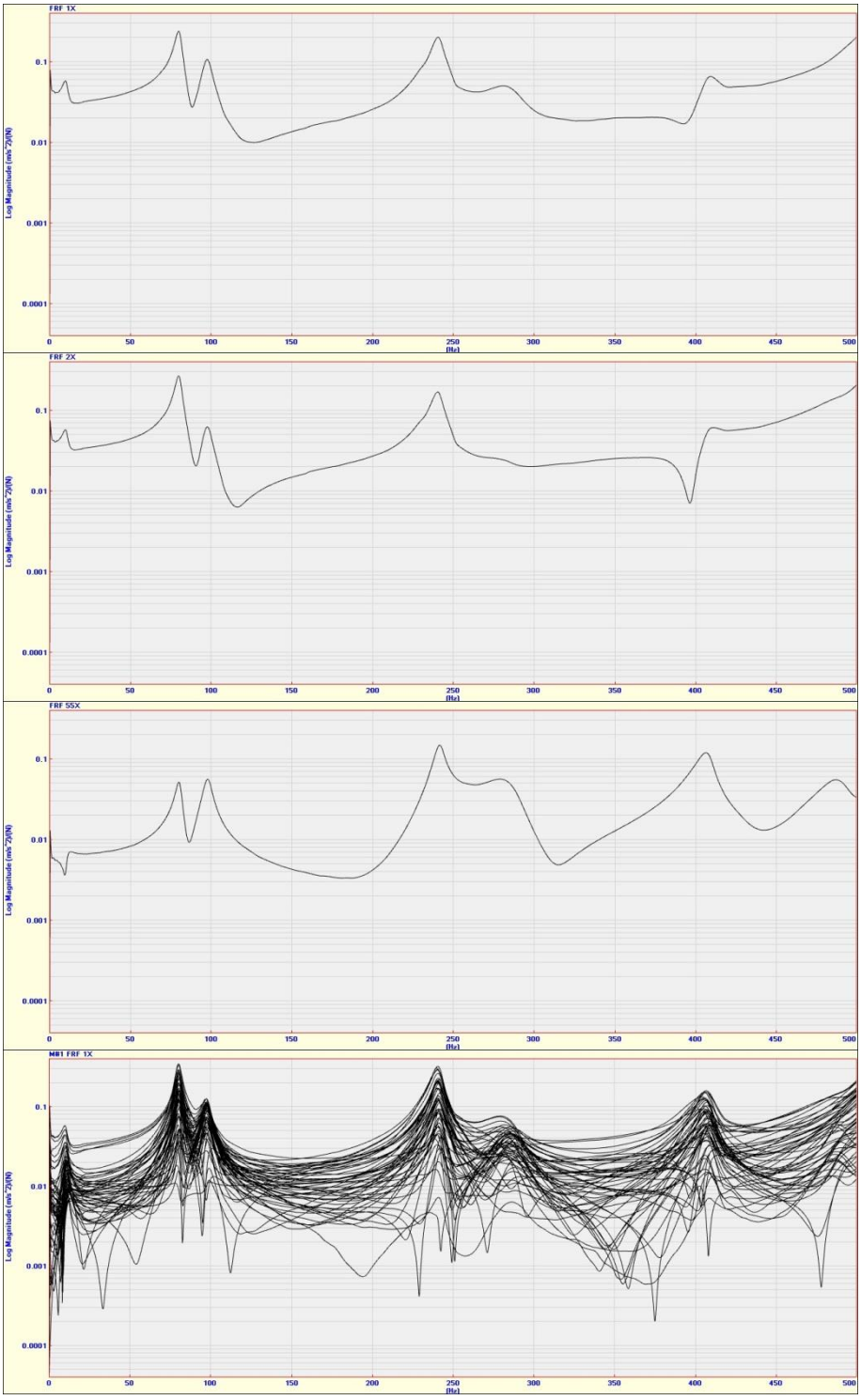

Figure 55 - Results of Frequency versus Magnitude for test 2V0H_1_nonstrengthened_a in points 1, 2, 55 and all points

5. POST PROCESS AND ANALYSIS OF DATA

After performing the 32 dynamic tests and computing the Fast Fourier Transforms (FFTs) and Frequency Response Functions (FRFs), the results must be verified with post processing data in ME'scopeVES software to accurately estimate the modes and damming. After that, first's modes of the walls (in range of 0 to 500 Hz) are presented in all tests. In addition the function of modal assurance criteria (MAC) are estimated for calibration of modes between strengthened specimen and non-strengthened. Finally, five different patterns of FRP will be compared in three ways: amount of FRP, influence of vertical and horizontal positions in FRP patterns and effect of angle on FRP patterns.

5.1 Post processing the experiments

Fifteen models of walls with their dimension were prepared and inserted in ME'scopeVES configuration file to be able to animate and visualize the modal movements. After computing the FRFs for each point that were discussed in section 4.4.4 and 4.6, all frequency response spectrums and signals were post processed with using the 500 Hz span and 0.2 Hz range of sensitivity frequency in software. Briefly, the final modes were estimated from three steps of curve fitting that will be explained in below.

5.1.1 Mode indicator

The first and most critical step of modal parameter estimation is to evaluate how many modes have been excited in a frequency range of a set of FRF measurements.

For this purpose,

1- The mode indicator will provide a best and single curve with resonance peaks for counting the number of mode in the frequency range

2- The mode indicator will limit the data used by the Frequency and Damping curve fitting methods to data surrounding each resonance peak. They would be used to weight the data from each reference during Residues curve fitting (next sections).

Figure 56 is presented these purposes

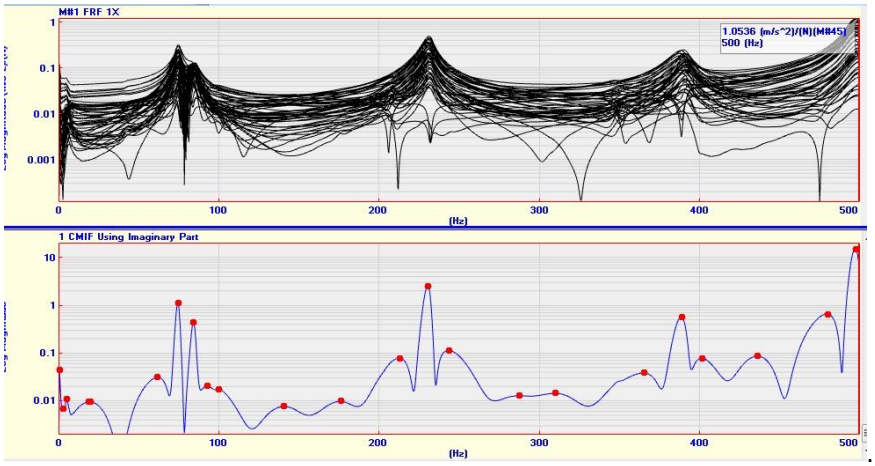

Figure 56 - Estimation peak and modes from FRF

Also, there are several methods for mode indicator. It is needed to use Complex Mode Indicator Function (CMIF) method for this kind of experiment at first step of curve fitting. The Complex Mode Indicator Function (CMIF) performs a singular value decomposition of the FRF data for resulting in a set of multiple frequency domain curves. The number of mode indicator curves equals the number of references which is 55 measured points or Traces[2] in these tests. Each peak in a curve is an indication of a resonance that is shown in Figure 57. In other word, multiple CMIFs are calculated from a multiple reference set of FRFs. Also, they will be used to locate closely coupled modes and repeated roots that will be discussed in section 5.1.2.2.

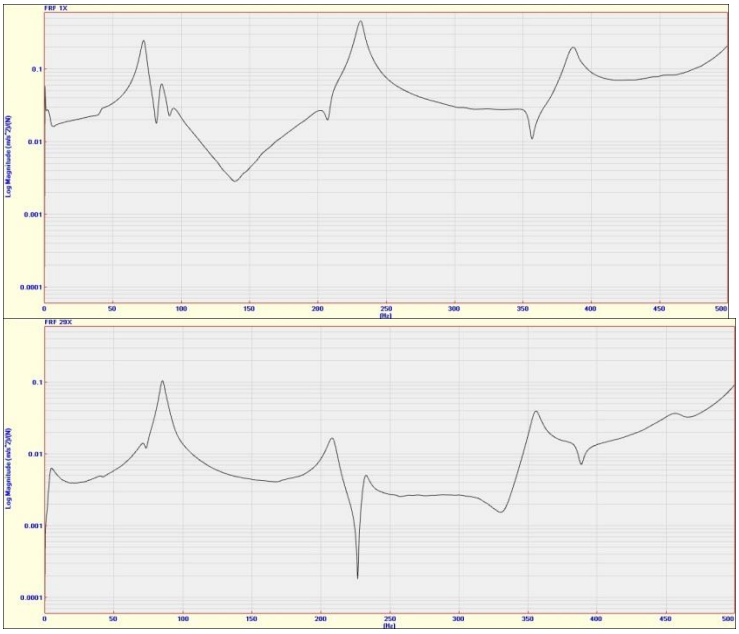

Figure 57 - Number of peaks for each FRF (4 modes for 1st FRF; 3 modes for 29th FRF)

[2] Each Trace contains values measured at a DOF(single channel measurement) on the structure

Furthermore, the Mode Indicator Function would be computed by processing of the Real, Imaginary and Magnitude of FRFs which is referred to chapter 2 and is seen in Figure 58.

Real: The Real will be used when there is a single resonance peak for each mode. This situation will happen when the response units are velocity.

Imaginary: The Imaginary will be used when there is a single resonance peak for each mode. This situation will happen when the response units are displacement or acceleration

Magnitude: The Magnitude can be used in any conditions when there is doubt condition for choosing valid Real or Imaginary part.

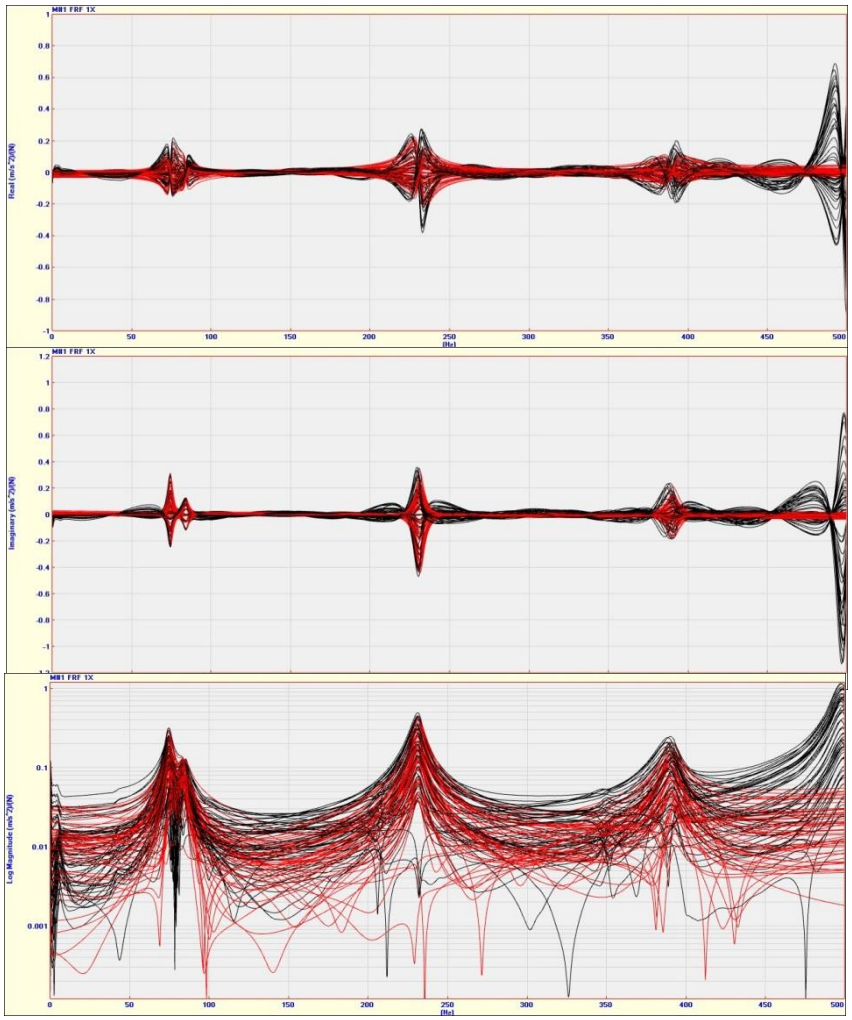

Figure 58 - Difference of computing modes for the Real, Imaginary and Magnitude part

5.1.2 Estimating real modes

In mode indicator which is described in previous sections deals with a lot of modes that they could not be correct because they are summation of all modes from all FRFs (55 FRFs). For solving, it is better to build up a list of modal frequencies and damping by curve fitting in small ranges by comparing the

imaginary and magnitude parts and choosing real modes when they are repeated in all FRFs. After that, the results will be performed and natural frequencies and damping could be estimated by picking the peaks manually. Figure 59 is shown this process.

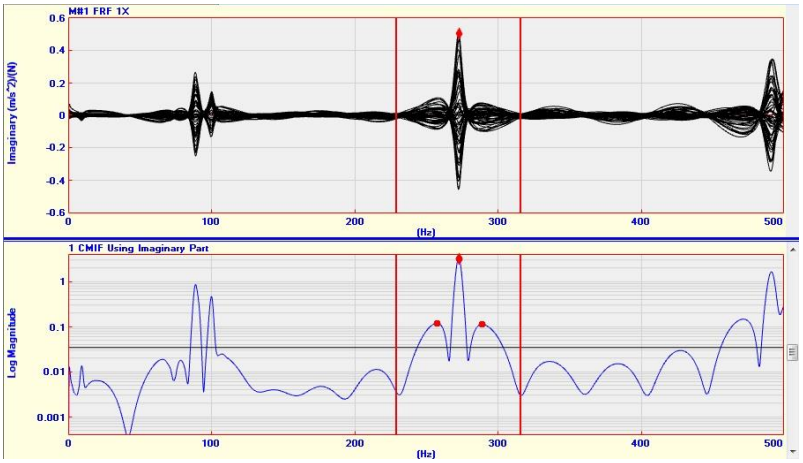

Figure 59 - Estimation frequencies and damping ratio

5.1.2.1 Damping comparison

To compare damping values between modes, the damping must be displayed in percentage value in instead of Hz rates. A large difference among values range in modal testing is usually not expected, unless there is a special damping mechanism that is affecting one mode more than another. In this experiment, the huge difference of damping should be controlled by the other result of FRFs.

5.1.2.2 Repeated roots and closely coupled modes

Two modes can be in the same frequency and can have damping with different mode shapes especially in geometrically symmetric structures. This condition is called a repeated root. Also, structures can have two or more closely coupled modes that are very close in frequency with sufficient damping, so their resonance peaks sum together and appear as one resonance peak in measurements. Then name of this situation is Closely Coupled modes. Figure 60 is presented this condition.

In general, sometimes the resulting mode shape will be looked like the summation of multiple mode shapes in viewed animation (complex mode, a traveling wave, instead of a standing wave) if the structure has closely coupled modes or repeated roots. Due to these situations, in the most case would be identified one mode where there are really two or more and it is impossible to divide them. From this experiment, it would be seen the separation of two modes will occur after strengthening automatically because of homogenizing the masonry materials.

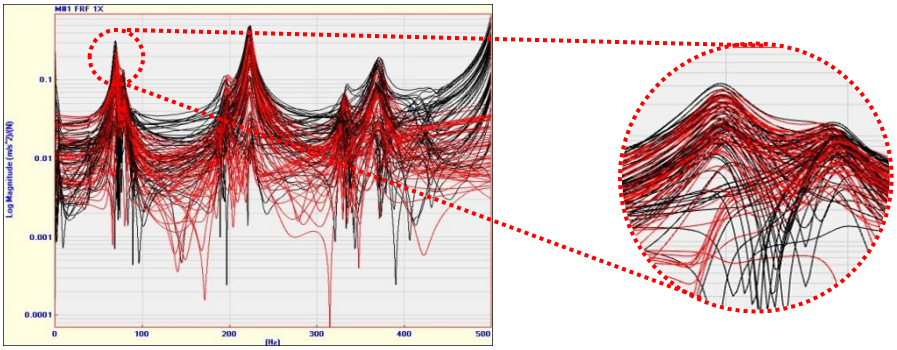

Figure 60 - Estimation modes in closely coupled conditions

5.1.3 Fit function and residues

After curve fitting is completed, a red Fit Function is displayed for each Trace that was curve fit. The Fit Function is overlaid on top of the Trace, so that is can be compared with the measurement data. The Fit Function is zero outside of the curve fitting band and each Fit Function should closely match its corresponding measurement over the curve fitting band as seen in Figure 61.

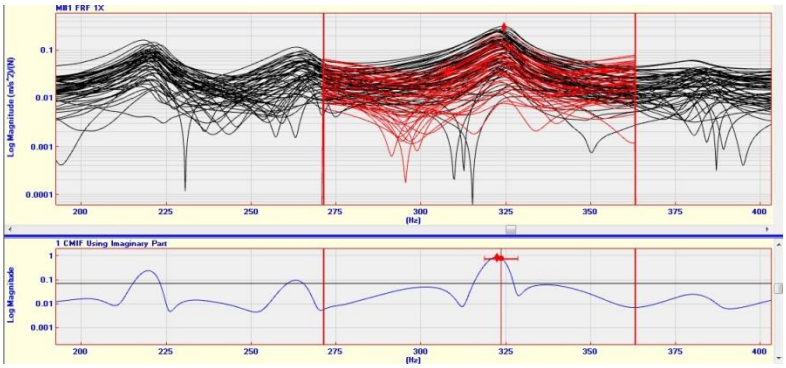

Figure 61 - Curve fitting of mode shapes

Experimental modal parameters are estimated by curve fitting an analytical Frequency Response Function (FRF) parametric model to a set of experimental derived data. The unknown parameters of the parametric model are the modal frequency, damping and residues for each mode. Each mode has a single frequency, damping estimate and a different residue estimate to each measurement that is curve fit. Each residue is a different component of the mode shape. In other words, residues are simply numbers that represent the "*strength*" of a resonance. In general, modal residues are complex numbers. Therefore, they are listed as magnitude and phase in the modal parameters spreadsheet and in a shape table as shown in Figure 62. Since the denominator of the FRF has units of Hertz, or (radians / second), residues must have the following units (Eq.30).

$$\text{Residue units} = (\text{FRF units}) \times (\text{radians / second}) \qquad (30)$$

The modal residues are estimated during a separate curve fitting step on the FRF data. During residue curve fitting, the coefficients of the numerator polynomial of each FRF are estimated by at least squared error curve fitting process. It should be mentioned, this parameter is not used for comparing results of this experiment; however, they were used for selecting the best mode shapes as real mode.

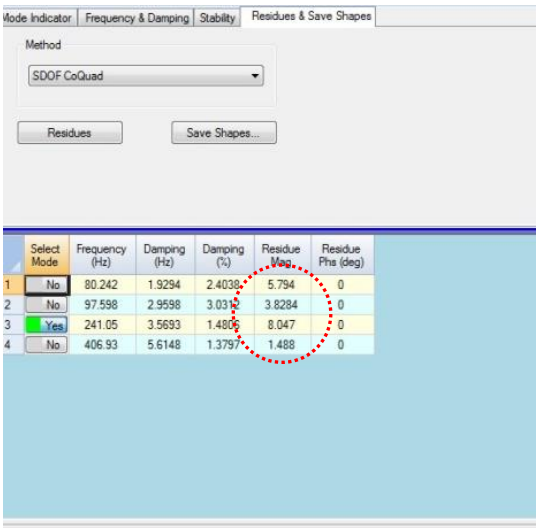

Figure 62 - Example of residue parameter

5.2 Analysis and comparison of specimens

To evaluate the main objective of the experiment and make a comparison between the identification of strengthening and non-strengthening experimental results, the fifteen specimens in five groups of FRP patterns were considered as discussed in chapter four. Moreover, they were compared from three aspects; amount of FRP, influence of vertical and horizontal positions in FRP patterns and effect of angle on FRP patterns that were mentioned in section 4.5. Finally all of three aspects were compared generally to appraise the best performance of FRP pattern.

Also it is possible to see the mode shapes and compare the data for estimation of frequencies, damping ratio, modal assurance criterion (MAC) and value of residue. For this purpose, fifteen exact geometric models were constructed and the points of impacts were defined with their directions. However to see exact behavior, the grids and points just are shown because the movement of edges and support will be following virtually from the measured points. Thus, the movements of non-measured points were simulated and they were depending on other points.

5.2.1 Location of accelerometer

As discussed in section 4.4.1, it was decided to locate the one accelerometer at top in left side of all walls because of its high amplitude, maximum displacement and contribution in each mode. However,

two tests were carried out with different position of accelerometer in 2V2H_1 specimen to evaluate the discrepancy of left and right side position for modes in specimen.

The results of test for non-strengthened and strengthened 2V2H_1 specimen at 2 positions of accelerometer are tabulated in Figure 63 and Table 16. In Figure 63 can be estimated there are different modes with different behavior. However, the first and second mode shapes around 74 and 84 Hz are the same in different positions of accelerometer even. Also, it should be specified the second mode shape with right accelerometer shows similar frequency but in different nodal line. It means, the position of accelerometer have affected on the displacement direction of wall, although, it is not possible to discuss about damping ratio exactly that will be discussed in section 5.2.2.2. Furthermore, the first compound mode shapes (1s lateral+1st Bending) were reached in the same frequency around 232 Hz before strengthening and 235.8 to 239.4 Hz after strengthening. In next section, it would be discussed the 3.6 Hz is not error of accelerometer in the high range of frequency whereas the FRPs were applied with 1 and 2 millimeters tolerance of adhesive. All of these facts confirm that the position of accelerometer could not be important even if other position of accelerometer cannot be received some excited modes.

2V2H_1_L	**Mode**	**1**	**2**	**3**	**4**	**5**	**6**
	Shape Label	**1st L**	**1st B**	**2nd B**	**1st L+1st B**	**3rd B**	**1st L+2nd B**
	Frequency Units	**(Hz)**	**(Hz)**	**(Hz)**	**(Hz)**	**(Hz)**	**(Hz)**
Non-strengthened_a	Frequency	74.687	84.844	207.550	232.290	352.830	391.640
	Damping ratio (%)	2.690	2.480	1.974	1.453	1.220	1.358
Strengthened_a	Frequency	76.930	89.456	222.940	239.400	378.360	
	Damping ratio (%)	2.663	2.664	1.960	1.614	1.231	
Difference	Frequency	2.243	4.612	15.390	7.110	25.530	
	Damping ratio (%)	-0.027	0.184	-0.014	0.161	0.011	
Difference %	Frequency (%)	3.003	5.436	7.415	3.061	7.236	
2V2H_1_R	**Mode**	**1**	**2**	**3**	**4**		
	Shape Label	**1st L**	**1st B**	**1st L+1st B**	**1st L+2nd B**		
	Frequency Units	**(Hz)**	**(Hz)**	**(Hz)**	**(Hz)**		
Non-strengthened_a	Frequency	74.504	84.244	231.440	390.630		
	Damping ratio (%)	2.674	2.611	1.487	1.348		
Strengthened_a	Frequency	76.079	87.881	235.810	425.670		
	Damping ratio (%)	2.720	2.998	1.733	2.161		
Difference	Frequency	1.575	3.637	4.370	35.040		
	Damping ratio (%)	0.046	0.387	0.245	0.813		
Difference %	Frequency (%)	2.114	4.317	1.888	8.970		

Table 16 - Details of frequency and damping estimation for the 2V2H_1 specimen with different position of accelerometer

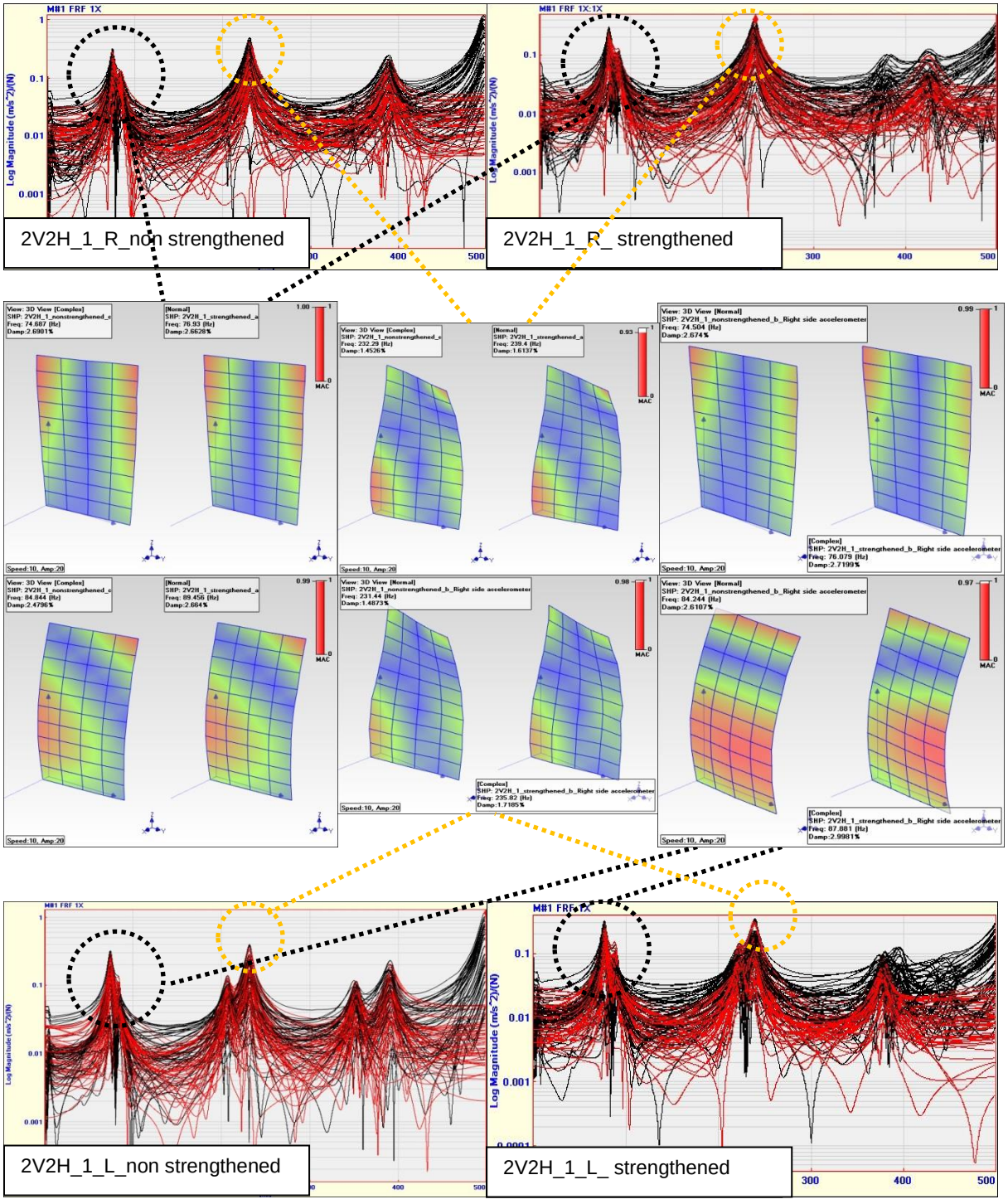

Figure 63 - Estimation the same modes and same frequencies with different position of accelerometer

5.2.2 Identification of the mechanical response of 15 specimens before and after strengthening for 5 FRP patterns

At first, frequency and damping ratio estimation of the recorded data for each specimen were compared with itself and then two other specimens to calibrate and discard the inappropriate data. In

the processes of modal identification, the difference of frequencies in similar mode shapes was identified to validate the results that were shown in tables and figures of each section. Also, Modal Assurance Criteria (MAC) value is a method for quantitatively comparing two complex shape vectors. In other words, MAC is calculated for two mode shapes from columns of the DOFs to evaluate the coherence of mode shapes. In addition, the percentage of frequency difference, damping ratio and residue difference of each specimen show the efficiency of patterns in each group that will be presented in each part.

5.2.2.1 Obtaining the modal parameter and discarding the strange data

a) 2V0H specimen

Figure 64, Figure 65, Figure 66 show the results parameter of three 2V0H specimens from six tests in non-strengthened and strengthened condition. The results were transformed from the time domain to the frequency domain, which are called FRF. The results of the FRFs and the frequency values can be obtained by picking up the peaks of the FRFs. From the below graphs, the FRFs for the walls have clear peaks, so that the frequency values can be determined without difficulty.

The 2V0H_1_nonstrengthened_a shows the first and second mode shapes around 75 Hz to 95 Hz that are close to each other and should be found from lonely FRFs or focusing on this range with regards to repeated roots and closely coupled modes as seen in Figure 64 part a. Furthermore, the FRFs of 2V0H_1_strengthened_a show the 18 FRFs (around 32%) were not excited in the range of 280 to 300 Hz; therefore there is no complete mode for evaluation, Figure 64 part b.

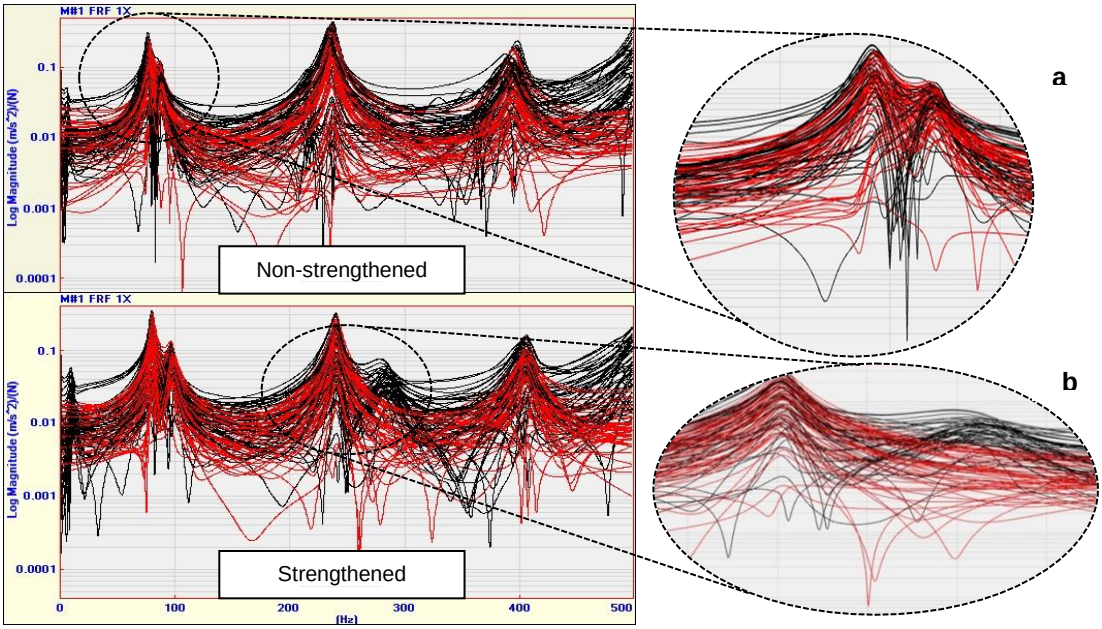

Figure 64 - FRFs of 2V0H_1 specimen before and after strengthening

Figure 65 presents six modes in both tests obviously. Also, Figure 65 shows the FRFs are shifted to the right to illustrate the effect of applying FRP on the frequency value. It can be indicated the frequencies are increased in three specimens as seen in Table 17.

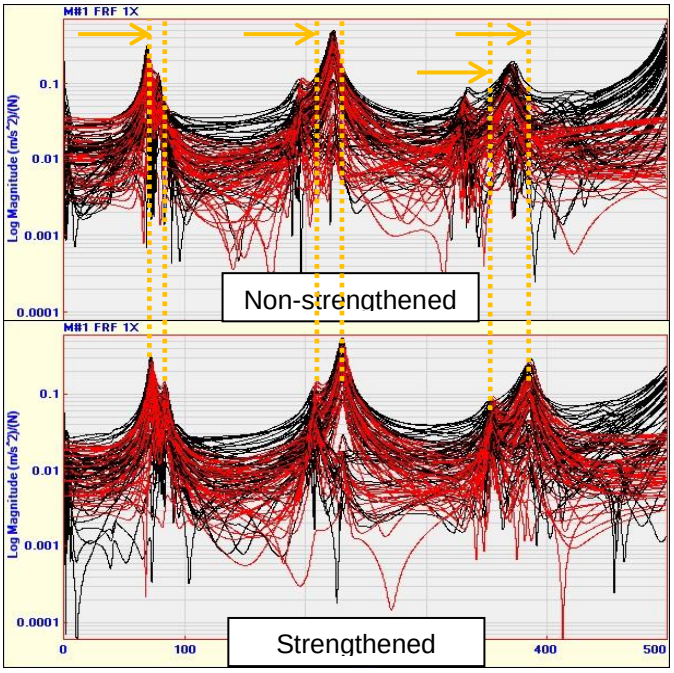

Figure 65 - FRFs of 2V0H_2 specimen shows shift of peaks after strengthening

It can be seen in Figure 66, the four modes are obtained from FRFs for 2V0H_3 model and two peaks are not absolutely clear. However, one peak is not complete mode shape in the 2V0H_3_strengthened_a specimen at 221.57 Hz due to location of accelerometer that discussed in section 5.2.1 and it is not obvious after strengthening too, Figure 66 part a. The second unclear peak is around 360 to 380 Hz that is compounded with fourth mode shape after applying FRP as seen in Figure 66 part b.

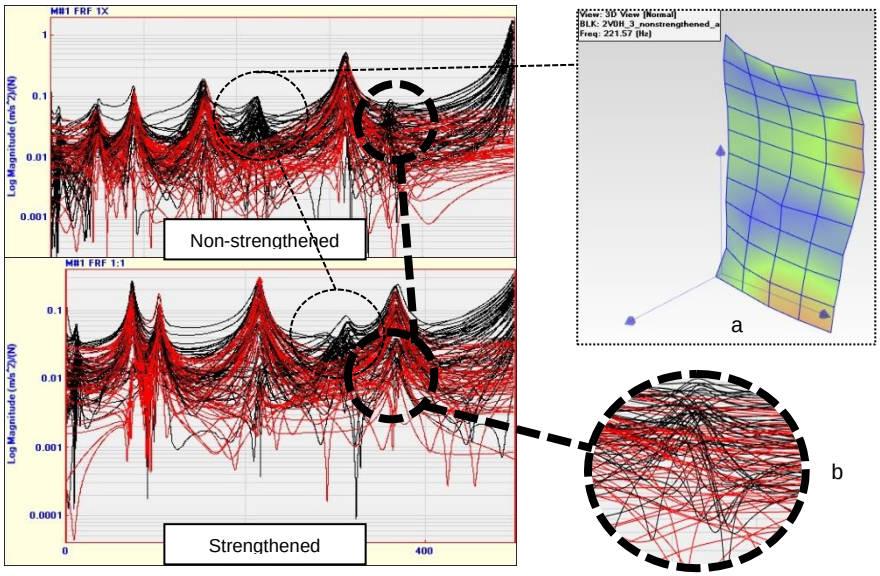

Figure 66 - Vague mode shapes of 2V0H_3 specimen

Table 17 and Figure 67 list the main points of results concerning the frequency values, the trend of frequencies and the mode shape configurations. It is obvious the frequencies of strengthened walls for

each mode have increased generally. However, the variations of frequency after strengthening for 2VH0_3 specimen are much different with regards to other specimens, especially in the first and third modes (around 45 and 30%) as seen in Table 17. Also, this strange increasing could be effect of other situations for the first, third and fourth mode shape that will be discussed and it is not calculated in average (the numbers are specified with red color).

2V0H_1	**Mode**	**1**	**2**	**3**	**4**	**5**	**6**
	Shape Label	**1st L**	**1st B**	**1st L+1st B**	**1st L+2nd B**		
	Frequency Units	**(Hz)**	**(Hz)**	**(Hz)**	**(Hz)**		
Non-strengthened_a	Frequency	77.202	88.089	236.960	395.200		
	Damping ratio (%)	2.704	2.669	1.412	1.450		
Strengthened_a	Frequency	80.242	97.598	241.050	406.930		
	Damping ratio (%)	2.404	3.031	1.481	1.380		
Difference	Frequency	3.040	9.509	4.090	11.730		
	Damping ratio (%)	-0.300	0.363	0.068	-0.070		
Difference %	Frequency (%)	3.938	10.795	1.726	2.968		
2V0H_2	**Mode**	**1**	**2**	**3**	**4**	**5**	**6**
	Shape Label	**1st L**	**1st B**	**2nd B**	**1st L+ 1st B**	**3rd B**	**1st L+ 2nd B**
	Frequency Units	**(Hz)**	**(Hz)**	**(Hz)**	**(Hz)**	**(Hz)**	**(Hz)**
Non-strengthened_a	Frequency	69.824	78.969	196.580	223.690	332.210	370.420
	Damping ratio (%)	2.757	2.536	1.752	1.296	1.150	1.540
Strengthened_a	Frequency	72.684	85.068	208.460	231.160	355.210	386.220
	Damping ratio (%)	2.662	2.419	1.628	1.206	1.051	1.239
Difference	Frequency	2.860	6.099	11.880	7.470	23.000	15.800
	Damping ratio (%)	-0.095	-0.117	-0.124	-0.090	-0.098	-0.301
Difference %	Frequency (%)	4.096	7.723	6.043	3.339	6.923	4.265
2V0H_3*	**Mode**	**1**	**2**	**3**	**4**	**5**	**6**
	Shape Label	**1st L**	**1st B**	**1st L+1st B**	**1st L+2nd B**		
	Frequency Units	**(Hz)**	**(Hz)**	**(Hz)**	**(Hz)**		
Non-strengthened_a	Frequency	51.110	89.998	165.970	317.870		
	Damping ratio (%)	6.655	2.398	2.495	1.163		
Strengthened_a	Frequency	74.537	104.770	215.720	368.230		
	Damping ratio (%)	3.067	2.124	1.964	1.566		
Difference	Frequency	23.427	14.772	49.750	50.360		
	Damping ratio (%)	-3.588	-0.274	-0.531	0.403		
Difference %	Frequency (%)	45.836	16.414	29.975	15.843		
2V0H	**Mode**	**1st L**	**1st B**	**2nd B**	**3rd B**	**1st L+ 1st B**	**1st L+ 2nd B**
Average of Increasing value	Frequency (%)	4.017	11.644	6.043	6.923	2.533	3.617

*: The columns with red color are discarded for average

Table 17 - Summary of frequency and damping estimation for the 2V0H specimens

Figure 67 shows the frequencies of the first six modes with two ratio of divergence between non-strengthened and strengthened walls. It can be seen that the applying FRP is increased the frequency of all modes. The magnitude differences of two specimens are around 3 to 11 Hz or 4 to 11% of non-strengthened specimens for first modes, although the behavior of third specimen (2V0H_3) is different as seen in Figure 68.

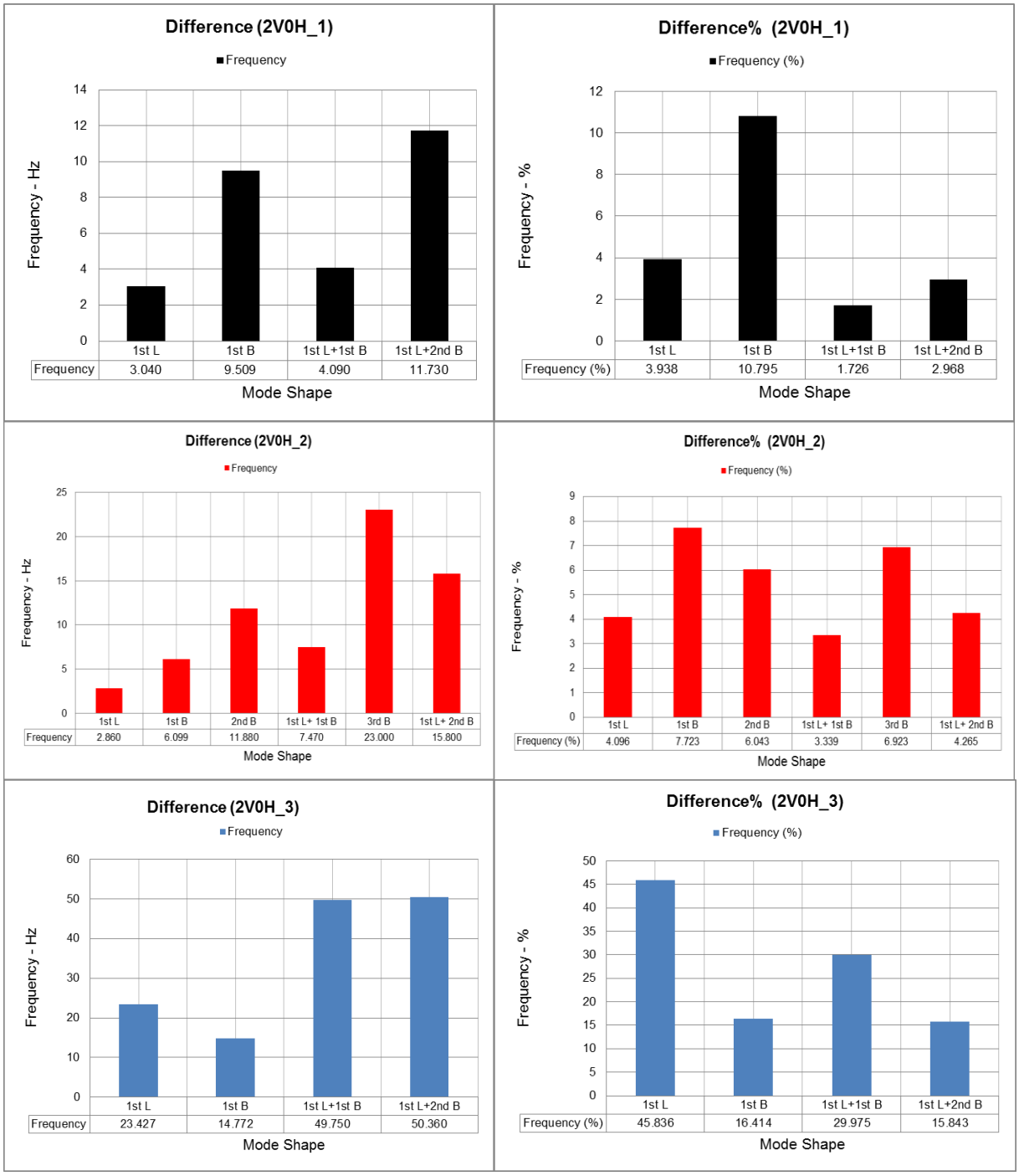

Figure 67 - Comparison of the difference of frequencies after and before strengthening for 2V0H specimens in Hz and percentage

Regarding to the frequency values, the influence of FRP is much more significant on the lower modes because the lower modes have much lower frequency values than the higher modes that is associate with maximum energy. The 2V0H_3_nonstrengthened_a and Figure 68 present the problem and the effect of FRP in first mode. In addition, it is more significant when the wall was not constructed carefully like drying mortar, full of small pore or other hypotheses. However, there is not real judgment

until next experiment (eccentrically loading test) for this wall. Also, it should be mentioned some points for homogenizing hypothesis in below and can be seen in Figure 68.

- Supposition of boundary condition is not true because the fractures of first mode shape was solved after strengthening but the conditions of support were not changed.
- The influence of fractures in 1st mode shape is continued for 2nd, 3rd and 4th mode shape at same location but the most effects were happened in first mode.
- After retrofitting with FRP, there are not a lot of fractures in all mode shapes
- With regards to unknown situation, the data of 1st, 3rd and 4th modes are discarded for average percentage in Table 17.

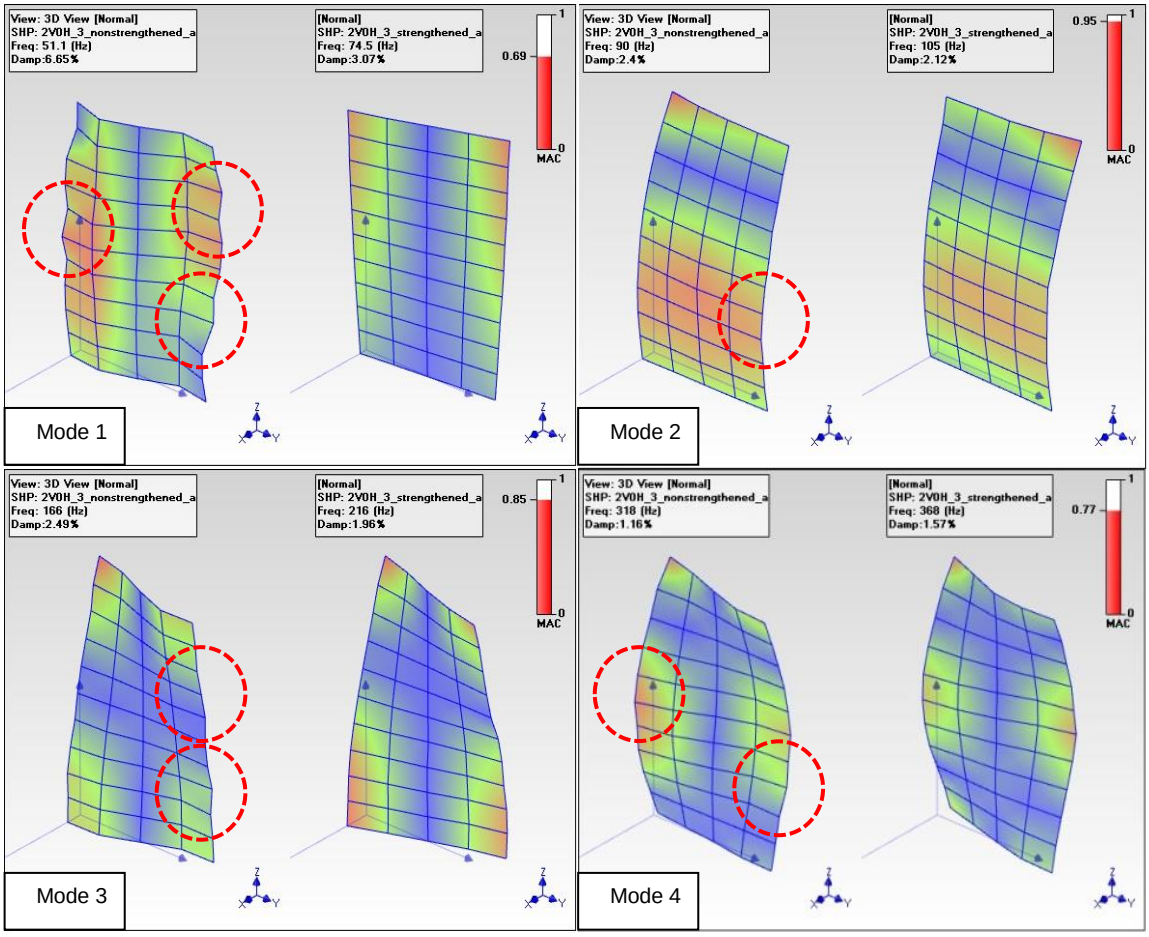

Figure 68 - Mode shapes of 2V0H_3 specimen

The mode shapes can be visualized and animated by using the models prepared as mentioned in section 5.1. Figure 68, Figure 69 and Figure 70 present the results of non-strengthened and strengthened specimens concerning the mode shape configurations through the MAC values.

It is clear the first modal displacement for all specimens occurs in vertical direction (1st Lateral mode shape around z-direction), while the 2nd mode shape corresponds to horizontal direction (1st Bending mode shape around y-direction). Also the third and fourth mode shapes of 2V0H_1 and 2V0H_2 are compounded from 1st and 2nd mode shapes whereas they are appeared in Mode 4 and 6 for 2V0H_3 specimens.

Figure 70 shows the third mode of 2V0H_2 specimen is 2nd bending mode shape because the vertical is changed to diagonal nodal line situation under accelerometer position as discussed before. Also the 2nd and 3rd bending mode shapes are not excited for the 2V0H_1 and 2V0H_3 specimens due to location of accelerometer as can be seen in Figure 68 and Figure 69.

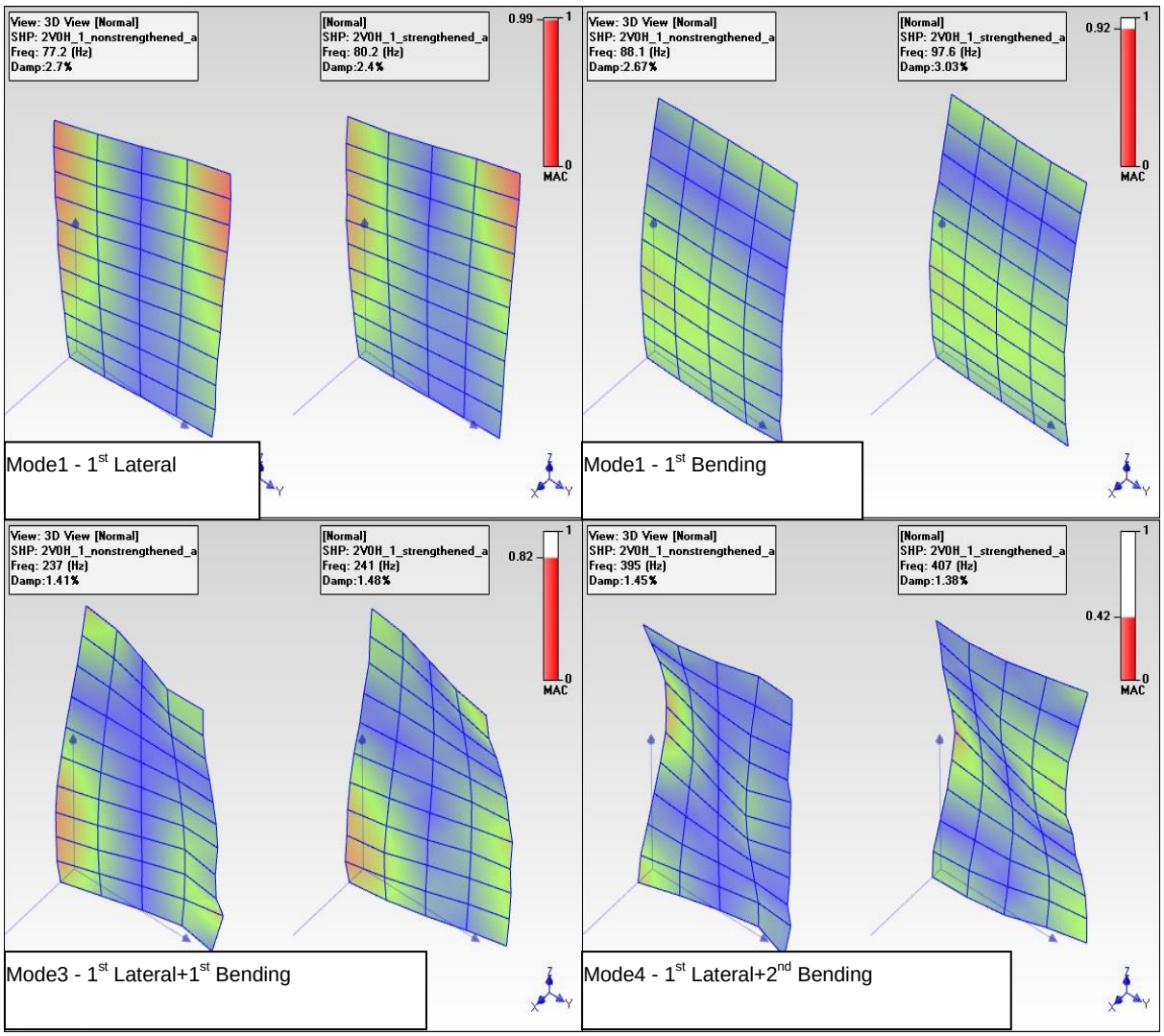

Figure 69 - Mode shapes of 2V0H_1 specimen

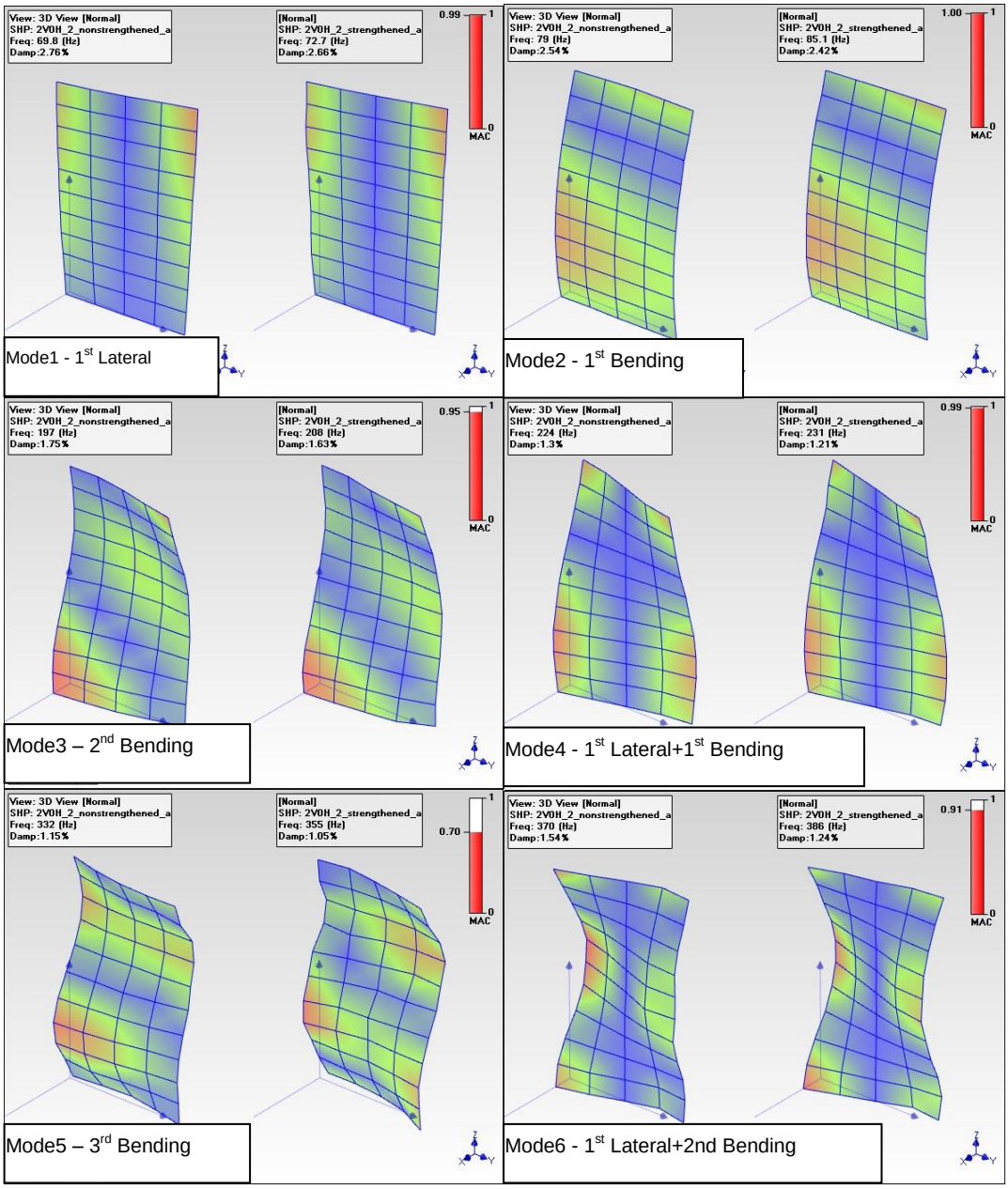

Figure 70 - Mode shapes of 2V0H_2 specimen

In Figure 71 the MAC Value of tests 2V0H are plotted for comparison. Most effective contribution of MAC value is seen on all modes except 1st mode shape of 2V0H_3 due to homogenizing that mentioned in pervious part. However, the MAC value shows the effect of strengthening is more significant for the lower modes, when the mode is getting higher frequency after strengthening and the MAC value is low. Hence, all mode shapes correlation is acceptable. It should be mentioned the 4th mode shape of 2V0H_1 is low but it is independent mode shape. Finally, all of MAC values are presented in animation of specimens when they are compared together.

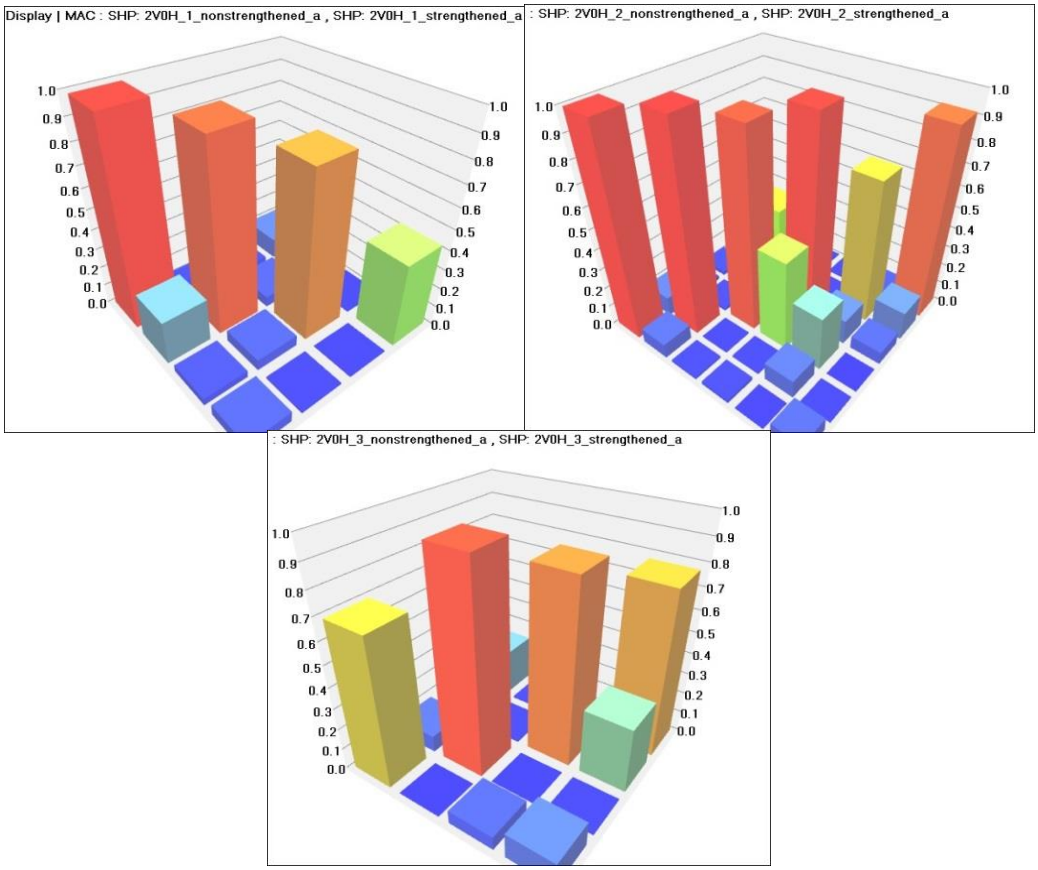

Figure 71 - Graph of MAC value for 2V0H specimens

b) 2V2H specimens

Table 18 and Figure 72 have summarized the frequency values, increased frequencies and some mode shape. Generally, the differences of frequencies have gone up and two mode shapes are disappeared. The 6th mode (1st Lateral+2nd Bending) of 2V2H_1 is hidden after strengthening due to no exciting in this location of accelerometer or increasing markedly and going out from frequency domain. The 2nd mode (1st Bending) of 2V2H_3 is disappeared before applying FRP because the FRP was made more homogeneous masonry, and then the 2nd mode (1st Bending) is separated as independent mode and it can be seen in Figure 72. In the 2V2H_2 specimen, the 2nd Bending mode shape in positive direction and negative direction are presented in Figure 72. It should be specified it is not possible to say that is torsional mode shape because the top and bottom movements are in the same direction. However, the strengthening is caused the nodal line be rotated in negative direction at the mode 3 (2nd Bending mode shape) in 2V2H_2 specimen. Due to separation of 2nd Bending mode shape in positive and negative direction (2V2H_2 specimen), they are deleted from the difference average values of specimens (the numbers are specified with red color in Table 18).

2V2H_1	**Mode**	**1**	**2**	**3**	**4**	**5**	**6**
	Shape Label	**1st L**	**1st B**	**2nd B**	**1st L+1st B**	**3rd B**	**1st L+2nd B**
	Frequency Units	**(Hz)**	**(Hz)**	**(Hz)**	**(Hz)**	**(Hz)**	**(Hz)**
Non-strengthened_a	Frequency	74.687	84.844	207.550	232.290	352.830	391.640
	Damping ratio (%)	2.690	2.480	1.974	1.453	1.220	1.358
Strengthened_a	Frequency	76.930	89.456	222.940	239.400	378.360	
	Damping ratio (%)	2.663	2.664	1.960	1.614	1.231	
Difference	Frequency	2.243	4.612	15.390	7.110	25.530	
	Damping ratio (%)	-0.027	0.184	-0.014	0.161	0.011	
Difference %	Frequency (%)	3.003	5.436	7.415	3.061	7.236	
2V2H_2*	**Mode**	**1**	**2**	**3**	**4**	**5**	**6**
	Shape Label	**1st L**	**2nd B+**	**2nd B-**	**3rd B**	**1nd L+ 2nd B**	
	Frequency Units	**(Hz)**	**(Hz)**	**(Hz)**	**(Hz)**	**(Hz)**	
Non-strengthened_a	Frequency	70.080	186.000	221.290	311.750	368.440	
	Damping ratio (%)	2.988	2.462	1.908	1.753	0.823	
Strengthened_a	Frequency	72.233	200.730	239.380	337.900	386.630	
	Damping ratio (%)	2.969	2.037	1.923	1.623	1.795	
Difference	Frequency	2.153	14.730	18.090	26.150	18.190	
	Damping ratio (%)	-0.019	-0.425	0.015	-0.130	0.971	
Difference %	Frequency (%)	3.072	7.919	8.175	8.388	4.937	
2V2H_3	**Mode**	**1**	**2**	**3**	**4**	**5**	**6**
	Shape Label	**1st L**	**1st B**	**1st L+1st B**	**3rd B**	**1st L+2nd B**	
	Frequency Units	**(Hz)**	**(Hz)**	**(Hz)**	**(Hz)**	**(Hz)**	
Non-strengthened_a	Frequency	68.301		222.620	312.180	356.920	
	Damping ratio (%)	2.760		1.558	1.651	1.778	
Strengthened_a	Frequency	74.167	81.549	237.360	354.000	385.340	
	Damping ratio (%)	2.781	2.459	1.604	1.423	1.751	
Difference	Frequency	5.866		14.740	41.820	28.420	
	Damping ratio (%)	0.021		0.047	-0.228	-0.027	
Difference %	Frequency (%)	8.588		6.621	13.396	7.963	

2V2H	Mode	1st L	1st B	2nd B	3rd B	1st L+ 1st B	1st L+ 2nd B
Average of Increasing value	Frequency (%)	4.888	5.436	7.415	9.675	4.841	6.449

*: The columns with red color are discarded for average

Table 18 - Summary of frequency and damping estimation for the 2V2H specimens

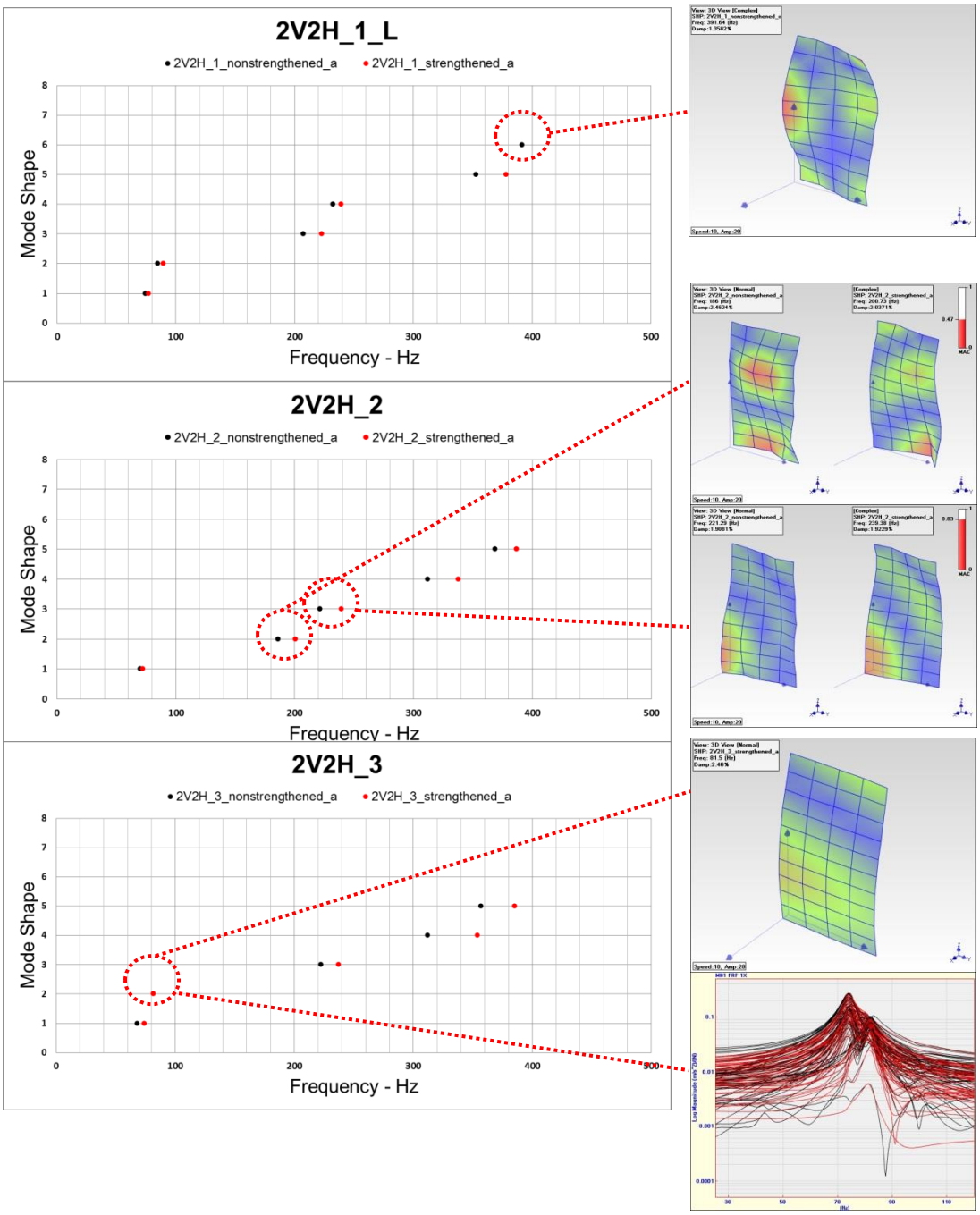

Figure 72 - Comparison of the frequency results for three specimens of 2V2H model

Figure 73 tabulates the difference of frequencies for the first six modes before and after strengthening 2V2H specimens. When the differences were plotted it was found that the disparity of frequency for all 2V2H specimens is steady. Among the three specimens the biggest variance magnitude is 41.82 Hz and 13.39% of 2V2H_3 specimen in 4th mode. However, the lowest difference magnitude is 2.15 Hz and 3.07% of 2V2H_2 wall in the 1st mode as can be expected.

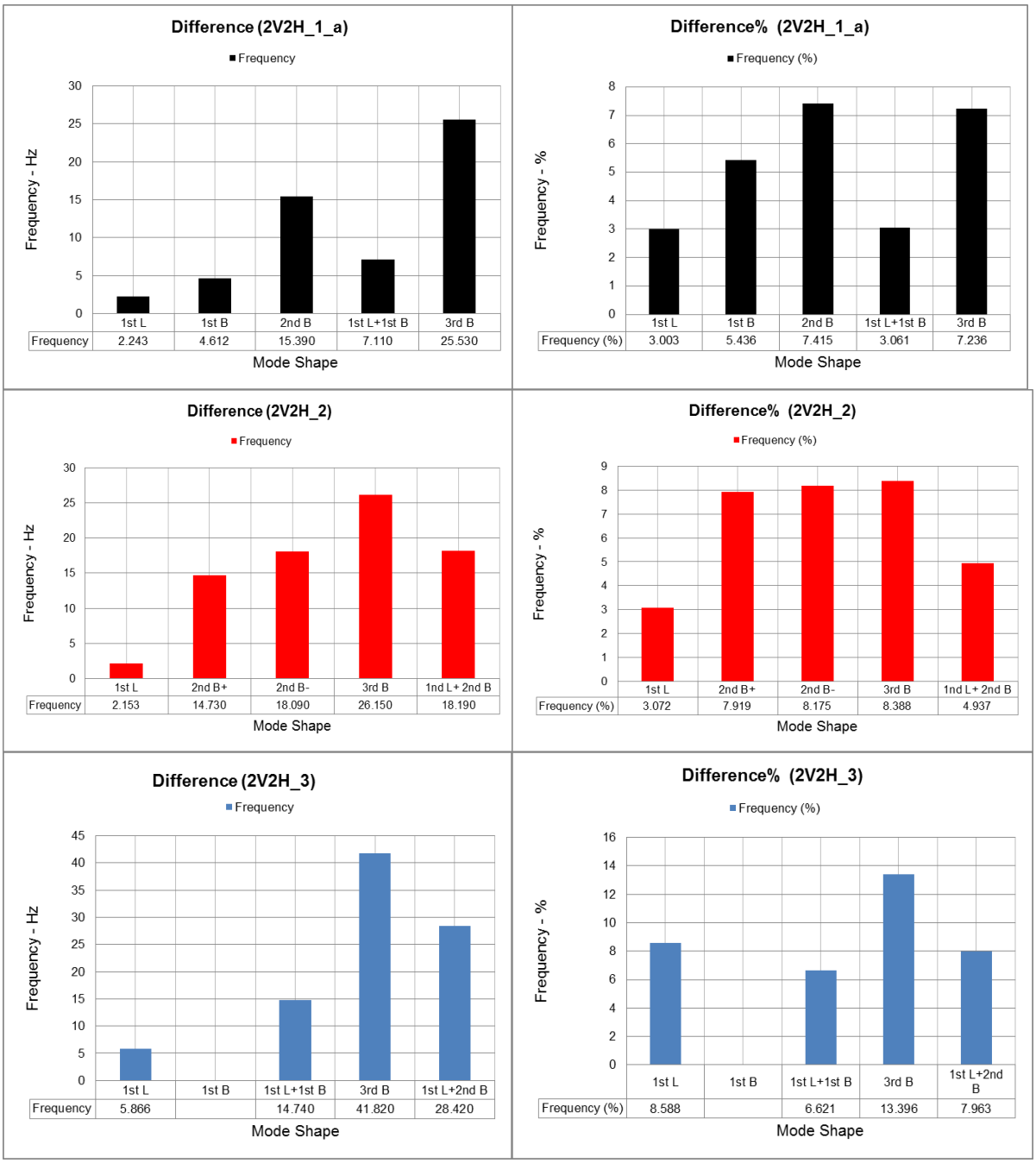

Figure 73 - Comparison of the difference of frequencies for 2V2H specimens in Hz and percentage

c) 3V0H specimens

The date of 3V0H specimens are shown in Table 19. The quality of results in 3V0H_1 is perfect and 5 mode shapes is evaluated. The 3V0H_2 is presented there is a problem in mode 4 (1^{st} Lateral+ 1^{st} Bending) because it could not be estimated the 1^{st} Lateral+ 1^{st} Bending mode before strengthening as seen in Figure 74. Briefly, the condition of repeated roots and closely coupled modes is main reason of this situation as discussed in section 5.2.2.1. However, it could not be considered the homogenizing activity in masonry structure and it is needed some other health monitoring like ultrasonic test. Thus, the results could not be included with this data.

In addition, the FRFs of 3V0H_3_strengthened_a show a compound mode shape in range of 380 to 400 Hz but as not good estimation of FRFs the MAC value is under 0.4 that is low value. So, the results could not be considered as shown with red column in Table 19. The reason is returned to location of accelerometer because it could not receive data from this excited mode. The Figure 74 shows the quality of FRFs.

3V0H_1	**Mode**	**1**	**2**	**3**	**4**	**5**	**6**
	Shape Label	**1st L**	**1st B**	**1st L+1st B**	**3rd B**	**1st L+2nd B**	
	Frequency Units	**(Hz)**	**(Hz)**	**(Hz)**	**(Hz)**	**(Hz)**	
Non-strengthened_a	Frequency	77.056	81.738	243.980	369.150	410.420	
	Damping ratio (%)	2.541	2.477	1.193	1.398	1.088	
Strengthened_a	Frequency	79.943	90.040	252.730	394.580	427.090	
	Damping ratio (%)	2.372	2.272	1.215	1.290	1.275	
Difference	Frequency	2.887	8.302	8.750	25.430	16.670	
	Damping ratio (%)	-0.169	-0.205	0.022	-0.109	0.186	
Difference %	Frequency (%)	3.747	10.157	3.586	6.889	4.062	
3V0H_2	**Mode**	**1**	**2**	**3**	**4**	**5**	**6**
	Shape Label	**1st L**	**1st B**	**2nd B**	**1st L+1st B**		
	Frequency Units	**(Hz)**	**(Hz)**	**(Hz)**	**(Hz)**		
Non-strengthened_a	Frequency	76.072	87.192	223.880			
	Damping ratio (%)	2.575	2.528	1.729	262.360		
Strengthened_a	Frequency	85.832	104.640	246.290	1.528		
	Damping ratio (%)	2.360	2.229	1.415			
Difference	Frequency	9.760	17.448	22.410			
	Damping ratio (%)	-0.216	-0.298	-0.314			
Difference %	Frequency (%)	12.830	20.011	10.010			
3V0H_3*	**Mode**	**1**	**2**	**3**	**4**	**5**	**6**
	Shape Label	**1st L**	**1st B**	**1st L+1st B**	**1st L+2nd B**		
	Frequency Units	**(Hz)**	**(Hz)**	**(Hz)**	**(Hz)**		
Non-strengthened_a	Frequency	71.055	86.587	229.380	388.550		
	Damping ratio (%)	2.904	2.518	2.055	2.348		
Strengthened_a	Frequency	73.786	95.525	236.030	407.610		
	Damping ratio (%)	2.714	2.325	1.425	2.194		
Difference	Frequency	2.731	8.938	6.650	19.060		
	Damping ratio (%)	-0.190	-0.193	-0.630	-0.155		
Difference %	Frequency (%)	3.844	10.323	2.899	4.905		

3V0H	Mode	1st L	1st B	2nd B	3rd B	1st L+ 1st B	1st L+ 2nd B
Average of Increasing value	Frequency (%)	6.807	13.497	10.010	6.889	3.243	4.062

*: The columns with red color are discarded for average

Table 19 - Summary of frequency and damping estimation for the 3V0H specimens

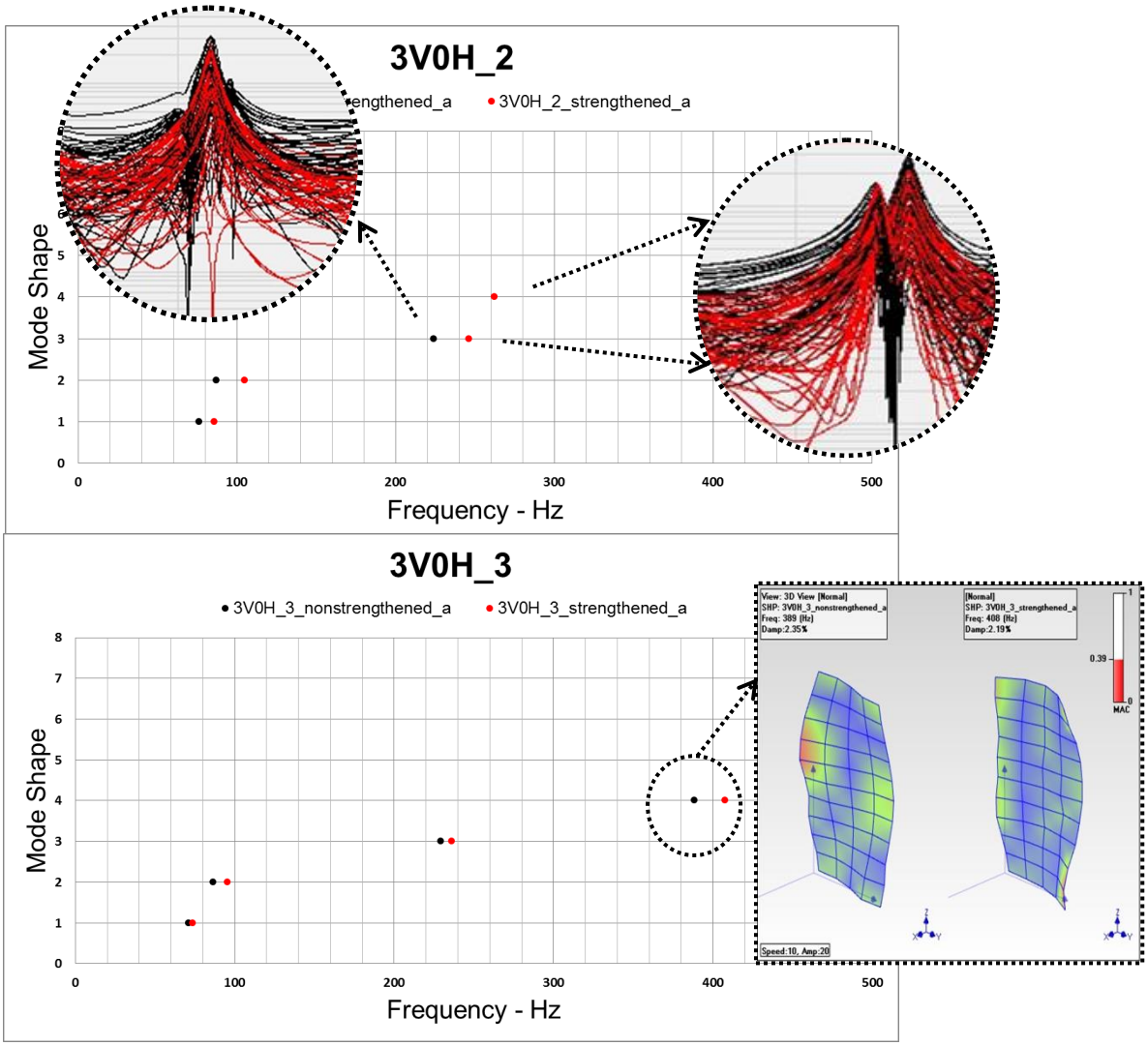

Figure 74 - Vague mode shapes of 3V0H specimens

d) 3V5H specimens

Considering the mode 1 (1st lateral) of 3V5H_1 specimen, difference in frequencies between two tests (179.99%) exhibits very high values in comparison 20% or 27% of increasing frequency for other specimens. Assuming that the geometric definition of the model is correct, source of difference can be addressed to inappropriate estimation of masonry homogenizing. However, all of condition was suitable for these tests and specimen. Figure 75 shows all FRFs, mode shapes and MAC values. Only the results for the first specimen are presented by figure because the influence is significant for other cases. However, Table 5-7 shows all of results for 3V5H pattern.

3V5H_1*	**Mode**	**1**	**2**	**3**	**4**	**5**	**6**
	Shape Label	**1st L**	**1st B**	**1st L+1st B**	**2nd B**	**1st L+2nd B**	**3rd B**
	Frequency Units	**(Hz)**	**(Hz)**	**(Hz)**	**(Hz)**	**(Hz)**	**(Hz)**
Non-strengthened_a	Frequency	27.712	81.104	143.490	199.100	303.970	337.420
	Damping ratio (%)	7.236	2.595	1.841	1.694	0.855	0.996
Strengthened_a	Frequency	77.592	102.070	235.200	324.700	405.320	
	Damping ratio (%)	2.713	2.182	1.471	1.372	1.177	
Difference	Frequency	49.880	20.966	91.710	125.600	101.350	
	Damping ratio (%)	-4.522	-0.414	-0.370	-0.322	0.322	
Difference %	Frequency (%)	179.994	25.851	63.914	63.084	33.342	
3V5H_2	**Mode**	**1**	**2**	**3**	**4**	**5**	**6**
	Shape Label	**1st L**	**1st B**	**1st L+1st B**	**2nd B**	**1st L+2nd B**	
	Frequency Units	**(Hz)**	**(Hz)**	**(Hz)**	**(Hz)**	**(Hz)**	
Non-strengthened_a	Frequency	50.203	87.699	162.090	220.520	264.600	
	Damping ratio (%)	5.027	2.461	2.051	1.877	2.038	
Strengthened_a	Frequency	64.100	102.700	192.760	285.040	330.290	
	Damping ratio (%)	4.157	2.233	2.348	1.628	2.010	
Difference	Frequency	13.897	15.001	30.670	64.520	65.690	
	Damping ratio (%)	-0.871	-0.229	0.297	-0.249	-0.028	
Difference %	Frequency (%)	27.682	17.105	18.922	29.258	24.826	
3V5H_3	**Mode**	**1**	**2**	**3**	**4**	**5**	**6**
	Shape Label	**1st L**	**1st B**	**1st L+1st B**			
	Frequency Units	**(Hz)**	**(Hz)**	**(Hz)**			
Non-strengthened_a	Frequency	72.077	84.344	217.880			
	Damping ratio (%)	2.808	2.582	1.676			
Strengthened_a	Frequency	86.658	103.860	260.760			
	Damping ratio (%)	2.453	2.094	1.297			
Difference	Frequency	14.581	19.516	42.880			
	Damping ratio (%)	-0.355	-0.488	-0.379			
Difference %	Frequency (%)	20.230	23.139	19.681			
3V5H	**Mode**	**1st L**	**1st B**	**2nd B**	**3rd B**	**1st L+ 1st B**	**1st L+ 2nd B**
Average of Increasing value	Frequency (%)	75.969	22.031	46.171		34.172	29.084

*: The columns with red color are discarded for average

Table 20 - Summary of frequency and damping estimation for the 3V5H specimens

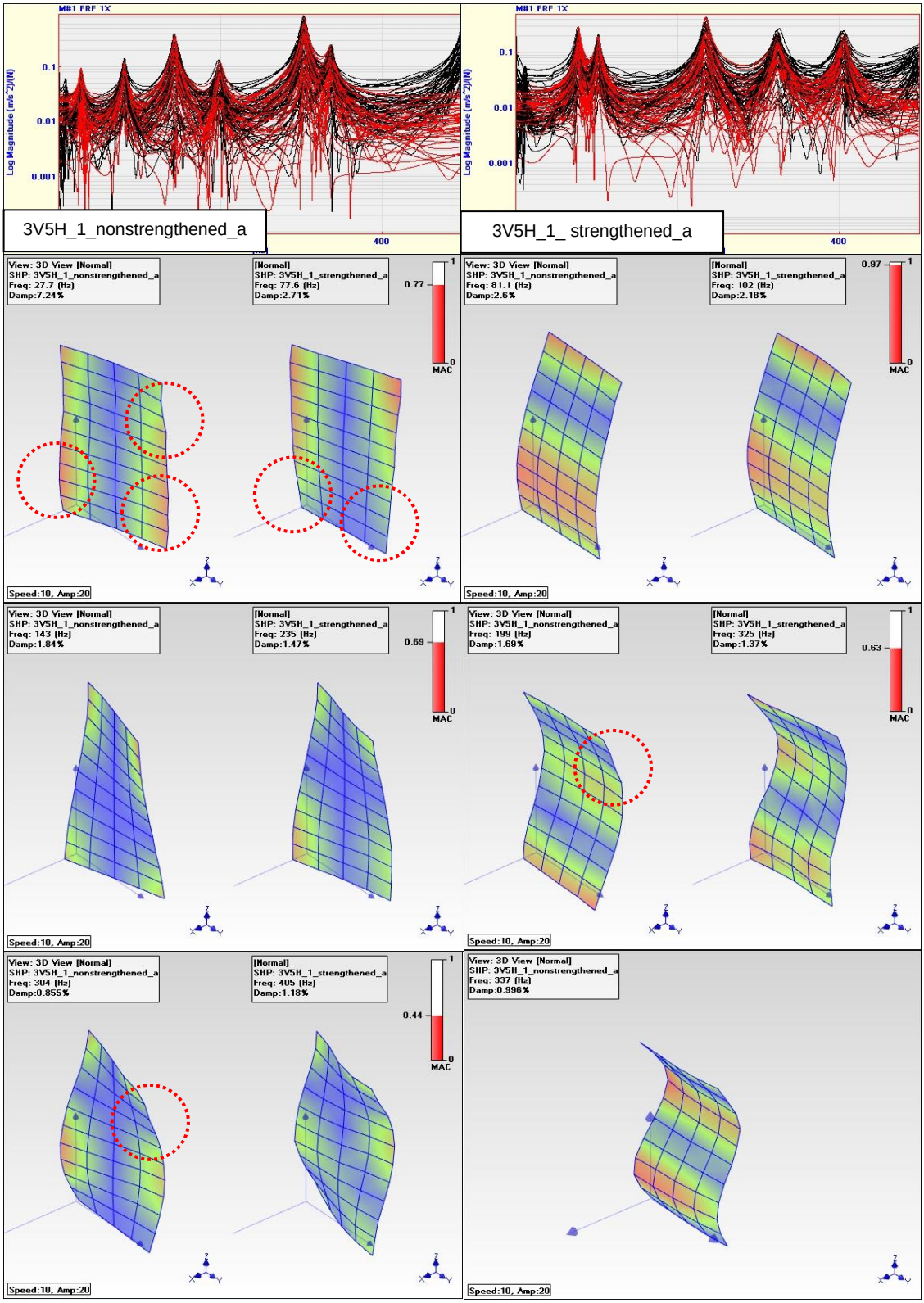

Figure 75 - Comparison between the non-strengthened and strengthened 3V5H_1 specimen (influence of homogenizing after strengthening)

e) 3I3I specimens

The frequency response spectrum of 3I3I_1 represented below can be used to easily evaluate the data and to locate the peaks which indicate resonant frequencies. Before strengthening, it is possible to identify peaks between 70-80, 200-210, 335-345, 340 and at 390 Hz although there are two peaks in 70-80 Hz that are Closely Coupled modes. So, judging on these values natural frequencies are expected in those ranges that are six modes. However, there are just three modes after strengthening of 3I3I_1 specimen as shown in Figure 76 and Table 21. In 3I3I_3 specimen, it has been realized that the second modal displacement is not excited completely (16 FRFs are excited among 55 FRFs) and the FRFs are reached after strengthening as can be seen in Figure 76 and Table 21.

Table 21 - Summary of frequency and damping estimation for the 3I3I specimens

3I3I_1	**Mode**	**1**	**2**	**3**	**4**	**5**	**6**
	Shape Label	**1st L**	**1st B**	**2nd B**	**1st L+1st B**	**3rd B**	**1st L+2nd B**
	Frequency Units	**(Hz)**	**(Hz)**	**(Hz)**	**(Hz)**	**(Hz)**	**(Hz)**
Non-strengthened_a	Frequency	71.680	77.569	204.420	223.140	339.280	388.970
	Damping ratio (%)	2.750	2.638	1.861	1.635	1.660	1.674
Strengthened_a	Frequency	90.250	102.560		274.410		
	Damping ratio (%)	2.881	2.306		1.235		
Difference	Frequency	18.570	24.991		51.270		
	Damping ratio (%)	0.131	-0.332		-0.400		
Difference %	Frequency (%)	25.907	32.218		22.977		
3I3I_2	**Mode**	**1**	**2**	**3**	**4**	**5**	**6**
	Shape Label	**1st L**	**1st B**	**1st L+1st B**	**1st L+2nd B**		
	Frequency Units	**(Hz)**	**(Hz)**	**(Hz)**	**(Hz)**		
Non-strengthened_a	Frequency	72.884	78.278	225.490	385.730		
	Damping ratio (%)	2.637	2.500	1.251	1.242		
Strengthened_a	Frequency	88.723	99.945	272.830	491.970		
	Damping ratio (%)	3.423	2.051	1.248	1.010		
Difference	Frequency	15.839	21.667	47.340	106.240		
	Damping ratio (%)	0.786	-0.449	-0.003	-0.233		
Difference %	Frequency (%)	21.732	27.680	20.994	27.543		
3I3I_3	**Mode**	**1**	**2**	**3**	**4**	**5**	**6**
	Shape Label	**1st L**	**1st B**	**1st L+1st B**	**1st L+2nd B**		
	Frequency Units	**(Hz)**	**(Hz)**	**(Hz)**	**(Hz)**		
Non-strengthened_a	Frequency	68.474		224.130	379.550		
	Damping ratio (%)	2.830		1.315	1.354		
Strengthened_a	Frequency	79.906	243.260	266.910	460.740		
	Damping ratio (%)	2.568	1.808	1.513	1.303		
Difference	Frequency	11.432		42.780	81.190		
	Damping ratio (%)	-0.262		0.199	-0.051		
Difference %	Frequency (%)	16.695		19.087	21.391		
3I3I	**Mode**	**1st L**	**1st B**	**2nd B**	**3rd B**	**1st L+ 1st B**	**1st L+ 2nd B**
Average of Increasing value	Frequency (%)	21.445	29.949			21.019	24.467

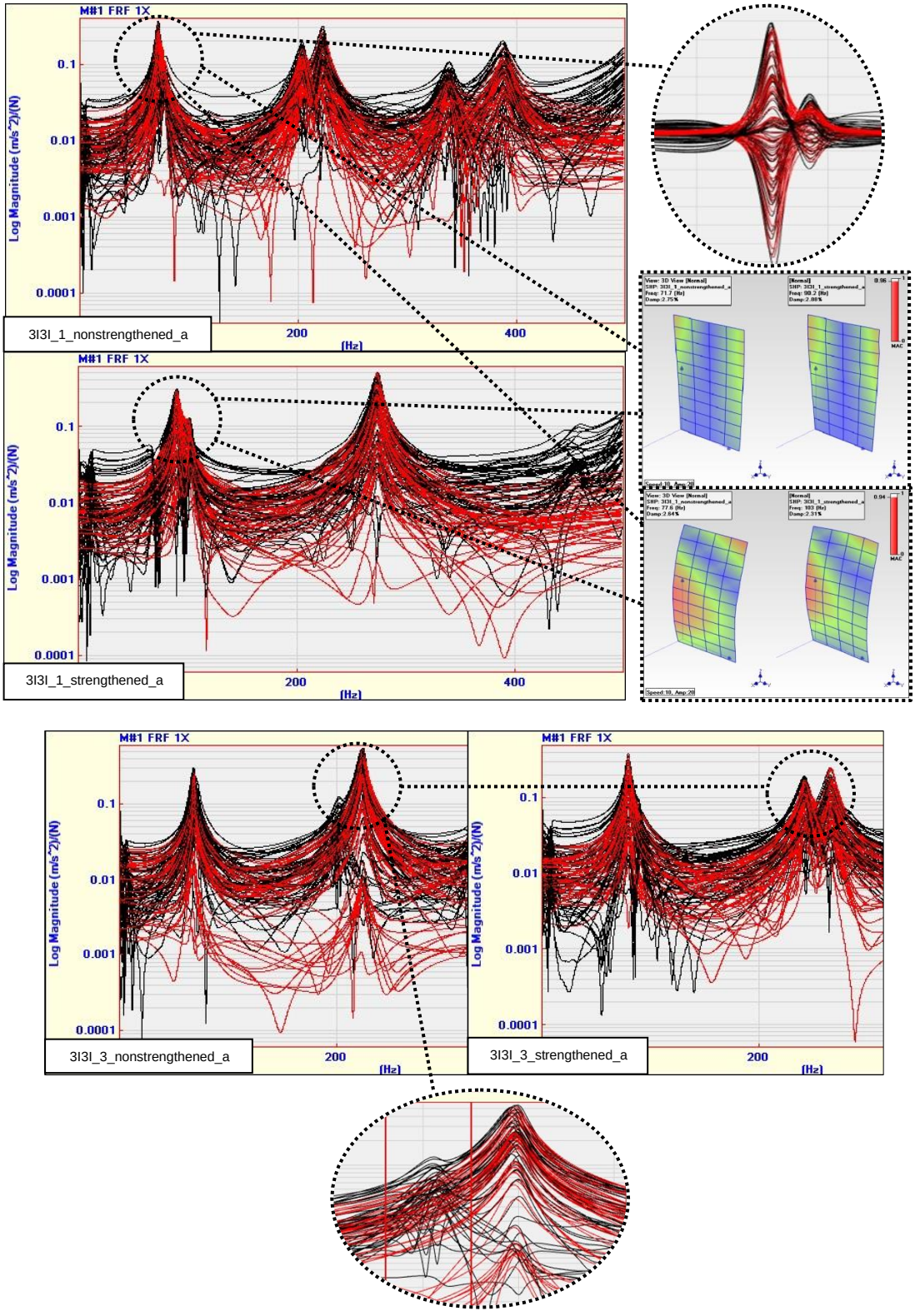

Figure 76 - FRFs of 3V3I_1 and 3I3I_3 specimens

5.2.2.2 Damping ratio parameter

Figure 77 and Table 17 to Table 21 are presented the damping ratio as second modal parameter to be evaluated. As can be seen, it is difficult to estimate a general relationship for damping ratio before and after strengthening with comparison the result of other 26 tests. Also, Salawu and Williams (1995) compared the damping parameter before and after strengthening of a concrete bridge and there was not clear relation to be established general behavior between structural improvement and damping ratio. Moreover, Park et al. (2006) stated that the effect of the damping change to the resonant frequencies is negligibly small in general. The average values of difference of damping ratio consecutively are 0.015, -0.137 and -1.00 % for 2V0H_1, 2V0H_2 and 2V0H_3 specimens.

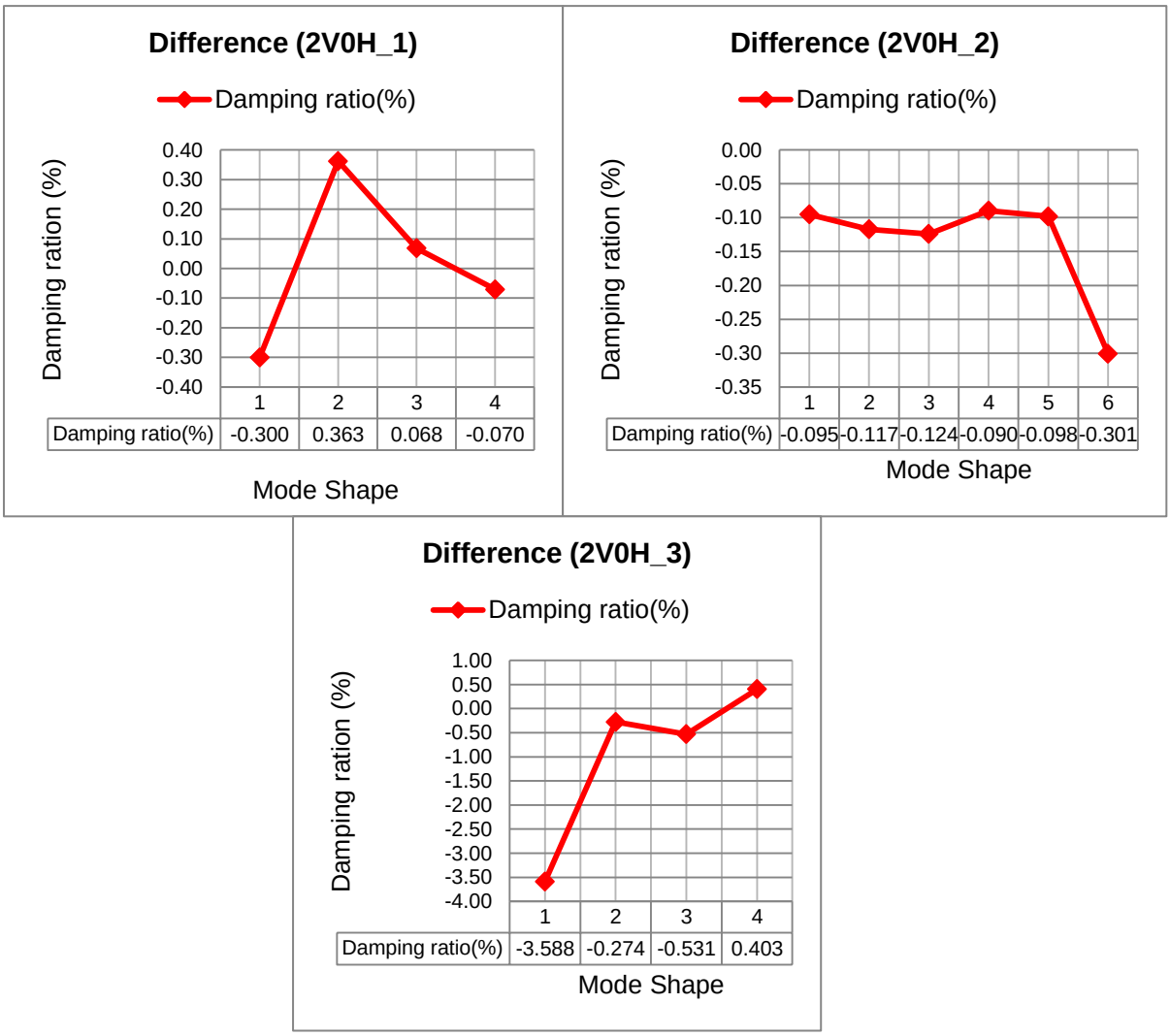

Figure 77 - Difference of damping ratio for the 2V0H_1, 2V0H_2 and 2V0H_3 specimens

5.2.3 Comparison the results of specimens

To compare the main objective of experiment and making a comparison between the identification of strengthening and non-strengthening experimental results, the average percentage of increasing frequencies are considered for five FRP patterns. For modal comparison, only the similar modes were selected because it is necessary to be specified the frequency difference of walls in same FRP pattern and same mode shape and also accurate estimation in experimental analysis is more important. Table 22 and Figure 78 represent the discrepancy of six common modes with regards to five FRP patterns. Finally, the results will be compared from three viewpoints; 1- Amount of FRP, 2- Influence of vertical and horizontal positions in FRP patterns and 3- Influence of angle on FRP patterns.

	Modes						
FRP patterns	Difference of frequencies %	1st L	1st B	2nd B	3rd B	1st L+2nd B	1st L+2nd B
	2V0H	4.02	11.64	6.04	6.92	2.53	3.62
	2V2H	4.89	5.44	7.42	9.68	4.84	6.45
	3V0H	6.81	13.50	10.01	6.89	3.24	4.06
	3V5H	23.96	20.12	29.26		19.30	24.83
	3I3I	21.44	29.95			21.02	24.47

Table 22 - Comparison the difference average of frequencies for each mode shape

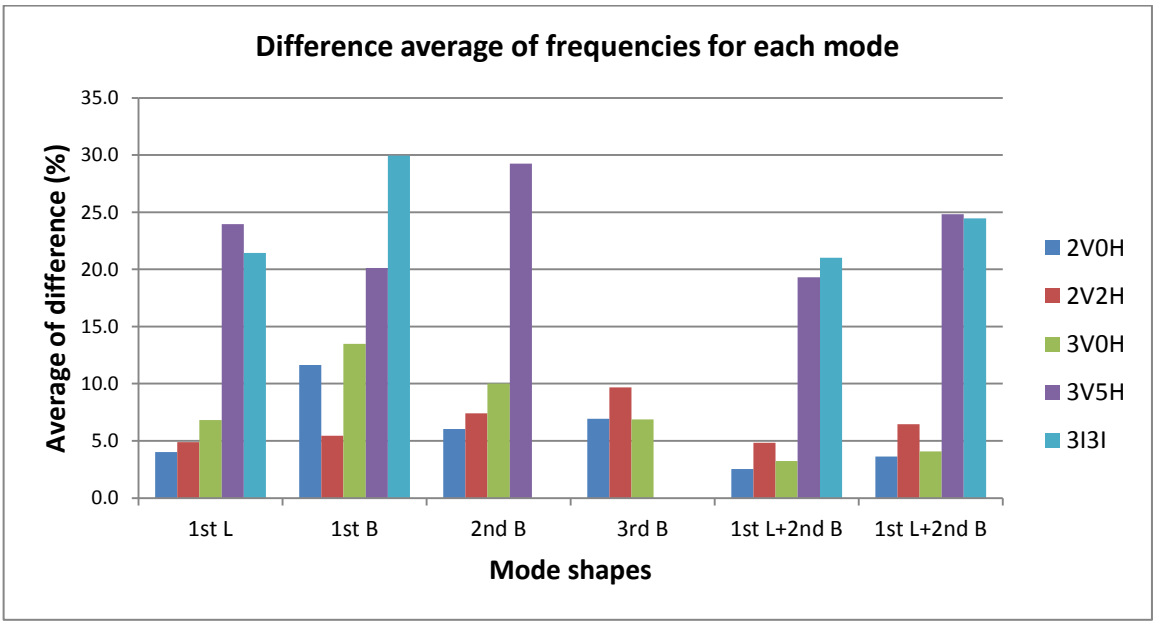

Figure 78 - Comparison the difference average of frequencies for each mode shape

5.2.3.1 Amount of FRP

Table 23 and Figure 79 compare the increasing frequency values obtained from the experiments whereas the amount of FRP is important to use minimum length of FRP with high efficiency of strengthening. The experimental results are the average values of the results from 2V0H and 3V0H patterns.

The bar graph illustrates increasing frequency in percent for selected 2V0H and 3V0H FRP patterns. Generally speaking, the most significant feature is that difference of frequency has boomed in almost mode shapes from 2V0H to 3V0H. First bending mode, in the most 2nd mode position, has far more increasing frequency than any other modes in the graph, starting from 11.64% to 13.5% in 3V0H. However, the growth of 2nd bending mode has been much more eye-catching in the modes. On the other hand, the 1st lateral+ 2nd bending mode has the least increasing, less than 0.44% in the 2V0H and 3V0H patterns; however, it is compound mode and can be significant in masonry walls. The discrepancy of 3rd bending mode was fixed and it is not important due to last single mode. In summary, while most of the modes show an increase, first lateral mode still maintains its position as the major modes of wall. In real masonry wall, it should be calculated the costs of strengthening and average 2.79 percent increasing frequency in 1st mode shape how much would be valuable from viewpoint of economy.

Modes						
Difference of frequencies %	**1st L**	**1st B**	**2nd B**	**3rd B**	**1st L+2nd B**	**1st L+2nd B**
2V0H	4.02	11.64	6.04	6.92	2.53	3.62
3V0H	6.81	13.50	10.01	6.89	3.24	4.06
divergence	2.79	1.86	3.97	-0.03	0.71	0.44

Table 23 - Comparison the difference average of frequencies and amount of FRP

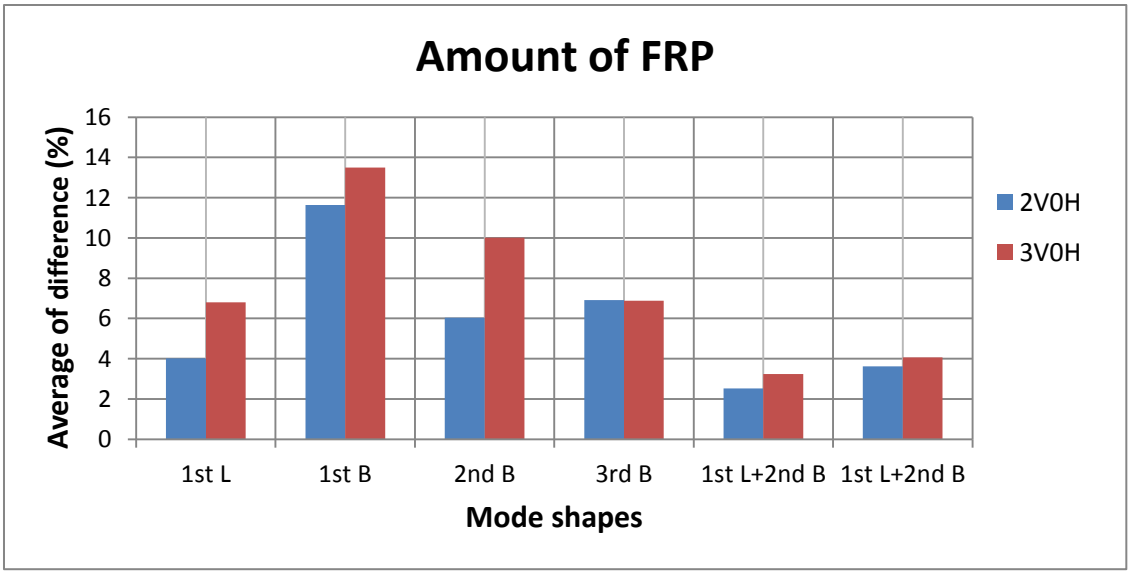

Figure 79 - Comparison the difference average of frequencies and amount of FRP

5.2.3.2 Comparison the grid and vertical patterns

As it was discussed in chapter 3, the data and difference of frequencies should be compared in the similar way. Table 24, Figure 80 and Figure 81 present the estimated frequency rates of single and compound mode shapes for grid and vertical patterns. Overall, the modes of 2V2H are increased substantially in front of 2V0H. Also, one notable trend seems to be that 2V2H pattern has steady become stiffer as applying FRP. Having considered the Table 24, it can be deduced that in both single and compound modes, the largest number of increasing frequency belongs to 2V0H. However, this situation could be influence of extra FRP with regard to section 5.2.3.2. Briefly, the 2V2H grid pattern has had an almost 2% increase in the 5 modes if the 1st bending mode is not considered.

It should be maintained the duty of vertical patterns in comparison with grid pattern is avoidance of the bending mode shapes with regard to 1st bending mode in Figure 80 and section 5.2.3.2. Considering Figure 81, the 1st lateral mode shape is provided the effect of 3V5H patterns is dramatically high with respect to other modes because the first mode shape has always associated the maximum energy. In addition, Table 24 shows the highest divergence of frequencies in 3V5H and 3V0H patterns that is 20.76%. It can be conclude the efficiency of 3V5H in comparison with 2V2H is better due to its influence on the lateral modes and rate of difference of frequencies.

Modes						
Difference of frequencies %	**1st L**	**1st B**	**2nd B**	**3rd B**	**1st L+2nd B**	**1st L+2nd B**
2V0H	4.02	11.64	6.04	6.92	2.53	3.62
2V2H	4.89	5.44	7.42	9.68	4.84	6.45
divergence	0.87	-6.21	1.37	2.75	2.31	2.83
Modes						
Difference of frequencies %	**1st L**	**1st B**	**2nd B**	**3rd B**	**1st L+2nd B**	**1st L+2nd B**
3V0H	6.81	13.50	10.01	6.89	3.24	4.06
3V5H	23.96	20.12	29.26		19.30	24.83
divergence	17.15	6.63	19.25	---	16.06	20.76

Table 24 - Comparison the difference average of frequencies for grid and vertical patterns

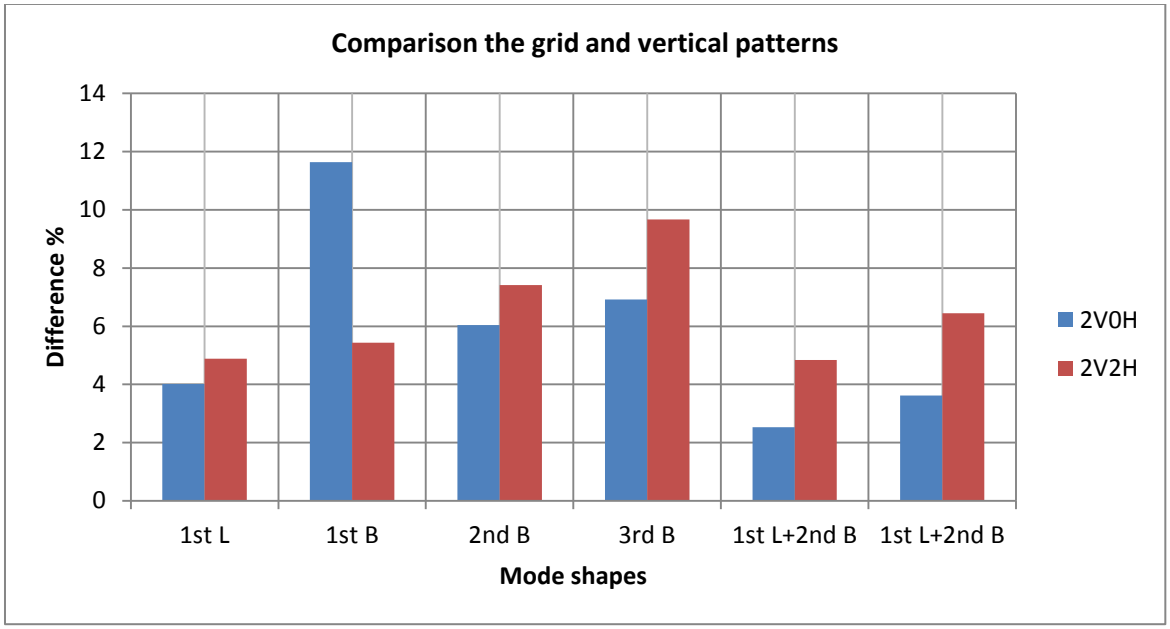

Figure 80 - Comparison the difference average of frequencies for grid and vertical patterns (2V0H-2V2H)

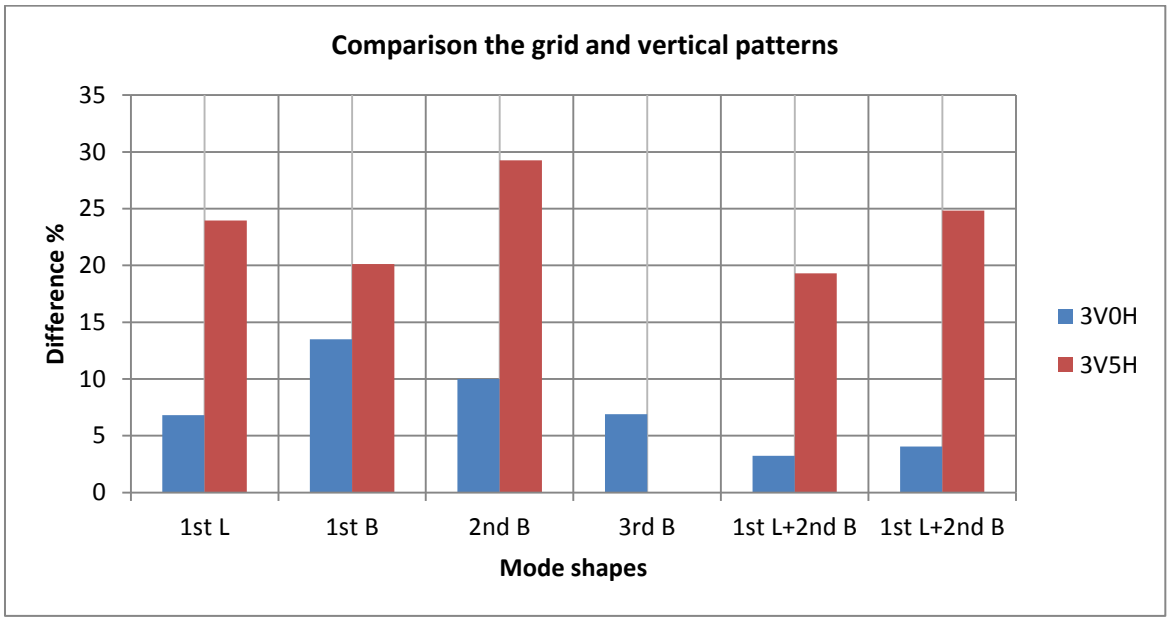

Figure 81 - Comparison the difference average of frequencies for grid and vertical patterns (3V0H-3V5H)

5.2.3.3 Influence of angle on FRP patterns.

The graph of mode shapes versus the difference of frequencies with 3I3I pattern (angles are 30-60 degrees) and 3V5H (angle is 90 degrees) was plotted based on the data obtained from the average of difference and is seen in Figure 82. The eight bars show the increasing frequencies of the specimen are more than 20% and close to each other. It can be noted that except 1st bending mode, the other

modes could not be compared exactly because the trend of difference of frequency is complicated in general and exponential trend-lines are similar. In addition, it can be mentioned 8.31 and 6.91 meters FRP material were used for 3V5H and 3I3I patterns, respectively. In brief, the efficiency of 3I3I pattern is higher than 3V5H because around 17% materials have been used more. Also, the rate of 1st Bending mode in 3I3I pattern is 29% that can be inducted using FRP in angle patterns is much more economical to control the dynamic behavior of masonry walls.

Modes						
Difference of frequencies %	**1st L**	**1st B**	**2nd B**	**3rd B**	**1st L+2nd B**	**1st L+2nd B**
3V5H	23.96	20.12	29.26		19.30	24.83
3I3I	21.44	29.95			21.02	24.47
divergence	-2.51	9.83	----	----	1.72	-0.36

Table 25 - Comparison the difference average of frequencies for angle (30-60 and 90)

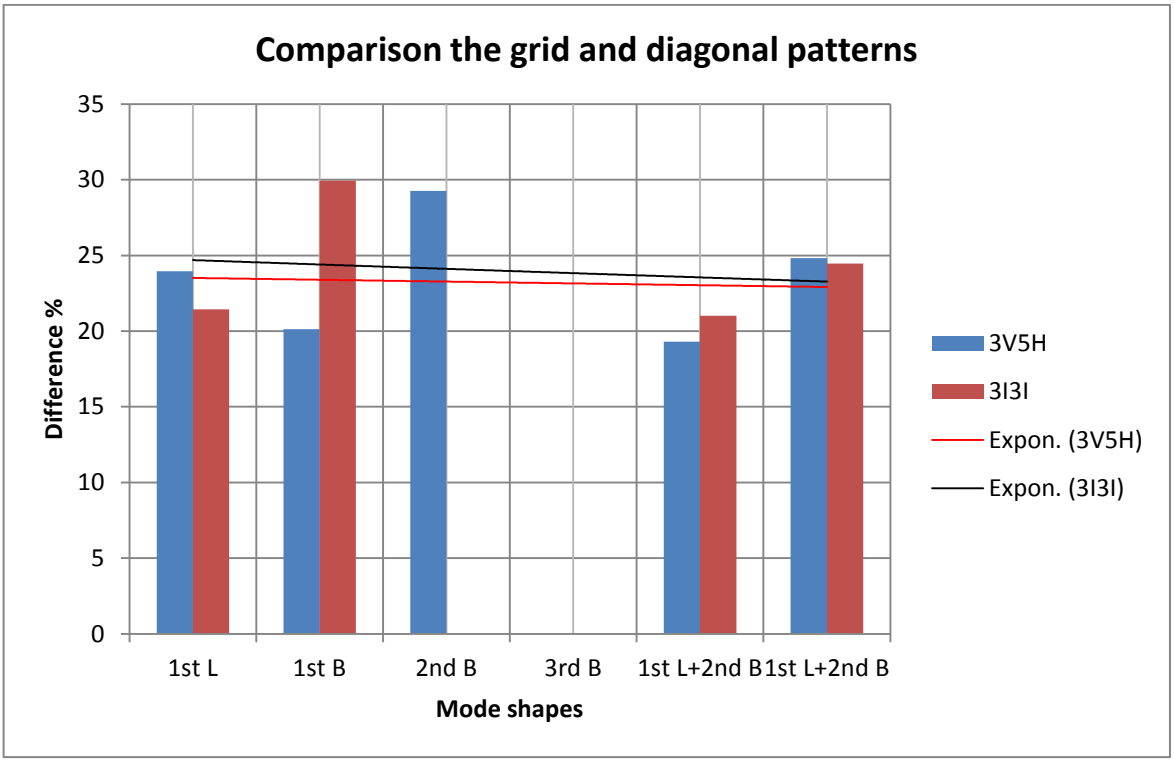

Figure 82 - Comparison the difference average of frequencies for angle (30-60 and 90)

6. CONCLUSIONS

Regards to the non-destructive tests, this research was carried out to identify the mechanical response of FRP strengthened brickwork walls with modal testing. The work was divided in three parts: a) a review about studying the scientific basis of the modal analysis, the data acquisition procedures and the post-processing theoretical formulation; b) defining the vibration tests and FRP patterns; c) applying FRP, performing the tests and obtaining relevant data for the mechanical characterization of the brickwork wall before and after the strengthening; Next, the main conclusions from the experiment are presented with proposing feasible improvements.

6.1 Dynamic experimental testing

- It was obtained in among of this experiment (Modal Testing) that the minimum space and equipment is required to carry out the test in comparison with other tests. Also, to measure the elements of masonry structure it would be better the measuring starts from centroid of elements.
- The results of non-strengthened and strengthened 2V2H_1 specimen at 2 positions of accelerometer show that the frequency associated with each mode is independent and equal. This condition was kept after applying FRP. However, the position of accelerometer have affected on the displacement direction (nodal line) of walls in some modes. For avoiding and calibrating the errors, supports of the accelerometer should be checked properly to avoid undesired noise. Moreover, frequencies record was taken in 55 points with 2 impacts of hammer. The coherence of 2 hammer impact and number of DOFs were checked between 2 impacts and among test. Records were pre-processed in the field to check the quality of the measurements. Finally, the sensitivity of frequency has been setup at 0.3125 Hz to have maximum accuracy meanwhile the minimum difference of frequency was around 2 Hz before and after strengthening.
- The applying primer was carried out in different times and one package of primer was used for each time because the process should be occurred maximum in 20 minutes. The best way to apply primer is to brush surface of walls like painting. For normal masonry walls, the average thickness of the primer layer should be between 1 and 2 mm. Then, the process of applying FRP usually was occurred 24 hours after applying primer. It is not necessary to apply primer for attaching two FRPs together. It should be mentioned, one package, around 5 kg primer, was a lot for five or seven walls with these dimensions in each time. So, it is better to get help from 6 workers for brushing. If there are not enough workers it should be painted whole of walls instead of locations of FRP on walls because it is faster and more useful for applying FRP with adhesive.

- Experimental dynamic identification tests should be performed with care in order to obtain reliable data. However, it was a very effective tool in determining the dynamic properties of a structure with regard to results of 15 specimens which was the main objective of this experiment. As computation time and cost decrease with the advent of new technology, it is natural that this kind of method should be developed for behavior of other masonry elements like arch and vault. Also, input-output modal analysis can be an attractive tool for historical construction and masonry elements.

6.2 Analysis of data and results

- It is most absolutely clear that the application of FRP to unreinforced masonry structures is feasible. The results show the masonry and historical constructions under dangerous situation could be preserved as soon as possible. In this case, masonry walls have been reached in strengthened condition with minimum 8 days for minimum 2.53 % frequency increasing as a dynamic parameter.
- In this experience 32 tests were carried out and there was possibility to make coherence among 30 tests (The trend of data was similar). However, source of difference in 2 tests can be addressed to inappropriate estimation of masonry homogenizing. This research shows if there is problem with the material, mortar or producing, it is possible to know. In the other hand, the system of strengthening was worked and modal testing was reacted very high. For example one of them around 75% increasing frequency has been shown after strengthening (3V5H_1 specimen) which is can be related to homogenizing.
- Totally, the Frequency Response Function (FRF) of walls has clear peaks; therefore the frequencies can be determined without difficulty. The first's natural frequencies of specimens are experimentally identified by measuring the FRF with manually applied horizontal impact. The mode shapes should be considered in the optimization process. Due to the maximum number of DOFs obtained in the experiments, the mode shapes were included in the optimization process that was explained in section 5. However the post-processing was carried out 3 times in limited time. Concerning the damping coefficient, there is a not a trend to its increase or decrease with process of this kind of modal equipment and due to difficulties in parameter estimation the results did not allow a final conclusion.
- The specimens with 2V0H FRP patterns showed the minimum increasing frequency was happened. The magnitude differences of specimens are around (3 to 11 Hz) or (4 to 11.6%) of non-strengthened specimens.
- For modal comparison, only the similar modes were selected because it is necessary to be specified the frequency difference of walls in same FRP pattern and same mode shape

- Regard to amount of FRP, the most significant feature is that difference of frequency has boomed in almost mode shapes from 2V0H to 3V0H. While most of the modes show an increase, the position of the first lateral mode is still important. In real masonry wall, it should be calculated the average of 2.79% increasing in 1st mode shape how much would be valuable from viewpoint of economy with regard to add 33% FRP laminate more.
- Regard to comparison the grid and vertical patterns, the modes of 2V2H are increased substantially in front of 2V0H generally. The 2V2H grid pattern has had an almost 2% increase in the 5 modes. It can be deduced the duty of vertical patterns in comparison with grid pattern is avoidance of the bending mode shapes with regard to 1st bending mode.

  For comparison between 3V0H and 3V5H in grid and vertical patterns, the 1st lateral mode shape is provided the effect of 3V5H patterns is dramatically high with respect to other modes because the first mode shape has always associated the maximum energy. It can be conclude the efficiency of 3V5H in comparison with 2V2H is better due to its influence on the lateral modes and rate of difference of frequencies.
- With respect to influence of angle on FRP patterns, the 3I3I and 3V5H was compared in 30-60 and 90 degrees, respectively. The trend of difference of frequency is complicated and close to each other in general and exponential trend-lines are similar. However, it can be mentioned 8.31 and 6.91 meters FRP were used for 3V5H and 3I3I patterns, respectively. In brief, using FRP in angle of 30-60 degrees pattern is much more economical to control the dynamic behavior of masonry walls.

To sum it up, it has to be said that the main aim of this research has been achieved. The performance of modal analysis at determining the vibrational response of FRP strengthened brickwork walls has been demonstrated. In addition, the influence of the different strengthening patterns has been noticed with this non-destructive testing method.

6.3 Future works

- For identification of the mechanical response of FRP strengthened brickwork walls, it seems that measuring the modal analysis is a good approach for the success of the dynamic parameter identification analysis. However, this experiment should be carried out in real structures. In addition, research needs to develop for behavior of other masonry elements like arch and vault and producing some software or toolbars under MATLAB software to predict the behavior of masonry wall after strengthening. Also, this experiment should be expended with applying FRP on both side of wall regard to load bearing research.

7. REFERENCES

Chopra A. (2001). Dynamics Of Structures, Theory and Applications to Earthquake Engineering (2nd Edition b.), New Jersey Prentice-Hall.

Smith, S.W. (1997). The Scientist and Engineer's Guide to Digital Signal Processing (1 ed.). USA: California Technical Publishing

Binda, L.; and Saisi, A. (2001): Non Destructive Testing Applied to Historic Buildings: The Case of Some Sicilian Churches, Proceedings of the 3rd International Seminar of Historical Constructions, Guimarães, Portugal, University of Minho

Ramos L. F. (2007). Damage Identification on Masonry Structures Based on Vibration Signatures, dissertation, university of Minho, Portugal

Casarin, F.; and Modena, C. (2007): Dynamic Identification of S. Maria Assunta Cathedral, Reggio Emilia, Italy, Proceedings of the 2nd Int. Operational Modal Analysis Conference, Copenhagen, Denmark,

Allemang J. R. (2003). The Modal Assurance Criterion – Twenty Years of Use and Abuse. Sound and Vibration , 14-21.

Alaboz M. (2009). Dynamic Identification and Modal Updating of S.Torcato Church Guimaraés, Portugal: University of Minho.

Ewins D. (1984). Modal Testing:Theory and Practise . Chichester: Research Studies Press LTD.

Gianni Bartoli, Michele Betti, Saverio Giordano, (2013),In situ static and dynamic investigations on the ''Torre Grossa'' masonry tower, Italy

Semih GÖNEN. (2012). Dynamic Identication and Modal Analysis of Ras Charratine Medersa in Fez, Morocco, Spain: Politechnical University of Catalunya.

Maia, N.M.; and Silva, J.M. (1997): Theoretical and Experimental Modal Analysis, Research Studies Press LTD, England

Bruel&Kjær Product Data Handbook

ME'scopeVES (2008), "Modal Analysis software", CD-Rom